NASA CONTRACTOR REPORT

NASA CR-157
c. 1

NASA CR-1570

INFORMATION REQUIREMENTS FOR SUPERSONIC TRANSPORT OPERATION

by Lewis Meier, Charles H. Wells, Sidney Serebreny, David M. Salmon, and John Peschon

Prepared by
STANFORD RESEARCH INSTITUTE
Menlo Park, Calif.
for Ames Research Center

NATIONAL AERONAUTICS AND SPACE ADMINISTRATION • WASHINGTON, D. C. • JULY 1970

NASA CR-1570

INFORMATION REQUIREMENTS FOR SUPERSONIC TRANSPORT OPERATION

By Lewis Meier, Charles H. Wells, Sidney Serebreny,
David M. Salmon, and John Peschon

Prepared under Contract No. NAS 2-5069 by
STANFORD RESEARCH INSTITUTE
Menlo Park, Calif.

for Ames Research Center

NATIONAL AERONAUTICS AND SPACE ADMINISTRATION

For sale by the Clearinghouse for Federal Scientific and Technical Information
Springfield, Virginia 22151 – CFSTI price $3.00

ABSTRACT

This report is the final report on Contract NAS2-5069. The report describes an investigation of the effect of atmospheric changes and errors in the measurements used to determine these changes on the vertical flight performance of an SST. Included in the report are descriptions of the models (engine, instruments, aerodynamics, atmosphere) and the optimal control theory (deterministic and stochastic) needed to determine optimal SST trajectories and their sensitivity to atmospheric variations and measurement errors. Descriptions are also given of computer programs for SST trajectory optimization and sensitivity analysis.

CONTENTS

CONTENTS (Continued)

CONTENTS (Continued)

CONTENTS (Concluded)

ILLUSTRATIONS

ILLUSTRATIONS (Concluded)

TABLES

INTRODUCTION

This report is the final report on NASA Contract NAS2-5069, "Information Requirements for Supersonic Transport Operation." The purpose of this introductory section is twofold: to summarize the results of the study and to act as a guide to the remainder of the report, which describes the results in full detail.

A. Background

This project follows two previous contracts: NAS2-2457 (Information Requirements for Guidance and Control Systems[1*]) and NAS2-3476 (Design of Guidance and Control Systems for Optimum Utilization of Information[2]). The goal of this project was to apply the theory developed in those contracts to the practical problem of flying an SST. In particular, it is well known that the performance of an SST (or any other airplane) is highly dependent upon atmospheric conditions. Thus the goal of the project was to determine what atmospheric parameters should be measured and how well to ensure optimal behavior under varying weather conditions.

One of the principal investigators on NAS2-2457 and NAS2-3476, John Peschon, left SRI to join Wolf Management Services, prior to the start of NAS2-5069. Portions of the research carried out under this contract and described in this report were carried out by him and other members

---

* References are listed at the end of this report.

of Wolf Management Services under a subcontract. Where not indicated otherwise, the tasks were carried out by Lewis Meier of SRI.

The philosophy developed in the previous contracts and applied in the present project was as follows: First, the problem is formulated as a stochastic control problem. This task involves selecting a suitable set of variables (referred to as the state) that describe the system to be controlled, a differential equation relating the behavior of state to the inputs of the system, an algebraic equation relating the measurements made on the system to the state, and a performance index to measure the performance of the system. Second, this stochastic control problem is solved to find the optimum controller for computing control on the basis of past and present measurements. Finally, the optimal performance of the system is computed as a function of measurement errors.

In the first contract (NAS2-2457), it was found that for linear systems and quadratic performance indices, the degradation in performance due to measurement errors was proportional to the covariance of the error in application of control due to the measurement errors. In the second contract (NAS2-3476), these results were extended to nonlinear systems and general performance indices by a suitable linearization. The result was that to second order, in the absence of constraints and for continuously differentiable system equations and performance indices, the cost of measurement errors was again proportional to the covariance of the error in application of control due to the measurement errors.

B. Description of Tasks Performed

To attain the goals of the project, the following tasks were performed.

1. Instrumentation Study

A survey was made of the instrumentation available on a modern jet airplane and the instrumentation that is likely to be present on a Supersonic Transport to ascertain what measurements will be available on an SST. This survey included descriptions of systems of instruments, which include processing of raw measurements and display, and others such as the air data computer, flight director, auto pilot and navigation system. The results of the study, which was performed by Charles Wells and John Peschon of Wolf Management Services, are described in Sec. III of Part One and Appendices B and C.

2. Atmospheric Study

An important aim of the project was to determine the effect of temperature variations on SST operation. Consequently a study was made of how temperature varies as a function of altitude for a standard day at various latitudes and times of the year, and how the actual temperature at cruise altitude has varied in the past on selected days along selected polar routes. This study was carried out by Sidney Serebreny and is described in Sec. II of Part One.

3. Selection and Development of Models

To describe the behavior of an SST several models had to be selected from existing models or developed. The atmospheric model (described in Sec. II of Part One and Sec. I of Part Three), the aerodynamic model (described in Sec. I of Part Three) and the Equations of Motion (described in Sec. I of Part Three) are all standard models. No suitable standard model of the engine existed; however, David Salmon, in conjunction with Mark Waters of NASA Ames Research Center, was able to develop such a model, which is described in Sec. I of Part One.

4. Theoretical Extensions

It was necessary to extend the theory of the previous contracts to treat the SST problem. These extensions came in the areas of optimization and sensitivity to measurement error and are described in greater detail below.

5. Program Development

Two programs were developed embodying the application of the theoretical developments of this and the predecessor contracts to the SST operation problems: an optimization program and a sensitivity program. These programs and results of their use are described in greater detail below; the programmer was P. H. Omlor.

C. Summary of Significant Theoretical Results

Part Two of this report summarizes the theoretical development performed on this project. This research was a continuation and refinement of the research performed during the two previous projects.

1. Stochastic Optimization Theory

To determine the effect of measurement errors on the performance of a control system, it is necessary to solve a general nonlinear stochastic control problem. Exact solution of such a problem while possible in theory is in practice computationally infeasible; therefore, approximate solutions must be resorted to. Section I of Part Two presents the development of one such approximate solution, which is described briefly below.

Consider a control law consisting of a nominal control plus a linear function of the difference between the estimate of the state, assumed to be unbiased, and the nominal state (i.e., the state that the

system would be in if the nominal control were applied and all random effects were absent). An expression for the performance of the system using this control law that is exact to second order can be developed. Note that inclusion in the control law of nonlinear functions of the difference between the nominal and the measured state of the system would have been pointless, since to second order the only affect of such terms is to shift the nominal trajectory. Optimization is performed by selection of the optimal linear gain and optimal nominal control. A necessary condition that the nominal control be optimal in the absence of measurement errors is that it maximize the Hamiltonian, which is a function of the state variables and an auxiliary set of variables called the adjoint variables.

If the minimum of the Hamiltonian does not lie on a constraint or on a discontinuity in the derivative of the Hamiltonian, then the derivative of the Hamiltonian with respect to the control is zero. In this situation optimal control about the nominal is determined by second-order considerations; specifically the optimum gain is found by solution of a linear control problem, where the state equations are the system equations linearized about the nominal trajectory and the cost matrices are the second derivatives of the Hamiltonian. These costs include not only the second-order terms from the original performance function, but also second-order terms from the state equations.

If the minimum of the Hamiltonian is on a constraint or on a discontinuity in the derivative of the Hamiltonian, then the derivative of the Hamiltonian (or its right and left derivatives in the case of a discontinuity) will not in general be zero. In this situation optimal control about the nominal is determined by first-order considerations; in particular the linear gain is chosen to maintain the control on the constraint or the discontinuity in the presence of variations of the

state from the nominal. Any other choice of gain will result in a first-order degradation in performance.

2. The Effect of Measurement Errors

In the presence of measurement errors the state of the system is not known exactly; hence the actual control will deviate from the optimum value that would be used if the state were known exactly. To second order the deviation in control is normally distributed about the optimum and hence can be parameterized by a standard deviation matrix. Again to second order this standard deviation is just the standard deviation of the errors in estimate of the state resulting from measurement errors multiplied by the gain used for control about the nominal.

When the optimum nominal control without measurement errors is not on a constraint or a discontinuity in the Hamiltonian, it is unchanged by the presence of measurement errors. In this situation, the lowest order term in the cost of measurement errors is second order; i.e., it is proportional to the square of the standard deviation of the control from optimum.

If the constraints on control are state dependent, then in the presence of measurement error it is impossible to tell exactly whether a given control meets the constraint or not. Thus it is necessary to tighten the constraint used in actual operation to ensure that the desired constraint is rarely broken. This means that those portions of the optimal nominal control without measurement errors that lie on a constraint must be shifted in the presence of measurement noise. In this situation, the lowest order term in the cost of measurement errors is first order; i.e., it is proportional to the standard deviation of the error in application of control as well as the standard deviation squared.

For a portion of the optimal nominal trajectory that lies upon a discontinuity in the derivative of the Hamiltonian, the presence of measurement noise leads to a first-order cost just as in the case of constraints. In this case the cause is the rectifying effect of the change of slope. This first-order cost can be minimized, but not eliminated, by shifting the nominal trajectory a slight amount from the measurement-error-free nominal.

3. Optimization Techniques

Finding the optimum nominal trajectory involves minimization of the Hamiltonian. Unfortunately the differential equations describing the state variable and adjoint variables must usually be integrated in opposite directions because their boundary conditions are not in the same place. This necessitates the use of iterative techniques for minimizing the Hamiltonian; i.e., a tentative control history is selected and the state equations integrated in one direction, the adjoint equations in the reverse direction and a new control history selected, the process being repeated until it converges. For this iterative process to work well it is desirable that the adjoint variable be insensitive to changes in control history. Section VI presents a method whereby the dynamics of the adjoint equations can be modified so that this sensitivity is minimal. This technique was used in this project to obtain very rapid convergence in the vertical control optimization problem described below.

4. Suboptimal Nominal Trajectories

It is not necessary that the nominal trajectory used in the developments described above be the optimal nominal. It is only necessary that the nominal lie within the region about the optimal nominal for which the second-order expansion of performance is adequate. Linear control

about the suboptimal nominal can then be used to correct for the nonoptimality of the nominal. This result is quite important, since it is often convenient to pick the nominal by solving a simplified version of the optimal control problem. The theory is not complete on the use of suboptimal nominal trajectories; although it is clear how to proceed in the absence of constraints and discontinuities in the derivative of the Hamiltonian, it is not clear how to proceed in their presence.

5. State Space Constraints

A major area of future research is the extension of the above techniques to handle state space constraints. Solution of a deterministic optimal control problem is difficult, but necessary conditions are known. Approximate solution of the stochastic optimal control problem with state space constraints and determination of the effect of measurement errors in the presence of state space constraints has not been achieved to date.

D. Flight Control of an SST

Control of the flight of the SST involves two tasks: controlling the motion of the center of mass of the SST and controlling the motion of the SST about its center of mass. The only dependence of the motion of the center of mass on the motion about the center of mass is provided by the attitude of the SST, which determines the forces acting on the center of mass. By use of the approximation technique described above, control of motion of the center of mass can be separated from the attitude control. For control of the center of mass, the attitude of the plane is taken as the control and the optimum control law is found. This control law will yield the desired attitude at any time and the cost (a quadratic cost found from taking second derivatives of the Hamiltonian) of not being at this attitude. This cost is then made part

of the attitude control performance criteria along with costs of effecting change in attitude. The goals of the attitude control system are thus inferred from the goals of the flight-path control system. The goal of the flight-path control system is given directly: It is to take the plane from its point of origin to its destination in a manner that minimizes time taken and fuel used while observing all air traffic, noise, and structural constraints.

In the following paragraphs a proposed method of controlling an SST is described. To implement that technique it is necessary to solve, among other problems, what is referred to herein as the vertical control problem. The research in the project was expended on this problem; it is described in greater detail below.

1. Horizontal Control

In general, the best path for an SST to take between two points is the shortest path. For ordinary jets it is sometimes worthwhile to modify the path somewhat to take advantage of favorable winds, but an SST travels so fast that it is not profitable to deviate from the shortest path.[3] In horizontal control the major state variables are the latitude and longitude and direction of the motion of the SST and the control variables are its roll and yaw angles. However, it is convenient to assume that the direction of motion of the aircraft can be changed instantaneously and that roll and yaw have nominal angles of zero. If ground track distance is taken as the independent variable, then the ground path can be optimized independently of the velocity.

2. Vertical Control

Given an optimal ground track to follow, there still exists the problem of determining the optimum cruise altitude and getting to and

from cruise at the beginning and end of the flight. In vertical control the major state variables are the altitude, velocity, and flight-path angle, and the control is the throttle and angle of attack. It is convenient, however, to assume maximum throttle during climb, minimum throttle during letdown, and throttle set to maintain velocity during cruise; hence this control can be eliminated. During cruise the vehicle is traveling at maximum velocity, and it is convenient to assume that altitude may be changed instantaneously. In this situation there are no state variables and the optimization is purely algebraic. During climbout and letdown, it is convenient to replace the altitude by the energy (potential plus kinetic) per unit mass and assume that velocity can be changed instantaneously.[4] If fuel used is taken as the independent variable, then the optimum climb and letdown profiles can be determined. Suitable nominal values of flight-path angle and angle of attack are used.

3. Autopilot Control

Suppose an optimum ground path and optimum climb, cruise, and letdown profiles have been specified; there remains the problem of selecting roll, yaw, and angle of attack (or pitch) to follow these paths. If we use the paths determined as above and the nominal values of the attitude as a nominal trajectory, then the approximation theory described above can be used to optimize control about this nominal. For the chosen nominal, vertical control and horizontal control should separate.

4. Realization

Refer to Fig. 1 for a block diagram of the realization of such a scheme of control. The vertical control computer takes measurements of the parameters which describe the atmosphere and measurements of the static

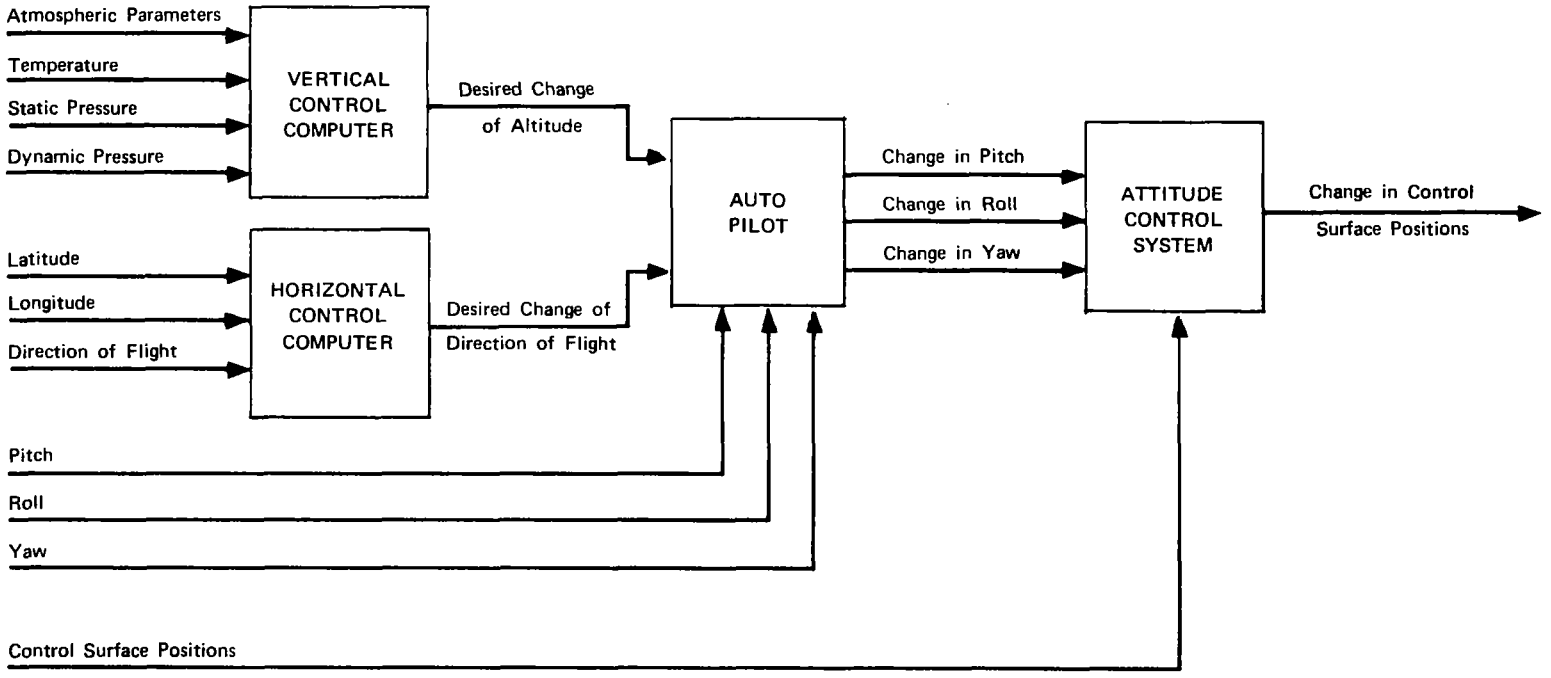

FIGURE 1 SST CONTROL SCHEME

and dynamic pressure and the temperature and then produces a desired change in altitude signal (exactly how this computation relates to the solution of the vertical control problem is spelled out in greater detail below). The horizontal computer takes measurements of the latitude and longitude and directions of motion and determines a desired change in the direction of motion signal. The altitude change signal and direction of motion signal are fed to the autopilot along with measurements of the attitude of the plane. The autopilot computes a desired change in attitude which can be either directly coupled to the attitude control system or displayed to the pilot on the flight director. The attitude control system takes the desired change in attitude signal from the pilot or autopilot and determines appropriate commands to the SST control surfaces.

E. Summary of Significant Results from Solution of the Vertical Control Problem

The vertical control problem, described briefly above, provides the ideal problem for the present study for two reasons:

- The major effect of atmospheric variations is on the optimal vertical flight profiles.
- The problem involves only control constraints; any of the other problems mentioned above involve state constraints--the theory has not, as yet, been extended to include the presence of state constraint.

Below, the vertical control problem is discussed in greater detail; most of the remainder of this report, except for Part Two, deals with it.

1. Problem Formulation

The state variable for this problem is the energy per unit mass, which is the sum of potential energy per unit mass (a linear function of altitude only) and kinetic energy per unit mass (a quadratic function of velocity only). As control variable either velocity or altitude may be used; velocity was chosen in the present study. The state equation can be written by using Newton's law to express rate of change of energy as a function of thrust, drag, mass, and velocity. To express the thrust and drag as functions of energy, velocity, and mass; the models of the engine, aerodynamics, and atmosphere were used. Section I of Part Four gives the derivation and simplification of the equations of motion, and the parameterization of the models of the engine, atmosphere, and aerodynamics.

Part Four, Sec. II, describes the formulation of the vertical control problem as an optimal stochastic control problem. Fuel used was chosen as the independent variable rather than time because mass could then be considered a function of the independent variable rather than a state variable. The performance function that one really wants to optimize is a trade-off between fuel used and time taken to go a fixed distance; however, it is easier to optimize a trade-off between time taken and distance covered for a fixed amount of fuel used. By running a family of the latter optimizations, it is possible to obtain a family of the former optimizations.

2. Problem Solution

When the SST is traveling at maximum velocity (i.e., during cruise), the only optimization that can be performed is minimization of the rate of fuel consumption. Determination of the optimum cruise is an algebraic

optimization (i.e., present optimum is independent of future optimum). At the beginning of the flight an optimum climb from the altitude and velocity at the end of take-off to cruise altitude and velocity must be performed. And at the end of the flight an optimum letdown to altitude and velocity suitable for landing from cruise altitude and velocity must be performed. These two optimizations are variational optimization (i.e., present optimum depends upon future optimum).

Section I of Part Four describes in detail the optimization equations needed for cruise, climbout and letdown, and Sec. I of Part Five describes an optimization program embodying those equations. To obtain an initial guess for the optimum climbout and letdowns, algebraic optimizations were performed. In running the program for a variety of parameters, it was found that the actual optimal climbouts and letdowns were always provided by the initial guess; thus optimal climb and letdown can be reduced to algebraic optimization.

In addition to knowing optimum climbout, cruise, and letdown as a function of various conditions, one is interested in the variation in performance with conditions and effect on performance of errors in the measurements made to determine the conditions obtaining at a given time. In Sec. II of Part Four equations that represent the application of the theory of Part Two, Sec. I, to the vertical control problem are given and in Part Five, Sec. II, a program (called sensitivity program) embodying these equations and the algebraic optimizations of the optimization program is described. Use of the sensitivity program gives, for any conditions parameterizable by the models used, the optimum climbout, cruise, and letdown, and the sensitivities of performance to measurement errors (made on certain assumptions about the measurements made and the nature of the errors). By use of the program for varying conditions, the effect

of changes in conditions on performance can be determined. Optimal cruise, climbout, and letdown and their sensitivities are discussed in greater detail below.

3. Realization of Vertical Control

In cruise, velocity is determined by a constraint that is a function of the outside temperature; optimization is performed by selecting the optimal pressure altitude as a function of fuel used and outside temperature, since engine and aerodynamics depend only on velocity, outside temperature, and outside pressure and not on geometric altitude. Climbout and letdown optimizations depend upon, in addition, the cruise temperature (through the cost function) and upon geometric altitude (through constraints and discontinuities in derivative).

Thus the vertical control computer needs to know fuel used, pressure altitude, outside temperature, velocity, geometric altitude, and cruise temperature. Pressure altitude is determined by measuring the outside static pressure; given the outside static pressure and temperature the velocity or airspeed may be determined by measuring outside dynamic pressure $[(1/2)\rho v^2]$. To determine geometric altitude and cruise temperature, it is necessary to have a model of the atmosphere. The model used in this development assumes that temperature is constant above the tropopause and falls at 6.3°C per km from sea level to tropopause; hence the atmosphere is specified by giving the temperature, pressure, and altitude of the tropopause. Cruise temperature (which is just the temperature of the tropopause) and geometric altitude can be determined from outside temperature and pressure and any two of the three conditions at the tropopause. Therefore the vertical control computer must have measurements of fuel used, outside temperature, outside static pressure, outside dynamic pressure and, say, pressure and altitude of the tropopause.

The first four quantities are currently measured on board; the conditions at the tropopause must come from external sources.

As pointed out above, the optimization is carried out by maximization of the appropriate function. This maximization may be carried out on board or on the ground. In the latter case, the results would be stored as a nominal control plus a linear function of the differences of measurements from nominal. Either realization appears well within the capability of available airborne digital computers. The commands will, under some circumstances (such as a dive through the second barrier during climbout), call for flight-path angles outside constraints. In these situations, the autopilot or pilot would select the permitted flight-path angle closest to that desired.

4. An Example

In this section the optimization and sensitivity of a typical SST is considered. The engine and aerodynamic parameters describing this SST are described in Part Three, Sec. I. For the nominal trajectory the values of the temperature, pressure, and altitude of the tropopause are: $\theta_{TROP} = -60°C$, $p_{TROP} = 295$ mb, and $h_{TROP} = 10$ km. Furthermore, along the optimum trajectory, range is maximized for a given amount of fuel.

Figures 2 and 3 describe the nominal trajectory for the typical SST. Note that the throttle setting is constant along the cruise. This will be true only if the temperature along the cruise (which is the temperature of the tropopause in the present model) is constant. In the real situation, temperature along cruise, and thus cruise altitude and power setting will vary. Both cruise and letdown as shown in Figs. 2 and 3 are quite well behaved. Climbout, however, shows much livelier behavior. The first piece of the climbout above the minimum altitude is caused by a discontinuity in derivative of the engine performance occurring when

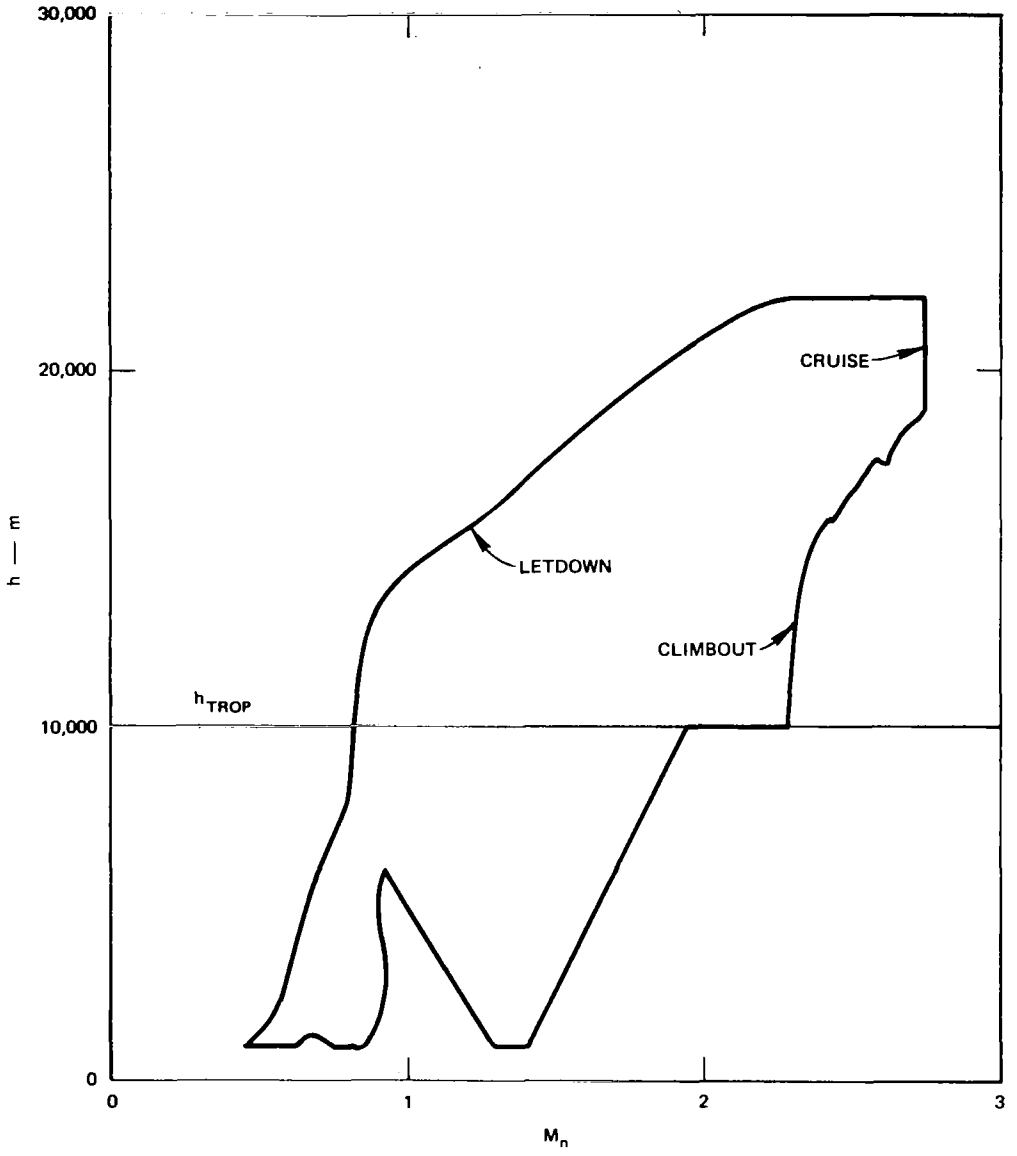

FIGURE 2 ALTITUDE

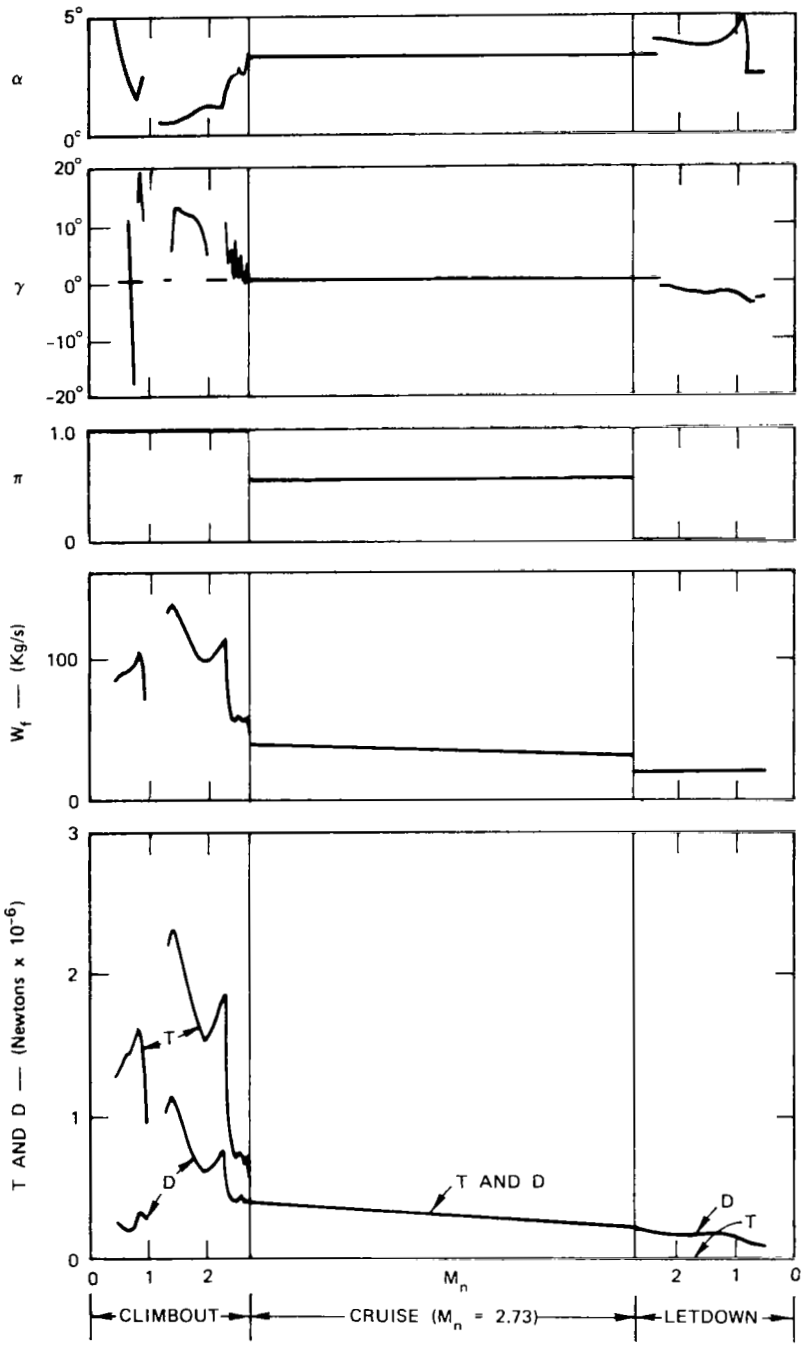

FIGURE 3 PROPERTIES OF OPTIMAL TRAJECTORY

the combustion chamber reaches its maximum total temperature. The optimum follows this discontinuity for a short period and then continuously returns to minimum altitude. The next major facet of the trajectory is a dive through the sonic barrier; in an actual trajectory, constraints on the SST will determine how fast this dive can be made. Note that in the supersonic climb, the trajectory follows the discontinuity of the atmosphere at the tropopause for awhile. The cause of the oscillation at the end of the climb is at present unknown.

Consider now the effect of variations in the atmosphere from nominal. In Table I the performance is given for perturbation of each of the atmospheric parameters from nominal; the value of the perturbed parameter is given in the table. Such variations in h_{TROP} and θ_{TROP} are shown to be common in Sec. II of Part One. Note that only the variations in

Table I

PERFORMANCE FOR PERTURBATION OF ATMOSPHERIC PARAMETERS FROM NOMINAL

Nominal	θ_{TROP} = $-80^{\circ}C$	θ_{TROP} = $-40^{\circ}C$	h_{TROP} = 0.7×10^4	h_{TROP} = 1.3×10^4	p_{TROP} = 280	p_{TROP} = 310
7.93×10^6	8.07×10^6	7.71×10^6	7.97×10^6	7.88×10^6	7.93×10^6	7.92×10^6

θ_{TROP} cause significant changes in performance. The reason for this is that cruise performance is affected only by θ_{TROP}, since the optimum cruise pressure altitude is a function only of θ_{TROP}. The effect of changes in h_{TROP} and p_{TROP} on cruise is to change the geometric altitude as illustrated in Table II, which gives the geometric altitude at the end of cruise for perturbations of h_{TROP} and p_{TROP}. Table III illustrates the

Table II

EFFECT OF CHANGES IN h_{TROP} and p_{TROP} ON CRUISE

$h_{TROP} = .07 \times 10^4$	h = 19,100	p_{TROP} = 280	h = 21,700
$h_{TROP} = 1 \times 10^4$	h = 22,100	p_{TROP} = 295	h = 22,100
$h_{TROP} = 1.3 \times 10^4$	h = 25,100	p_{TROP} = 310	h = 22,400

Table III

EFFECT OF CHANGES IN θ_{TROP} ON CRUISE

	h	p	v	$V/\dot{W}_f$	$1/\dot{W}_f$	π
$\theta_{TROP} = -40$	22,200	49.3	773	74.5	0.0964	0.634
$\theta_{TROP} = -60$	22,100	42.6	801	76.6	0.0956	0.539
$\theta_{TROP} = -80$	21,800	36.7	829	77.4	0.0934	0.446

effect of changes in θ_{TROP} on cruise by giving several quantities at the end of cruise; $v/\dot{w}_f$ is the distance covered per unit of fuel, $1/\dot{w}_f$ is the time taken per unit of fuel, and π is the power setting. The major conclusion is that performance is not changed very much with changes in atmospheric parameters when the control used is optimal for these actual parameters.

The second sensitivity of interest is the sensitivity to measurement noise. Table IV gives the percentage loss on performance of 1-percent errors in measurement of fuel used μ, outside temperature $\hat{\theta}$, outside

Table IV

PERCENTAGE LOSS ON PERFORMANCE FROM MEASUREMENT NOISE

	μ (percent)	θ (percent)	p (percent)	q (percent)	p_{TROP} (percent)	h_{TROP} (percent)
Cruise	0.009	0.37	0.71	0.70	0	0
Climbout	≈ 0	0.006	0.033	0.012	0.02	0.036
Letdown	0.002	≈ 0	0.004	0.002	0.002	0.005
Total	0.011	0.38	0.75	0.75	0.02	0.04

static pressure p, outside dynamic pressure q, p_{TROP} and h_{TROP}. Note that performance is relatively sensitive to errors in θ, p, and q and relatively insensitive to errors in μ, p_{TROP}, and h_{TROP}. The major cause of this sensitivity to error in θ, p, and q is the constraint on v during cruise. For this example it was assumed that the constraint on v was tightened by three standard deviations to ensure that it would seldom be exceeded because of measurement errors. If, for example, this constraint need be met only on the average, then sensitivity would be far less. In any event it appears that existing instrumentation would be quite adequate.

F. Areas of Future Research

Much has been accomplished in the application of modern control theory to the optimal operation of SST's, but much remains to be accomplished. Some of the areas of remaining research are listed below.

1. Broadening the Present Program

In the present program simple models were used for the constraints acting on the SST; more realistic models would be desirable. For some routes (see Sec. II of Part One), the changes in temperature and

temperature gradients can be quite large; the effects of these temperature changes upon cruise should be investigated. Programs should be developed to permit easy selection of model parameters in the engine and aerodynamics to fit experimental values. All the above areas are refinements of the programs developed in the present project rather than major revisions.

2. Two-State Vertical Control

In the present program, a one-state model is used for optimization of vertical control. In some situations, such as the transition from subsonic to supersonic in climbout, the computed control demands a flight-path angle exceeding the constraints. This difficulty can be handled heuristically by using the limiting flight-path angle in such situations. It would be desirable to optimize with a two-state model in which energy and velocity are state variables and flight-path angle the control variable. If the one-state optimum (heuristically modified where necessary) is sufficiently close to the two-state optimum (i.e., within the region that second-order approximation holds), then it is adequate for vertical control; otherwise a two-state optimum is necessary.

3. Autopilot Control and Altitude Control

Development of algorithms for optimal autopilot control and altitude control is the logical extension of the optimization of vertical control.

4. Theoretical Research

To study Items 2 and 3 above, further development of the stochastic control theory presented in Sec. I of Part Two is needed. In particular, the problem of including state variable constraints must be solved.

For Item 2, the two-state vertical control, the problem is the effect of state variable constraints on the nominal control; for Item 3, autopilot and altitude control, the problem is the effect of state variable constraints on control about the nominal.

PART ONE

MODELS NEEDED FOR THE OPTIMIZATION OF SUPERSONIC TRANSPORT OPERATION

I THE ENGINE

A. Introduction

This section presents two models for a supersonic transport (SST) engine. The models are based on information supplied by Mark Waters of the NASA Ames Research Center. A brief development of some relevant thermodynamic relations is given in Appendix A.

The first model includes many relationships between internal engine variables and models more accurately than the second model the processes occurring in the engine. However, for finding optimal SST trajectories, it is sufficient to consider the engine merely as a device for converting the input variables (the total pressure and temperature of the free stream atmosphere, the aircraft Mach number, and the engine power setting) into the output variables (thrust and fuel consumption). Accordingly, a second model is derived by simplifying the first model to provide only the required information.

B. Detailed Engine Model

Figure 4 shows a diagrammatic representation of the engine and defines the points at which the gas conditions will be considered.

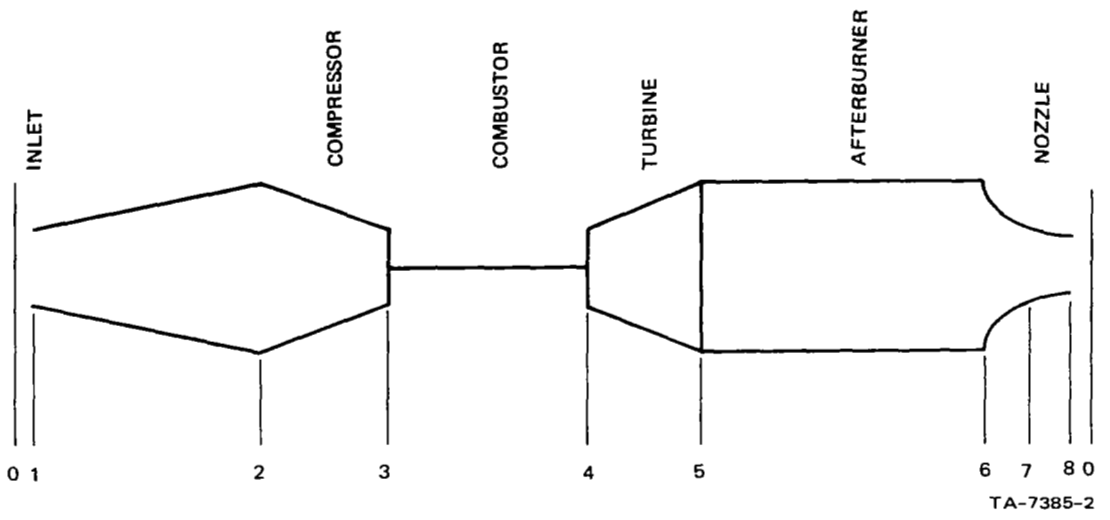

FIGURE 4 A DIAGRAMMATIC VIEW OF THE SST ENGINE

1. Ram Recovery and Compressor Characteristics

The total pressure* $p_2^\star$ at point 2 is determined by the ram recovery, which for a given inlet geometry depends on the flight Mach number M_n. Typically the relation is as in Fig. 5.

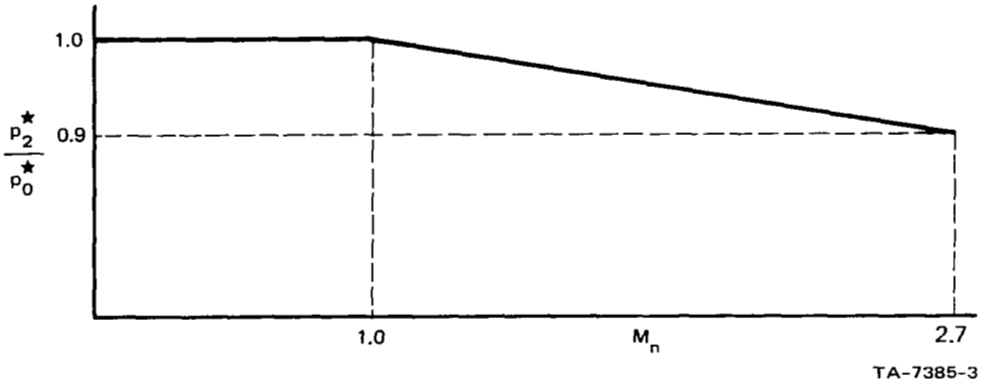

FIGURE 5 RAM RECOVERY

*Total temperatures and pressures are denoted by stars. The relationship between the total or stagnation quantities and the actual temperature and pressure is given in Appendix A.

The optimal rotor speed N for a given engine is a function of the total temperature $\theta_2^\star$ at 2 (which is equal to the total temperature $\theta_0^\star$ in the free stream). The relationship is typically as in Fig. 6. The airflow, W_a, for given rotor speed and total conditions at point 2 can be found from a characteristic like the one in Fig. 7. For given

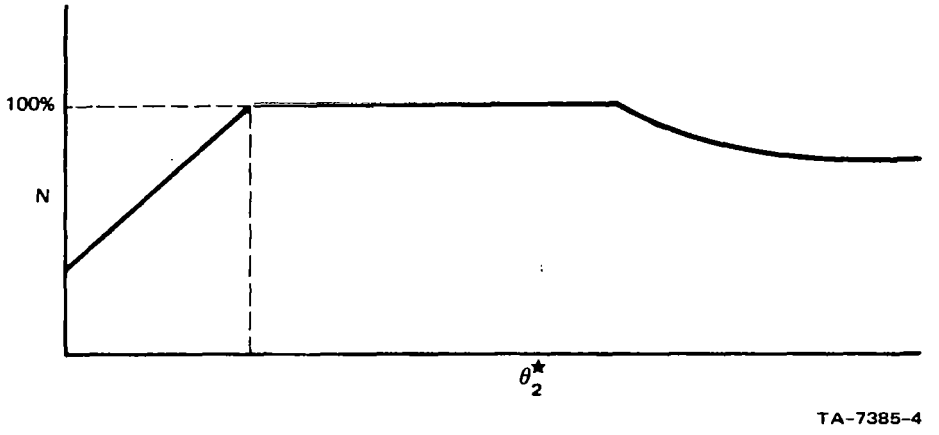

FIGURE 6 ROTOR SPEED AS A FUNCTION OF TOTAL TEMPERATURE

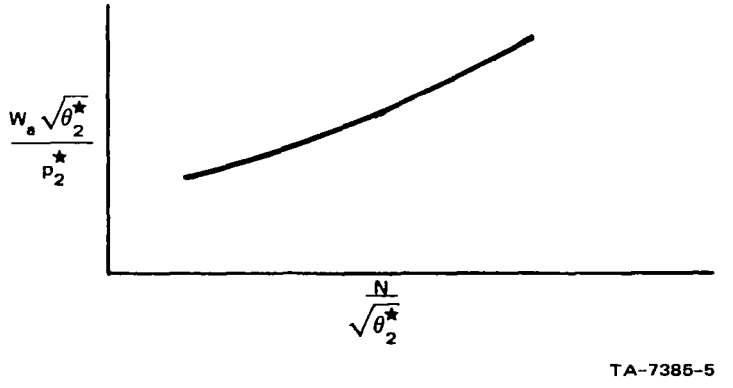

FIGURE 7 AIRFLOW AS A FUNCTION OF ROTOR SPEED

airflow and total conditions at point 2, the compressor characteristic shown in Fig. 8 can be used to determine the total pressure $p_3^\star$ at 3. (It is assumed in the derivation of this curve that the compressor efficiency, η_c, is constant.)

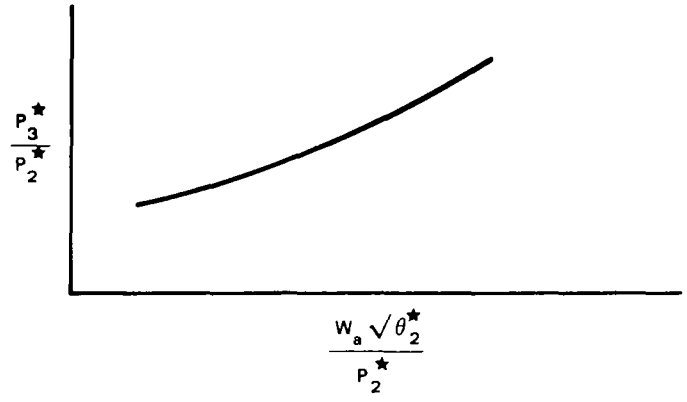

FIGURE 8 COMPRESSOR CHARACTERISTIC

2. Combustor, Turbine, and Afterburner Characteristics

The effect of the compressor and combustor is to raise the total temperature of the gas at 4 above that at 2, as in Fig. 9; $\theta_4^\star$ increases linearly with $\theta_2^\star$ until the temperature limitation of the engine is reached, at which point the engine control prevents further increase.

The afterburner further increases the total temperature $\theta_6^\star$ at point 6 according to the power setting Π of the engine. Figure 10 shows the combined effect of the compressor, combustor, and afterburner.

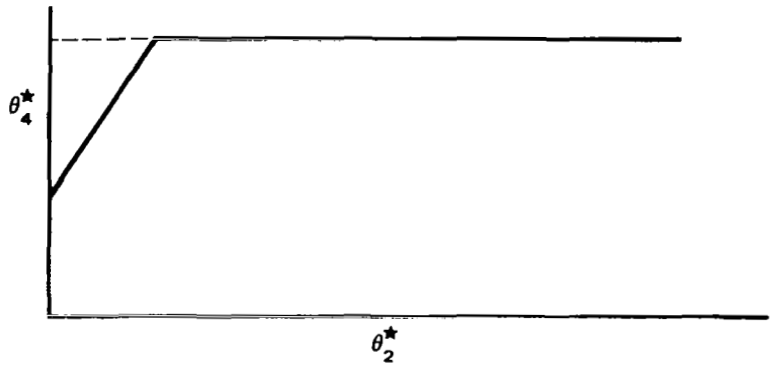

FIGURE 9 TYPICAL TOTAL TEMPERATURE INCREASE DUE TO COMPRESSOR AND COMBUSTOR

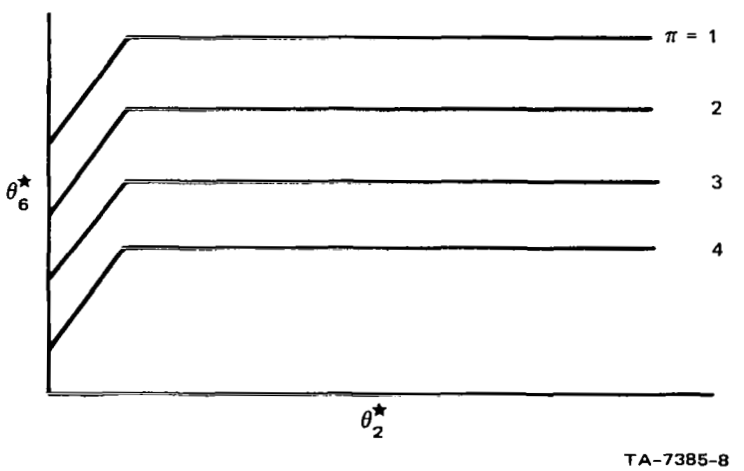

FIGURE 10 TYPICAL TOTAL TEMPERATURE INCREASE DUE TO COMPRESSOR, COMBUSTOR, AND AFTERBURNER

The gas condition at 5, which is needed to determine the pressure drop across the afterburner, can be found by equating the work done by the compressor and the turbine, while allowing for inefficiencies, i.e.,

$$\eta_c\left(\theta_3^\star - \theta_2^\star\right) = \eta_T\left(\theta_4^\star - \theta_5^\star\right) \tag{1}$$

where

η_T is the turbine efficiency

η_c is the compressor efficiency.

Assuming adiabatic compression in the compressor,

$$p_2\theta_2^{\star\frac{\gamma}{\gamma-1}} = p_3\theta_3^{\star\frac{\gamma}{\gamma-1}} , \tag{2}$$

and Eq. (1) can be rewritten

$$\frac{\theta_5^\star}{\theta_4^\star} = 1 - \frac{\eta_c X_c}{\eta_T \alpha} , \tag{3}$$

where

$$X_c = \left(\frac{p_2^\star}{p_3^\star}\right)^{\frac{\gamma-1}{\gamma}} - 1$$

$$\alpha = \frac{\theta_4^\star}{\theta_2^\star} .$$

The total pressure drop across the afterburner is a function of the total temperature increase across it, as shown in Fig. 11.

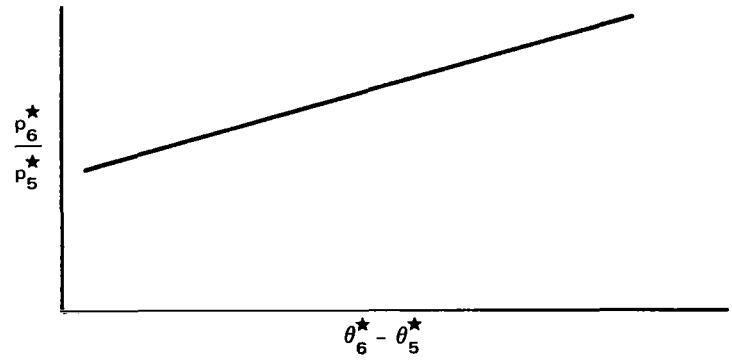

FIGURE 11 AFTERBURNER TOTAL PRESSURE DROP

3. Computation of Net Thrust

The net thrust T_N is defined here as

$$T_N = T_G - D_r \quad , \tag{4}$$

where

T_G is the gross thrust due to expulsion of gas

D_r is the ram drag due to slowing of inlet gas.

This definition of net thrust ignores the following drags normally attributed to the engine: the inlet spillage drag, which arises whenever not all of the air corresponding to the engine inlet area actually flows through the engine; the inlet cowl drag, which arises because the engine inlet walls have finite thickness causing a separation of the airflow; and the nozzle boat-tail drag, which arises because the nozzle walls have finite thickness.

The gross thrust T_G is defined as

$$T_G = c_g T_{GI} \quad , \tag{5}$$

where

T_{GI} is the ideal gross thrust

c_g allows for the inefficiency of the nozzle.

The ideal gross thrust is given by the ideal rate of change of momentum of the exhaust gases, i.e.,

$$T_{GI} = W_a \Delta V = W_a \sqrt{2} \left(H_6 - H_0 \right)^{\frac{1}{2}}$$

$$= W_a \sqrt{2} \left[c_p \left(\theta_6^{\star} - \theta_0^{\star} \right) \right]^{\frac{1}{2}} \qquad (6)$$

where

H_6 is the enthalpy and kinetic energy at 6

H_0 is the enthalpy of the free stream gas.

The nozzle has a characteristic similar to that shown in Fig. 12. The ratio $p_6^{\star}/p_0$ can be computed from

$$\frac{p_6^{\star}}{p_0} = K_1 K_2 \frac{p_3^{\star}}{p_2^{\star}} \left(\frac{\theta_5^{\star}}{\theta_4^{\star}} \right)^{\frac{\gamma}{\gamma-1}} \frac{p_2^{\star}}{p_0^{\star}} \frac{p_0^{\star}}{p_0} \quad , \qquad (7)$$

where

$$\frac{p_0^{\star}}{p_0} = \left(1 + \frac{\gamma - 1}{2} M_n^2 \right)^{\frac{\gamma}{\gamma-1}} \quad , \qquad (8)$$

$$K_1 = \frac{p_4^{\star}}{p_3^{\star}} \approx 0.94$$

$$K_2 = \frac{p_6^{\star}}{p_5^{\star}} \quad .$$

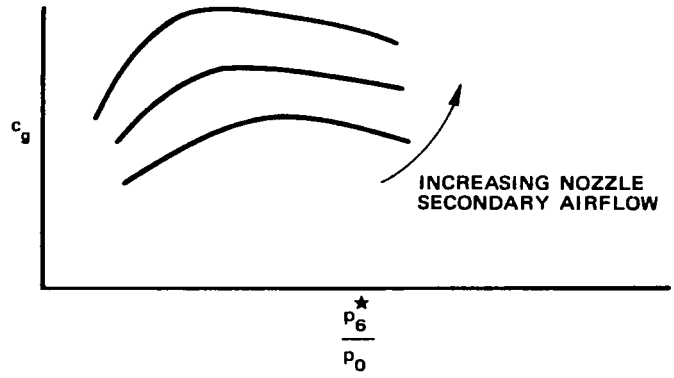

FIGURE 12 NOZZLE CHARACTERISTIC

The ram drag is computed from

$$D_r = W_a V_0 \quad , \tag{9}$$

where

$$V_0 = M_n \sqrt{\gamma R \theta_0} \tag{10}$$

$$\theta_0 = \theta_0^* \left(\frac{1}{1 + \frac{\gamma - 1}{2} M_n^2} \right) \quad . \tag{11}$$

4. Fuel/Air Ratio and Specific Fuel Consumption

The fuel/air ratio f is given by

$$f = f_g + f_{a/b} \quad , \tag{12}$$

where

f_g is the combustor fuel/air ratio

$f_{a/b}$ is the afterburner fuel/air ratio.

For a crude calculation of f the following formulas may be used:

$$f_g = c_p \frac{\theta_4^\star - \theta_3^\star}{\eta_{BG}\bar{H}} \tag{13}$$

$$f_{a/b} = c_p \frac{\theta_6^\star - \theta_5^\star}{\eta_{B\,A/B}\bar{H}} \quad , \tag{14}$$

where

η_{BG} is the combustion efficiency of the gas generator

$\eta_{B\,A/B}$ is the combustion efficiency of the afterburner

$\bar{H}$ is the heat obtained from a unit mass of fuel

and $\theta_3^\star$ may be found from

$$\eta_c \left(\theta_3^\star - \theta_2^\star\right) = \theta_2^\star \left[\left(\frac{p_2^\star}{p_3^\star}\right)^{\frac{\gamma-1}{\gamma}} - 1\right] \quad . \tag{15}$$

The specific fuel consumption is given by

$$SFC = \frac{w_a f}{T_N} \quad . \tag{16}$$

C. A Simplified Engine Model for Trajectory Optimization

Since the internal variables of the engine are not needed for trajectory optimization, it is desirable to find direct relationships between the input and output variables. It has been found that for a given power setting, the ratio $T_N/p_2^\star$ is a single-valued function of the ratio $\theta_6^\star/\theta_0^\star$. Figure 13 shows a family of curves, derived from theoretical performance of a typical SST engine. For the same engine, the curves relating $\theta_6^\star$ to $\theta_0^\star$ (as in Fig. 10) are given in Fig. 14. The two characteristics can also be combined into a single relationship between $T_N/p_2^\star$ and $\theta_0^\star$, as shown in Fig. 15. Similarly, it has

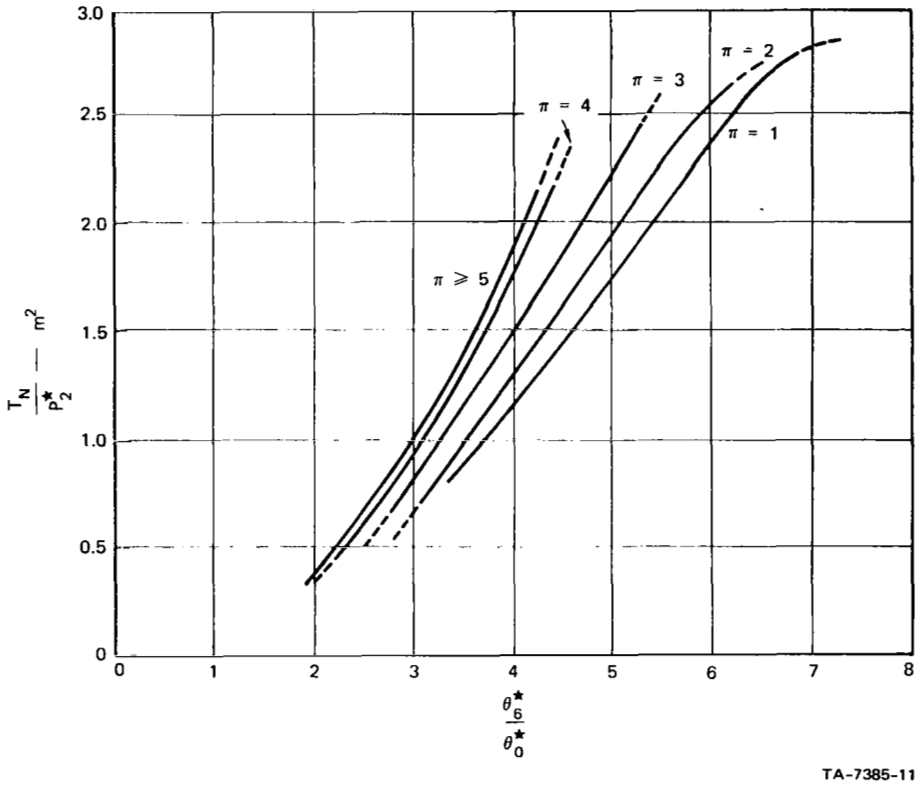

FIGURE 13 THRUST AS A FUNCTION OF $\frac{\theta^*_6}{\theta^*_o}$

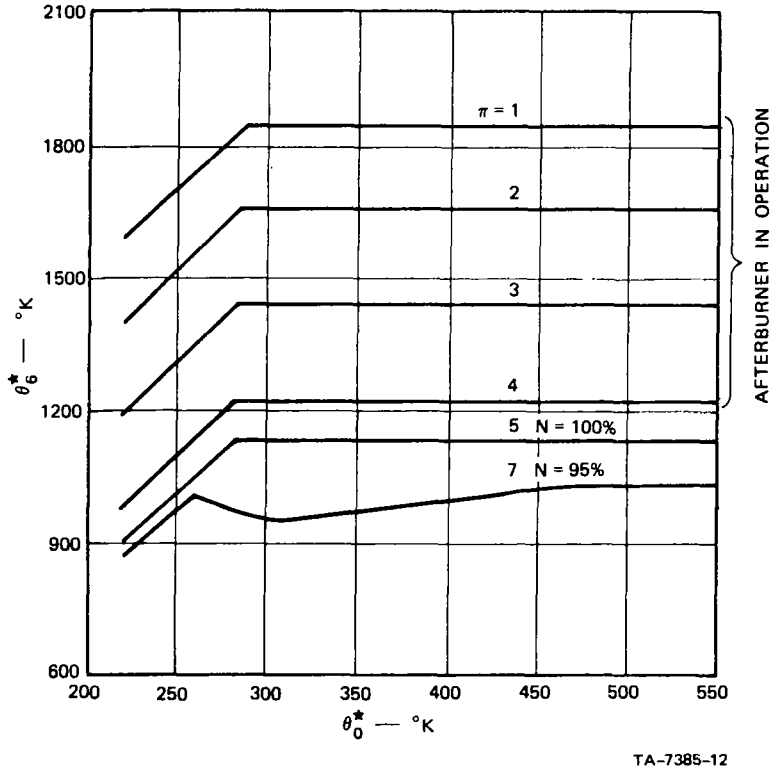

FIGURE 14 TOTAL TEMPERATURE INCREASE DUE TO COMPRESSOR, COMBUSTOR, AND AFTERBURNER

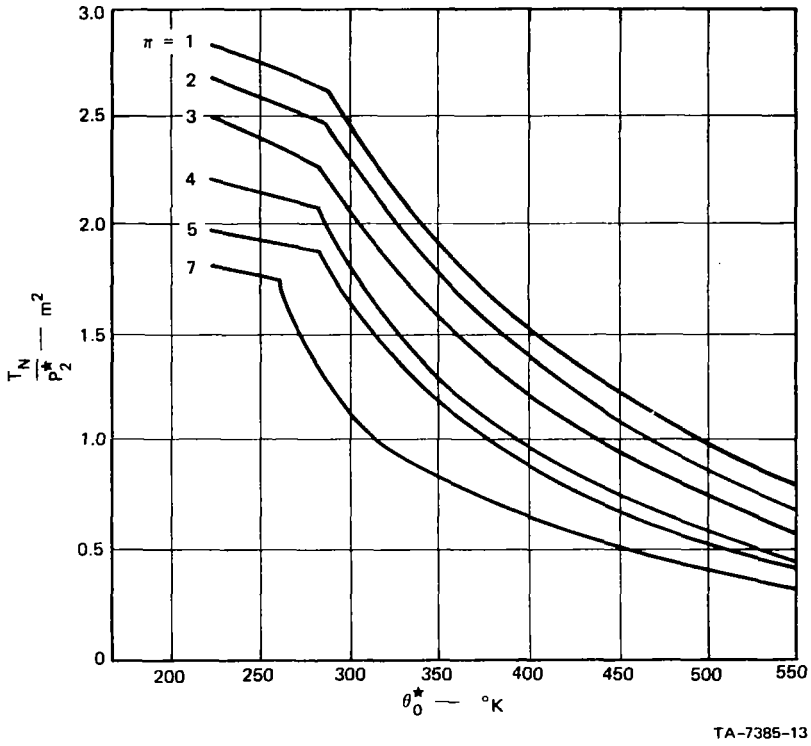

FIGURE 15 THRUST AS A FUNCTION OF θ^*_o

been found that the fuel flow, $W_a f$, can be found from a single relationship between $W_a f/p_2^*$ and θ_0^*, as shown in Fig. 16.

To summarize, the steps required to use the simplified engine model are as follows:

(1) Compute the total conditions in the free stream p_0^*, θ_0^*, and the aircraft Mach number, M_n

(2) Using Fig. 5, obtain the total pressure, p_2^*

(3) Using Fig. 15, obtain the net thrust, T_N

(4) Using Fig. 16, obtain the fuel flow, $W_a f$.

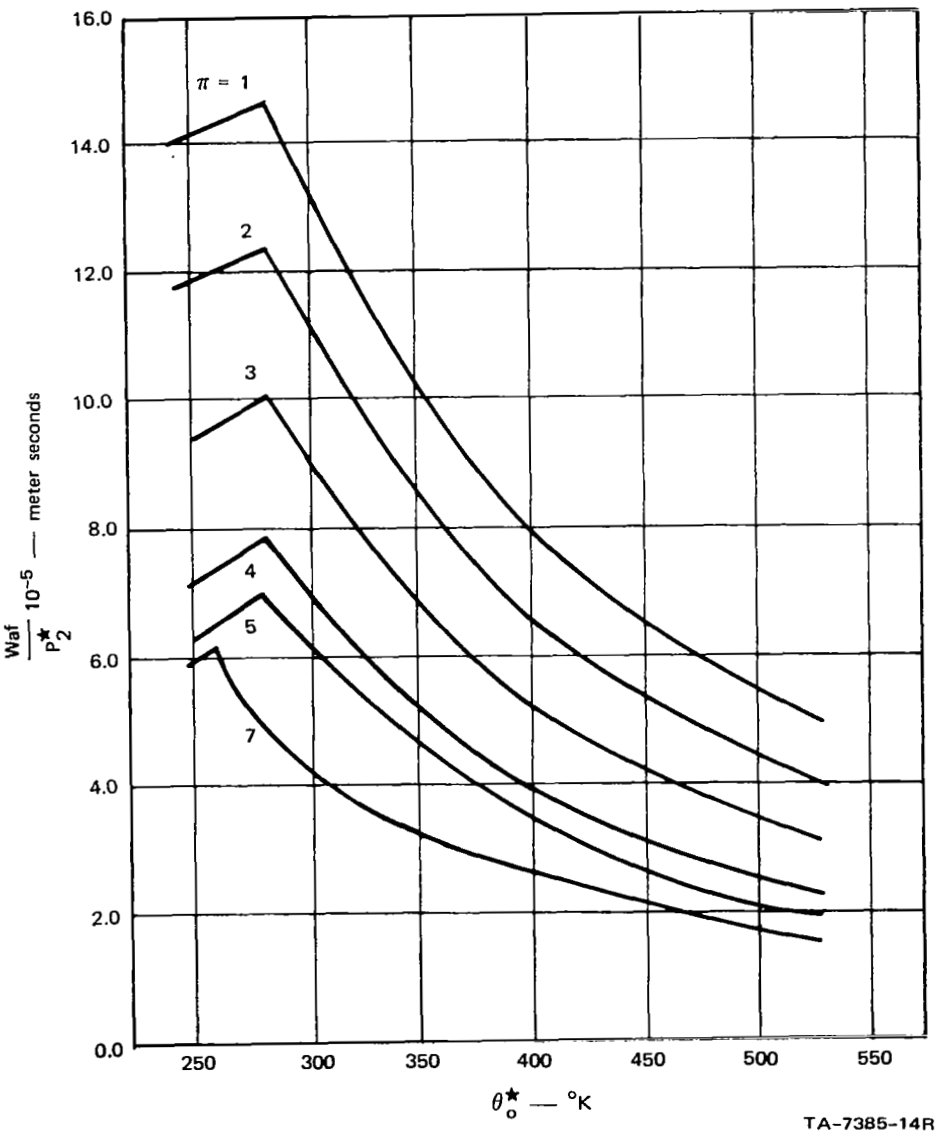

FIGURE 16 FUEL FLOW AS A FUNCTION OF $\theta_o^\star$

D. Conclusions

Two models for an SST engine have been presented. The first requires the computation of a number of internal engine variables as an intermediate step between the input variables and the output variables of thrust and fuel flow. The second model minimizes the number of internal variables and consists essentially of just two families of curves. As a result the second model can readily be transformed into two analytical expressions by fitting polynomials to the curves of Figs. 15 and 16 in the regions of most interest. (See Sec. I-C-3 of Part Three).

II THE ATMOSPHERE

A. Introduction

In this section, models of the atmosphere are considered. First the variation of temperature with altitude at a given geographic location is considered; then the variation of temperature at cruise altitudes is considered as a variation of geographic location. To illustrate the extreme case, polar routes were considered for the exposition of geographic variations.

B. Altitude Temperature Profiles

In the region of interest to an SST, the temperature profile can be closely approximated as decreasing linearly up to an altitude called the tropopause, at which point it becomes constant. This is borne out in Figs. 17-19. In all three figures, the lapse rate (i.e., rate of change of temperature with altitude) is very close to a constant (and the same constant) below the tropopause. Furthermore, only in the equatorial case (Fig. 19) does the temperature vary significantly from a constant above the tropopause.

C. Polar Region Temperature Distributions

Studies by Kochanski,[5] Godson,[6] Lee,[7] Behr et al.,[8] and others have demonstrated that there are great variations in temperature during the winter in the polar regions at altitudes which will probably serve as cruise altitudes for supersonic transport vehicles that might operate over transpolar routes. Large variations in these temperatures occur both within a given season and from one season to another.

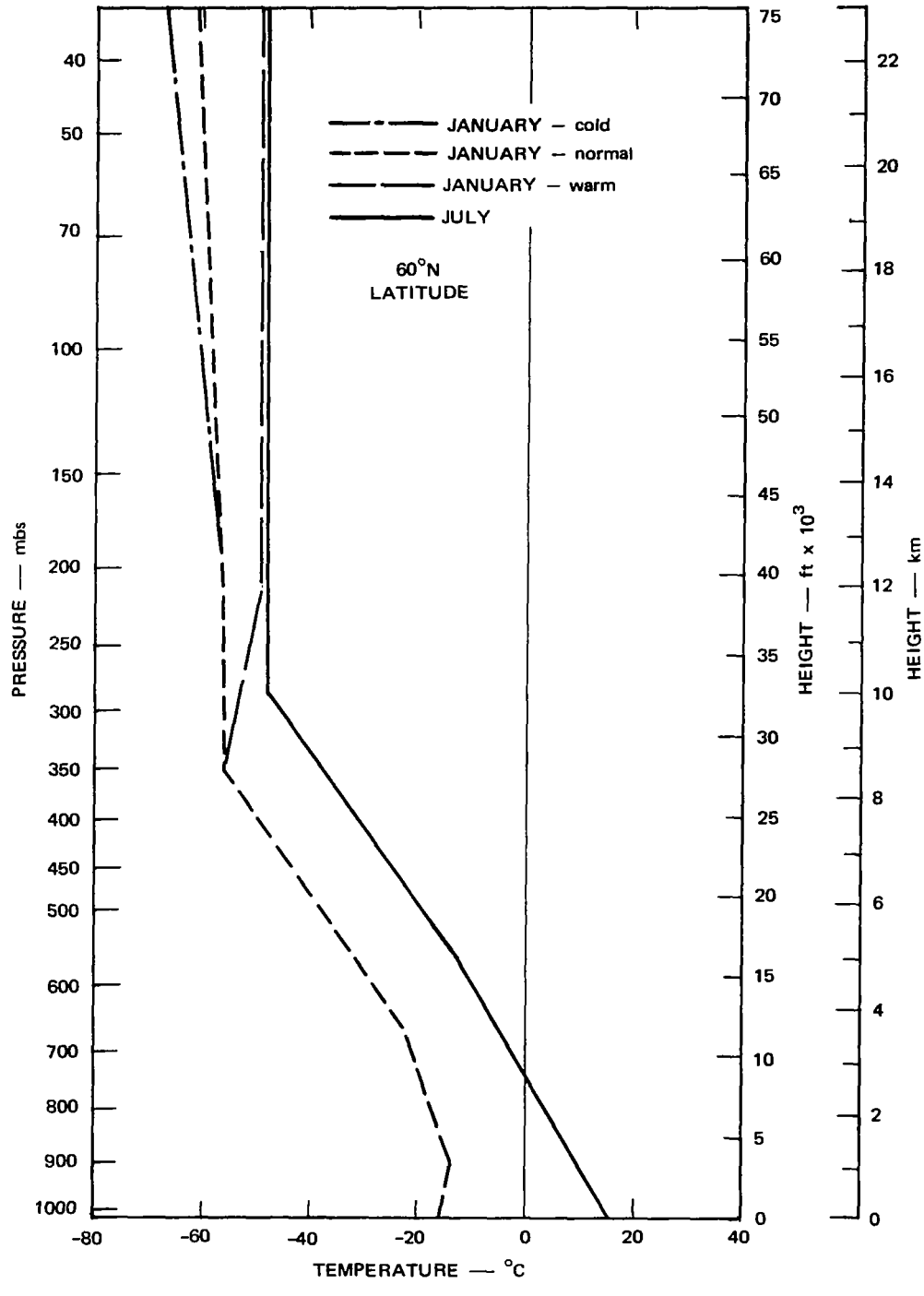

FIGURE 17 STANDARD TEMPERATURE PROFILES, 60° N LATITUDE FOR VARIOUS MONTHS AND CONDITIONS

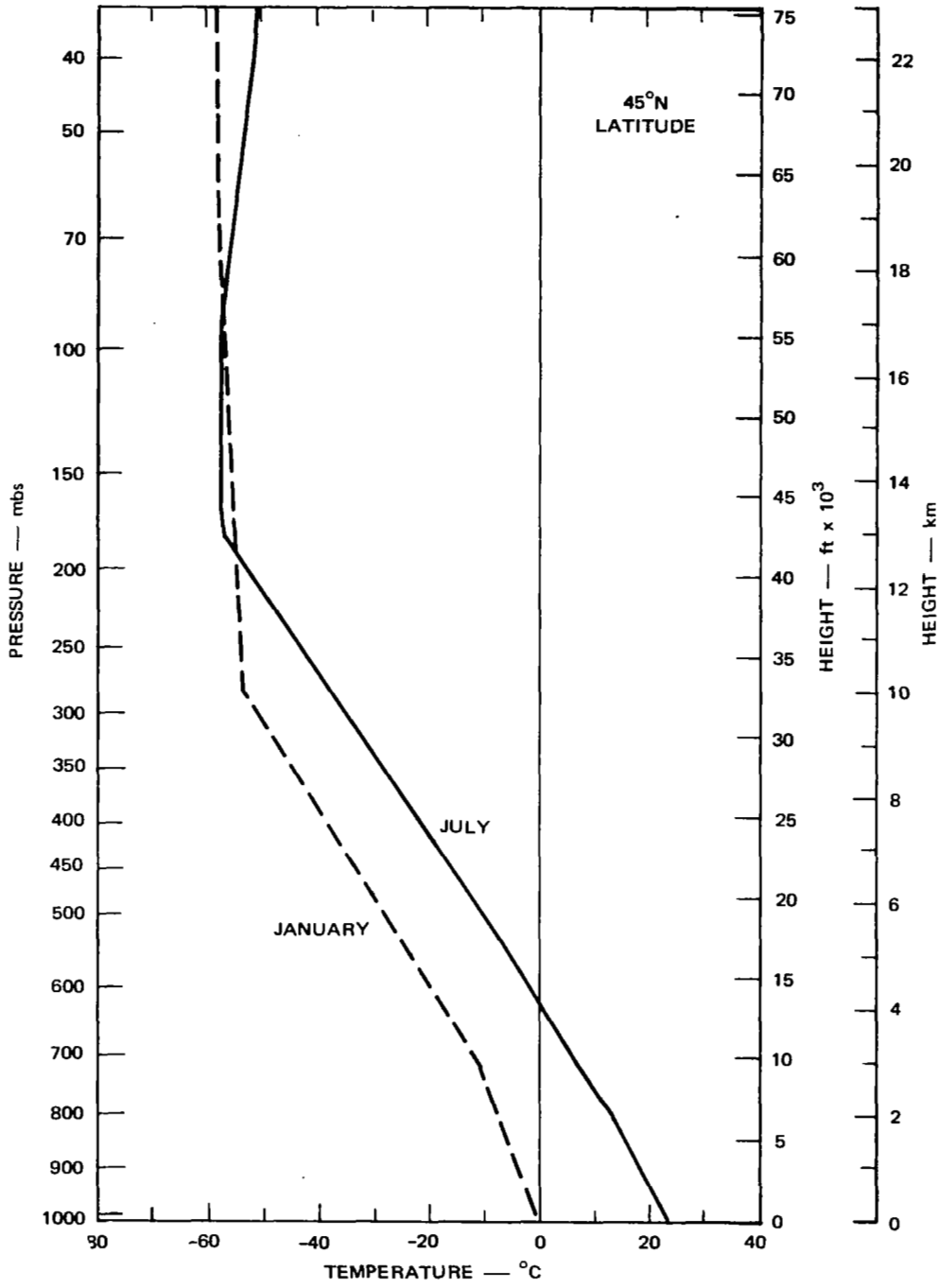

FIGURE 18 STANDARD TEMPERATURE PROFILES, 45° N LATITUDE FOR NORMAL JULY AND JANUARY

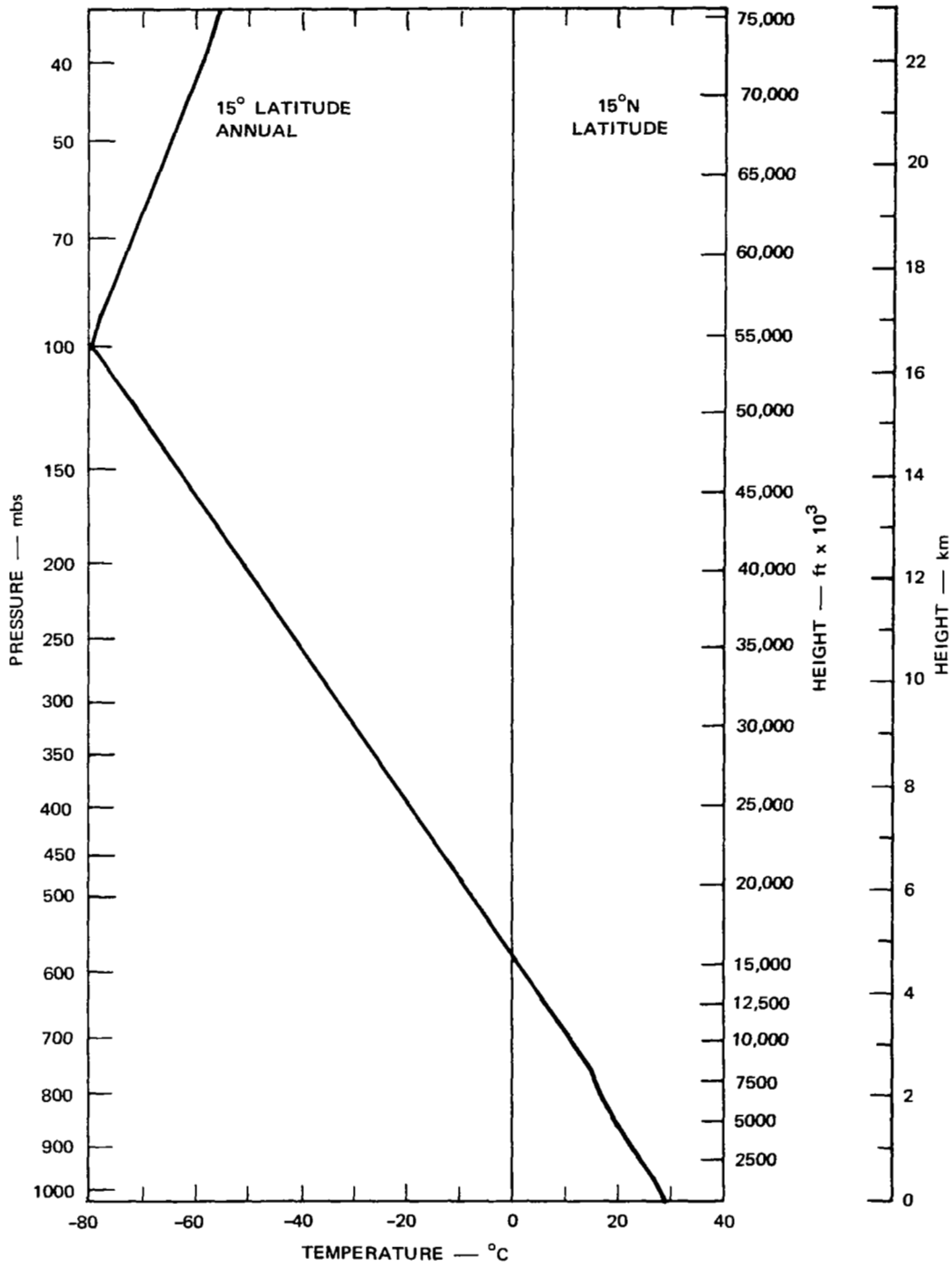

FIGURE 19 STANDARD TEMPERATURE PROFILES, 15° N LATITUDE

In all probability, a number of supersonic transport routes between major population centers of the world will penetrate polar regions in part, if they are not in fact transpolar routes. Therefore, an important and timely consideration is the possible impact of temperature variations in polar regions on supersonic transport operations during the cruise phase.

The following notes are intended first to present examples characterizing temperature distributions and their variations from a series of maps* analyzed by Behr et. al.[8] in the polar regions during winter, and, second, to demonstrate from these maps the ranges of temperatures encountered over two selected polar routes on the days illustrated.

D. Temperature Distributions

The maps characterizing January temperature distributions in the northern hemisphere polar region during seasons of early and late polar warming are presented in Figs. 20 (a)-(e) and 21 (a)-(d). Figures 20 (a)-(e) are for January 1963--this winter season was one in which early (in January--so-called explosive) warming of the polar regions occurred. Figures 21 (a)-(d) are for January 1964--in this winter season the polar warming was gradual and late (in March). These maps serve to illustrate the distribution of temperature and temperature gradients that

---

* These maps are available only for 30 mbs (78,500 feet). However, at lower altitudes (probable altitudes of SST operations), similar differences in temperatures and gradients prevail since the previously discussed atmospheric conditions are reflected in the pressure and temperature field throughout the upper atmosphere in the polar regions of the northern hemisphere. In fact, the mean positions of the level of maximum wind speed (jet stream core) is at about 20 kilometers (67,617 feet), more nearly the probable cruise altitude of the supersonic transport aircraft.

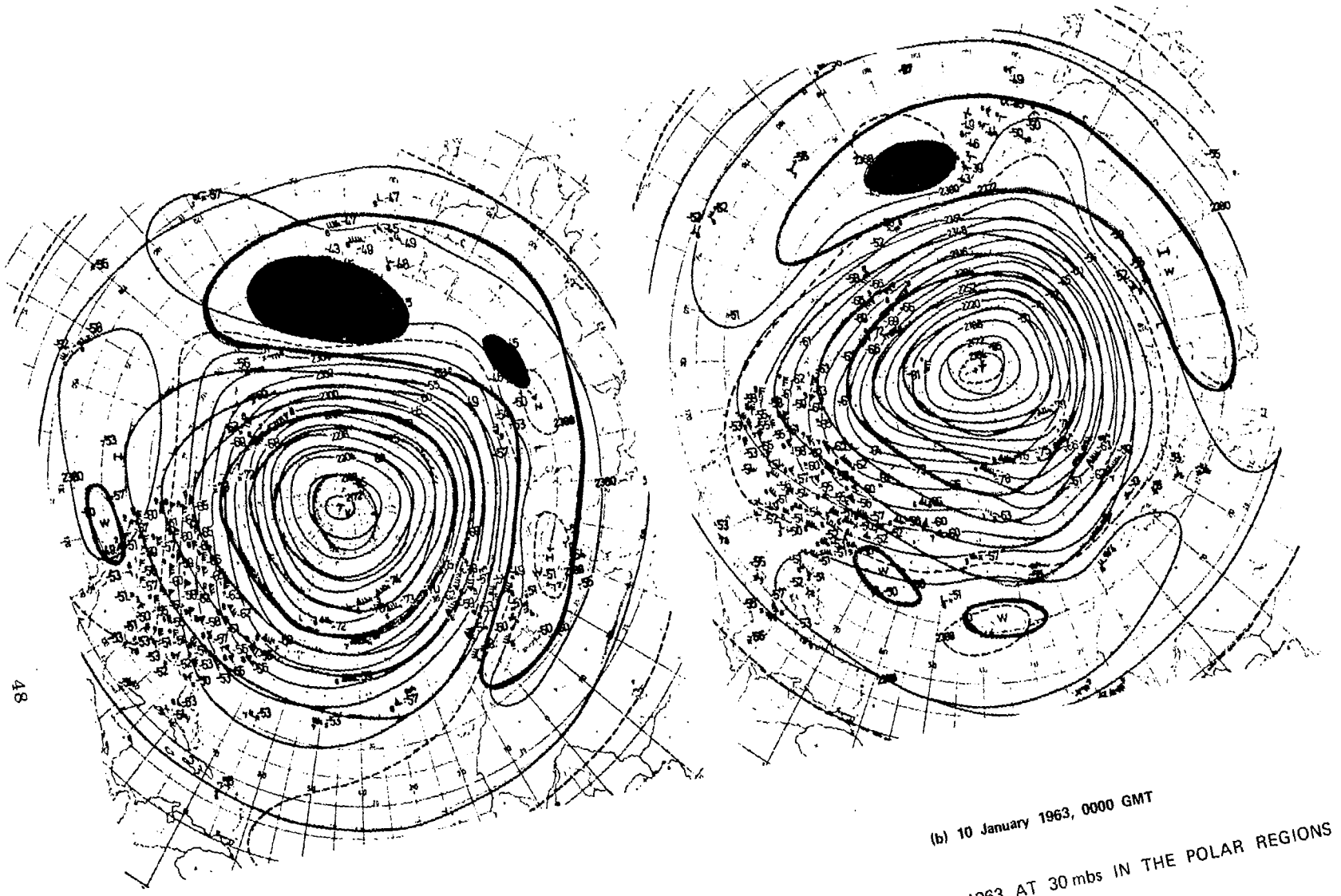

(a) 7 January 1963, 0000 GMT

(b) 10 January 1963, 0000 GMT

SELECTED DAYS DURING JANUARY 1963 AT 30 mbs IN THE POLAR REGIONS

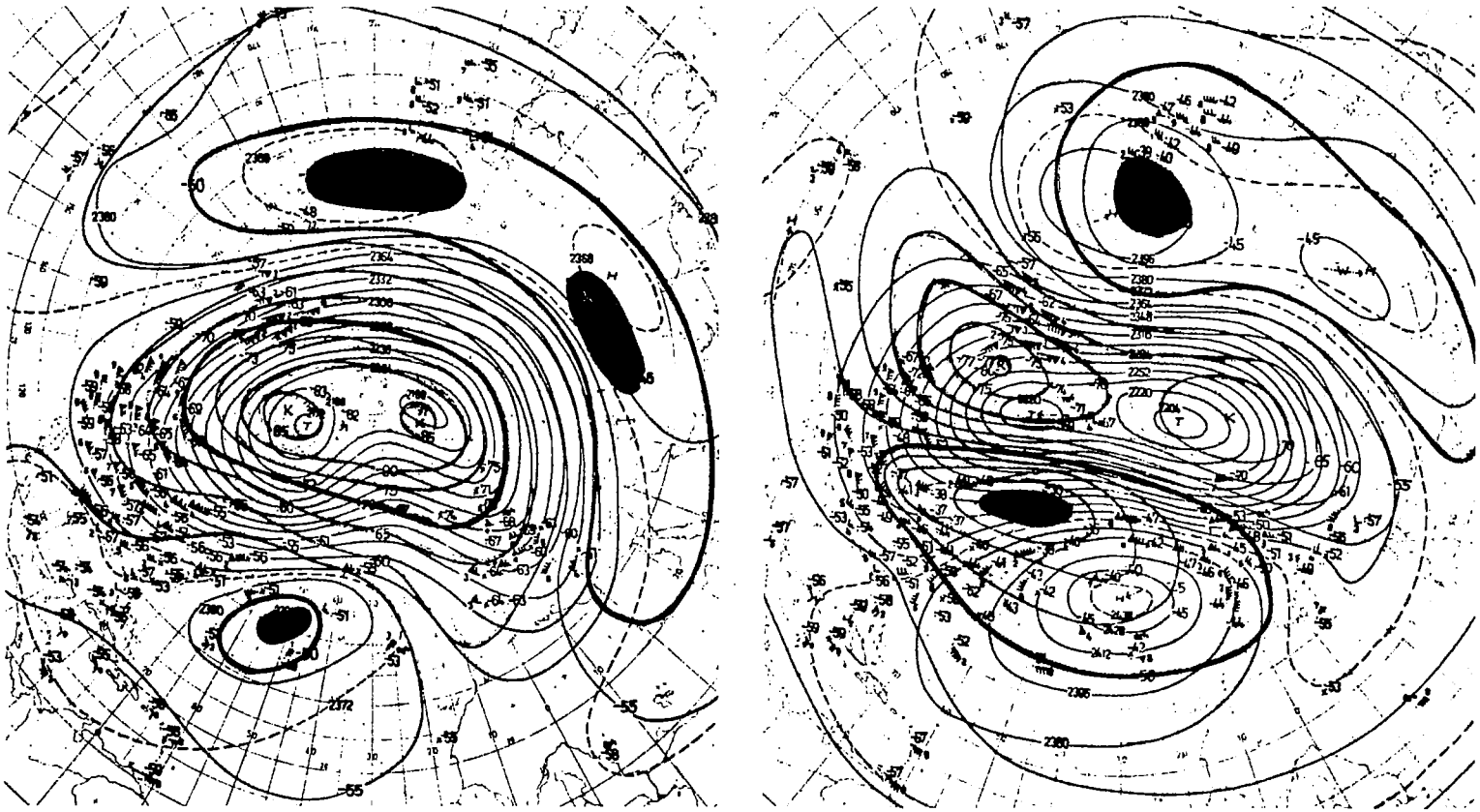

(c) 16 January 1963, 0000 GMT

(d) 23 January 1963, 0000 GMT

FIGURE 20 Continued

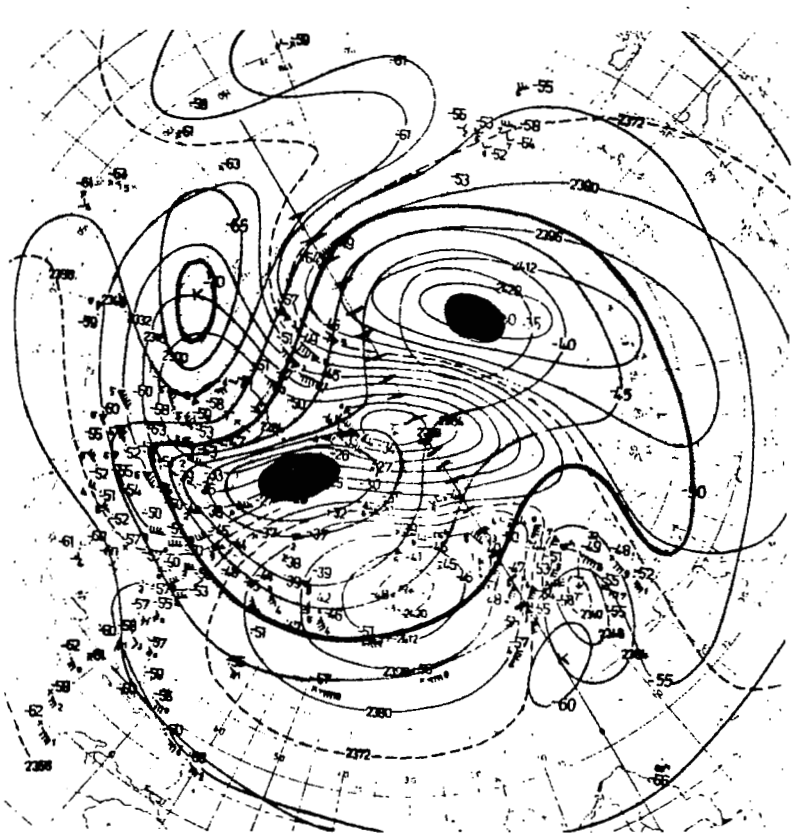

WARM CENTER

COLD CENTER

(e) 29 January 1963, 0000 FMT

FIGURE 20 Concluded

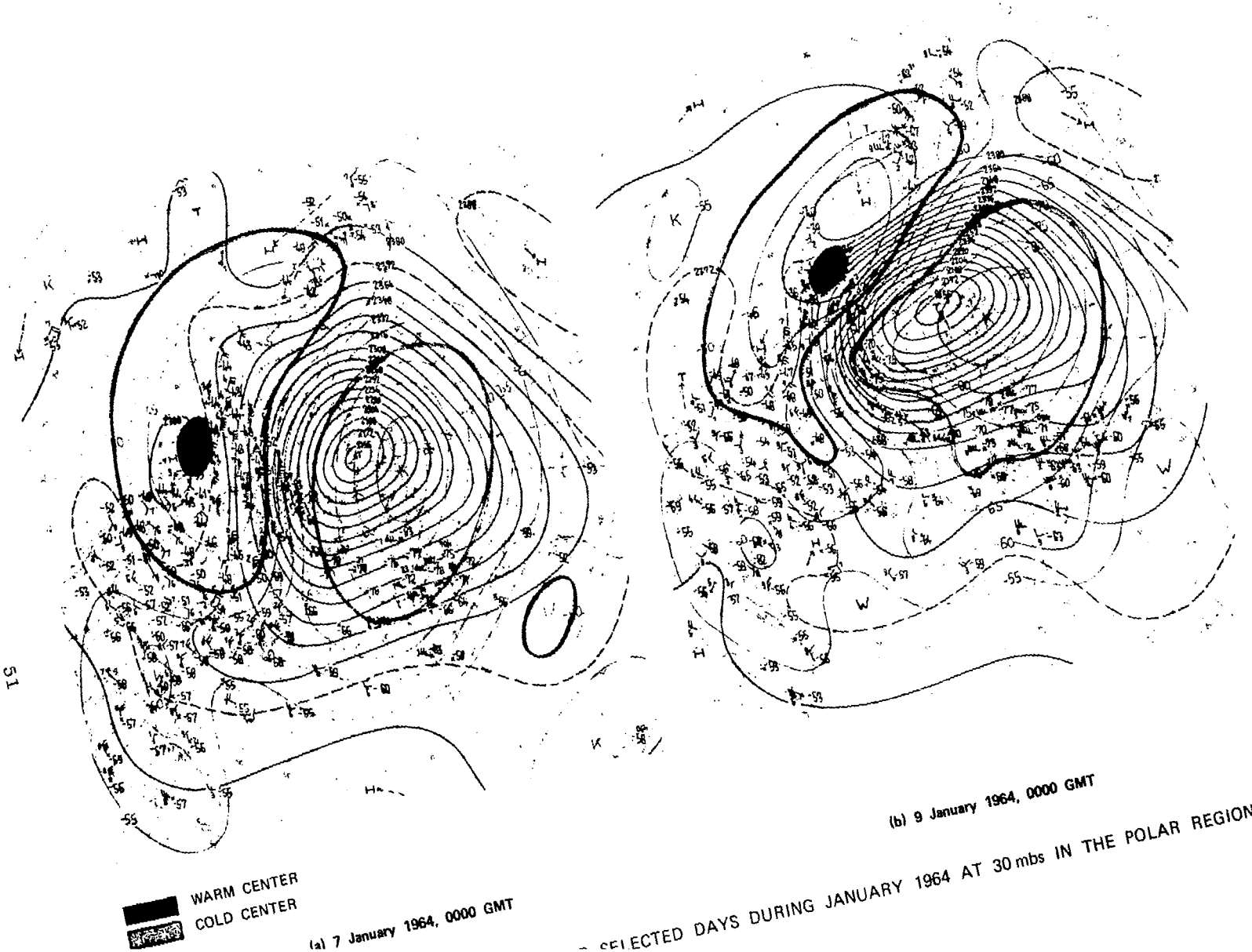

(a) 7 January 1964, 0000 GMT

(b) 9 January 1964, 0000 GMT

SELECTED DAYS DURING JANUARY 1964 AT 30 mbs IN THE POLAR REGIONS

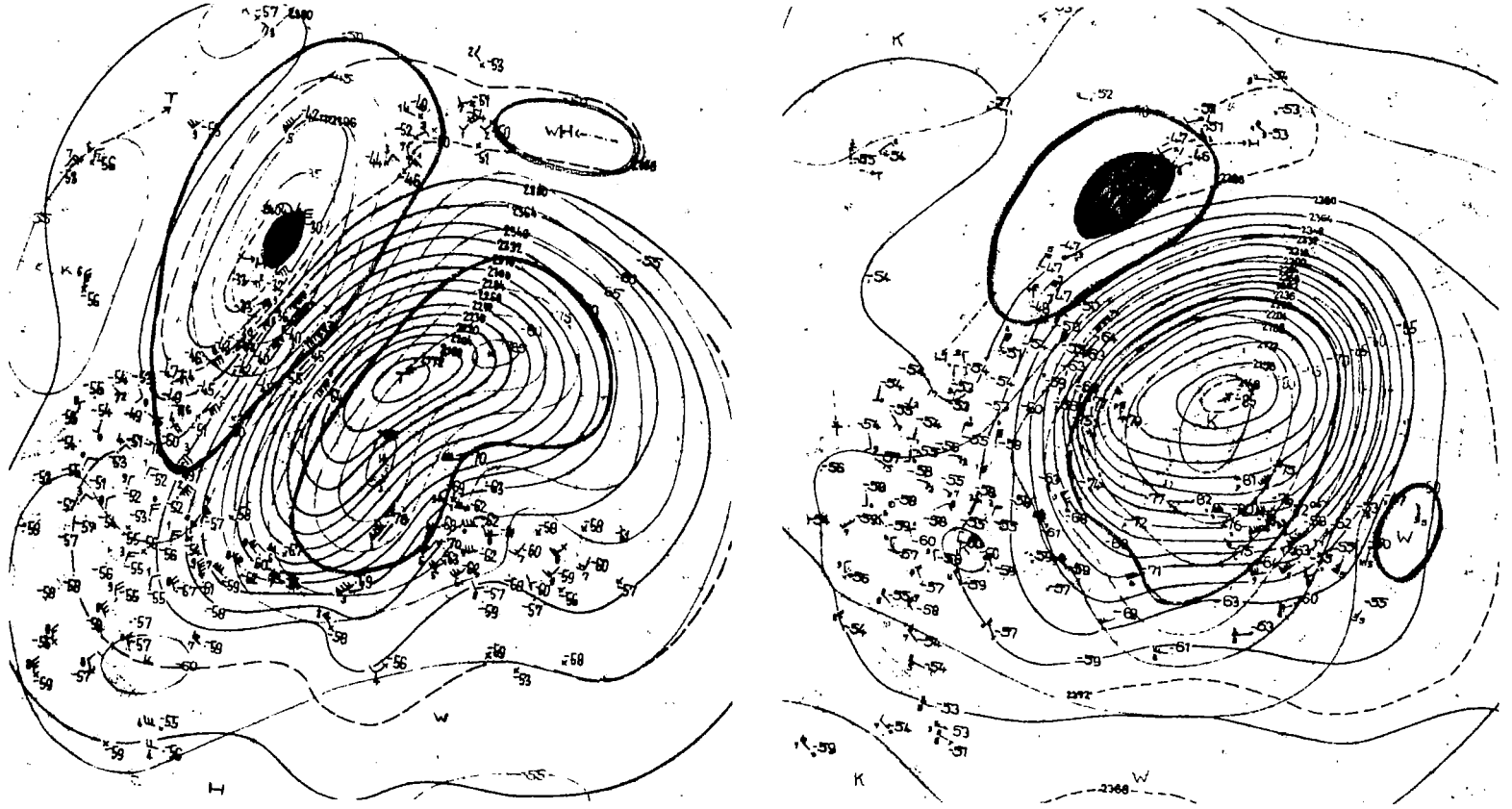

(c) 15 January 1964, 0000 GMT

(d) 29 January 1964, 0000 GMT

FIGURE 21 Concluded

occur and the variations of these distributions during any given winter of from one winter to the next.

During January 1963 [Figs. 20 (a)-(e)] the circumpolar vortex of cold air was predominantly nearly concentric with the pole during the first half of the month [Figs. 20 (a) and (b)]. In the middle of the month the cold core split in two, with one lobe of minimum temperature over northern Russia and the other over southern Canada and extending into the Bering Sea [see Figs. 20 (c) and (d)]. During this period the isothermal patterns became narrow and elongated, and warm air cores became juxtaposed on both sides of the cold air. Thus the maximum temperature gradients in the polar region north of 45° North Latitude occurred on the 19th (not illustrated) and 23rd of January [Fig. 20 (d)]. The absolute maximum gradient of 1°C per 36 km occurred on the 23rd of January. However, vis à vis the two transpolar routes selected, the orientation of the isotherms was such that at these altitudes only a small enroute temperature change would result.

By the 29th of January [Fig. 20 (e)] explosive warming had occurred, and cold air was completely absent from the polar regions. Temperatures in these regions had increased in excess of 40°C, and the gradients were very weak.

During the month of January 1964, the cold core of low temperatures persisted for most of the month [see Figs. 21 (a)-(d)] as a single elongated area of low temperatures eccentric with the polar regions. Throughout the period, the cold core was displaced over Siberia, Northern China, and Japan. Also an extensive region of warm air persisted for the entire month juxtaposed along the Pacific Ocean perimeter of the cold air. Stratospheric warming of the polar regions did not occur until the last few days in March and was gradual and not explosive.

Figure 22 shows the latitudinal distribution (in 5° increments) of temperatures for two days in January 1963 and 1964 over the polar regions of the northern hemisphere along a meridian through the pole.

Note the following:

(1) The wide divergence in temperature distribution between the middle and the end of the month of January 1963

(2) The near coincidence of the distribution on January 16th and 29th, 1964

(3) The near coincidence of the temperature distribution in the mid-month of January 1963 and January 1964

(4) The difference in temperature distributions at the end of January 1963 when compared with the end of January 1964.

The effects of early so-called explosive warming are quite striking. In the extreme polar regions the difference in temperature was 47.5°C

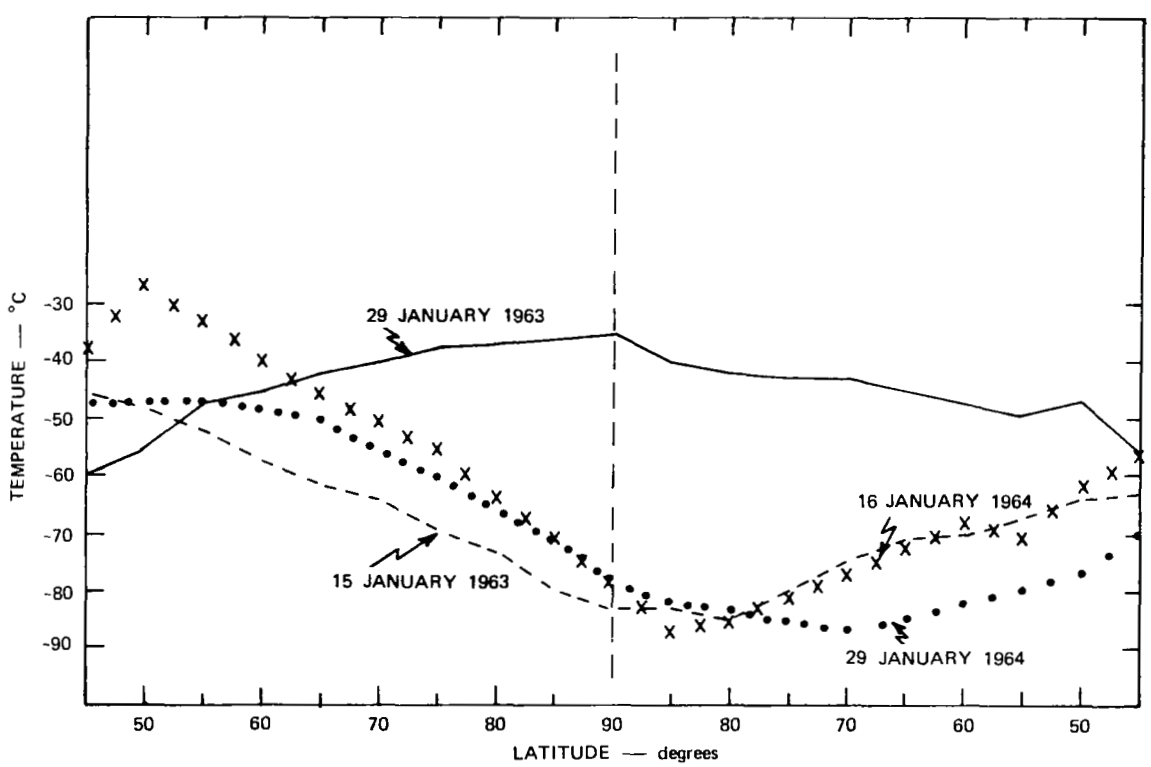

FIGURE 22 COMPARISON OF TEMPERATURE DIFFERENCES AT 30 mbs DURING SELECTED DAYS IN JANUARY, 1963 AND 1964, FOR 5° INCREMENTS NORTH OF LATITUDE 45° N ALONG THE 0°-180° MERIDIAN THROUGH THE NORTH POLE

between that on January 29, 1963, and that on January 29, 1964. It must also be emphasized that after such warming occurs the temperatures in the polar regions at supersonic cruise altitudes remain fairly high and the gradients fairly small.

Moreover, the gradients are reversed, so that from year to year the coldest and warmest temperatures along a crosspolar route will be encountered in reverse order.

Further illustrations of the variation and persistence in temperature and temperature gradients that exist in the polar regions are the mean monthly temperature maps for February 1956 and 1957 [Figs. 23 (a) and (b), respectively].[9] February 1956 showed no effects of early explosive warming, and in fact the minimum temperatures (-103°C) are considerably lower (approximately 18°C) than in January 1964. In February 1957, a year in which explosive warming was also evident, the highest temperatures were equal to those in January 1963.

E. Route Temperatures and Gradients

Two routes were selected connecting cities (Winnipeg, Canada; Fairbanks, Alaska; and Stockholm, Sweden) at high latitudes that might logically serve as the terminals of air routes over which supersonic transports might be operated. Consideration of the temperatures and temperature changes at these terminals and enroute temperature gradients and variations at near probable operating altitudes might serve to indicate the extent of the problems these temperature distributions may pose to supersonic transport operations over crosspolar terminal routes. For each of the days illustrated, temperature distributions and gradients at altitudes proximal to the SST cruise altitude along these two preselected transpolar routes (Winnipeg - Stockholm and Fairbanks - Stockholm) were obtained from the isothermal analysis of the maps illustrated in

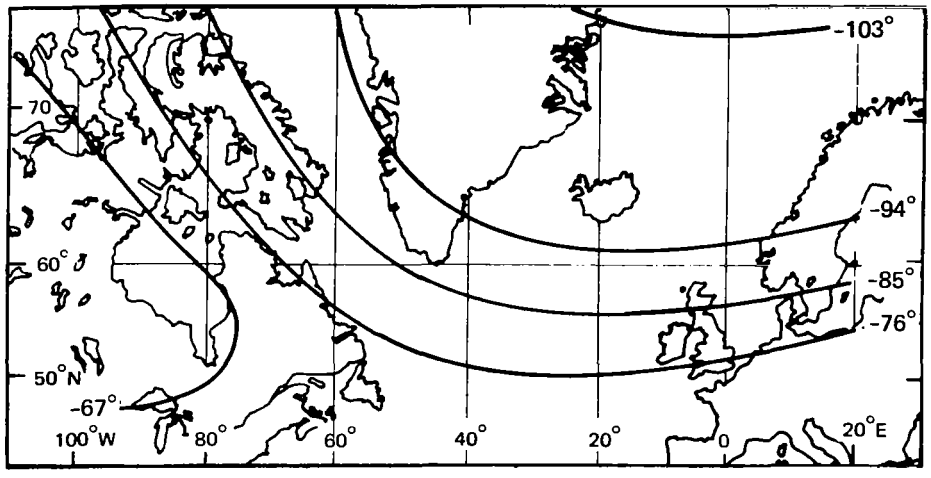

(a) FEBRUARY 1956

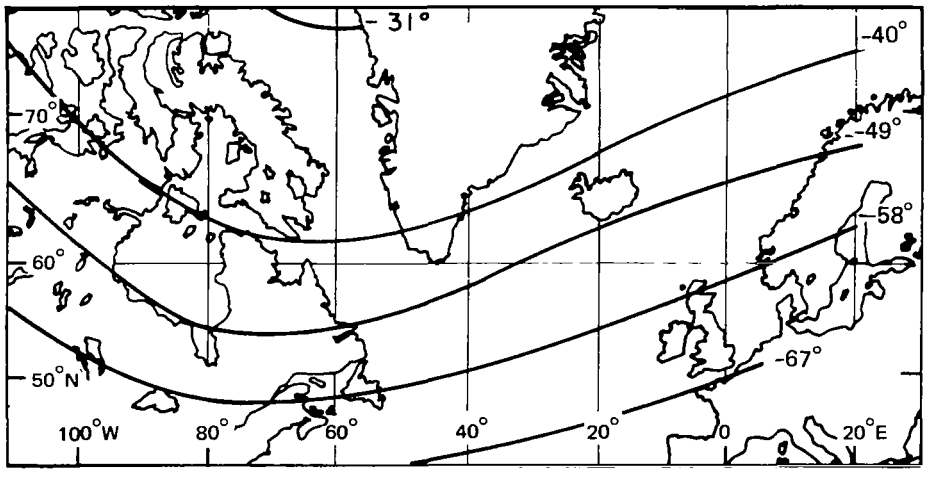

(b) FEBRUARY 1957

SOURCE: Reference 8.

FIGURE 23 HORIZONTAL DISTRIBUTION MEAN MONTHLY TEMPERATURES AT 30 mbs OVER THE NORTH ATLANTIC FOR FEBRUARY 1956 AND 1957.

igs. 20 (a)-(e) and 21 (a)-(d). These distributions as well as the emperatures (at 30 mbs, 78,500 feet) at the terminals of the routes are iven in Table V as follows:

(1) Temperatures at the terminals

(2) Temperature differences between the terminals

(3) Maximum enroute temperature differences

(4) Distance in kilometers per degree centigrade between the -50° C and the -70° C isotherms in the polar regions at 30 mbs

(5) Maximum gradients (km/$^{\circ}$ C) for any combination at 20° C.

The lowest temperatures in the polar regions (line 1) in both years vere equal throughout most of January, with the most obvious differences in our data sample) on 29 January. The warmest temperatures (line 2) vere also fairly close in both years, except in the latter part of the nonth, and along the selected routes the maximum enroute differences (lines 7 and 11) were considerably less in 1963 than in 1964. Very much the same pattern was in evidence over the entire polar regions as reflected in the maximum gradients found anywhere in the polar regions, when expressed as gradients between the -50°C and -70°C isotherms (line 12) or any other combination of 20°C temperature range (line 13). The absence of information on line 13 indicates that the -50°C to -70°C isotherms form the only 20°C isothermal gradient in the latitudes north of 45°.

Enroute maximum temperature differences between Winnipeg and Stockholm (line 7) on 29 January in both years were almost equal (25°C and 26°C, respectively), but they occurred at different ambient temperatures. Along the Fairbanks-Stockholm routes on these days there was both a large difference in the maximum enroute temperature differences (line 11) and the ambient temperatures (line 8 and 9). The orientation of the isothermal field with respect to a given route dictates the gradients that will be

Table V

DISTRIBUTION OF TEMPERATURES AT 30 mbs (78,500 FEET) FOR SELECTED DAYS IN JANUARY 1963 AND 1964 FOR SELECTED ROUTES

Line	45°N to 90°N	Date (January)									
		7	10	16	29	Average	7	9	15	29	Average
1	Coldest Temperature °C	-85	-85	-85	-70	-81.2	-85	-85	-85	-85	-85.0
2	Warmest Temperature °C	-43	-45	-45	-20	-38.2	-40	-35	-30	-45	-37.5
3	Difference °C	42	40	40	50	43.0	45	50	55	40	47.5
4	Winnipeg Temperature	-65	-63	-65	-30	-55.7	-48	-50	-50	-57	-51.2
5	Stockholm Temperature	-66	-68	-72	-50	-64.0	-81	-75	-62	-79	-74.2
6	Difference	1	5	7	20	8.3	33	25	12	22	23.0
7	Maximum Enroute Temp. Diff.	17	16	10	26	16.0	34	27	35	25	29.4
8	Fairbanks Temperature	-73	-71	-75	-48	-66.8	-43	-45	-40	-54	-45.5
9	Stockholm Temperature	-66	-68	-72	-50	-64.0	-81	-75	-62	-79	-74.2
10	Difference	7	3	3	(2)	2.8	38	30	22	25	28.7
11	Maximum Enroute Temp. Diff.	19	14	9	13	16.0	41	36	44	31	37.4
12	Maximum Gradient km/° C -70° to -50°	67	97	100	90	88.5	72	35	60	71	59.5
13	Any other combination (if greater) over a 20° Range	61	85	62	29	59.2		34	56	69	53.0

encountered. The distribution of ambient temperature in the polar regions for a given winter depends on whether or not explosive warming has occurred.

In most instances the enroute gradients (lines 7 and 11) in January 1964 were almost twice those in January 1963.

If such temperature variations are significant factors in cruise fuel consumption in supersonic transport operations, then further studies should be made of the details of temperatures and temperature changes in the polar regions over a number of possible transpolar routes.

III INSTRUMENTATION

A. Introduction

A prerequisite to the development of a mathematical model for control of an SST aircraft is the investigation of existing and planned aircraft instrumentation systems. The purpose of this section is to list the commercial aircraft instrumentation systems currently available. The ranges and accuracies are presented for those systems with known accuracies.

This section considers flight, navigation, engine sensors, and digital computers. Flight instruments used to control an aircraft in planar flight are considered first. The remaining flight instruments are described in the remainder of Sec. C. Navigation systems are discussed in Sec. D, and a description of present-day airborne digital computers is contained in Sec. E. Engine sensors are described in Sec. F. A definition of terms used is given in Sec. B.

B. Definition of Terms

Direct-Sensing Flight Instruments--Direct-sensing flight instruments transduce physical properties of the aircraft environment into signals which can be used to indicate a characteristic of the aircraft motion. Generally, flight instruments measure quantities related to the state of the aircraft, and often they provide a direct measurement of a state variable. The term state is used to describe a set of nonredundant variables that, when perfectly known, may be used to compute the future behavior of the aircraft. The relation between the sensed physical quantity and the output of the instrument is both one to one and as near linear as is practical.

Computed-Output Flight Instruments--Computed-output flight instruments present flight variables that are generally a function of several variables. The outputs usually represent states of the aircraft motion. The relation between the sensed quantity and the instrument output is generally nonlinear.

Gyro-Driven Flight Instruments--Gyro-driven instruments are generally stabilized by gyroscopes. These instruments provide indications of aircraft attitude.

External-Referenced Navigation Instruments--External-referenced navigational instruments depend on external references or position fixes. These references may be radio transmitters, optical devices, stars, satellites, or visual landmarks.

Internal-Referenced Navigation Instruments--Internal-referenced navigation aids require no external sources. The Doppler radar and inertial systems fall into this class.

Direct-Sensing Engine Instruments--Direct-sensing engine instruments have characteristics similar to those of direct-sensing flight instruments. The physical quantities sensed are usually of the static type rather than dynamic. For example, engine pressure is a static quantity whereas the airspeed indicator operates on dynamic pressure.

Computed-Measurement Engine Instruments--Computed quantities may be nonlinear functions of several variables. On-off sensors fit into the computed-measurement category also.

General-Purpose Computers--A general-purpose computer has software programming capability. Several functions may be serviced almost simultaneously. Reprogramming is possible, and memory allocations are not fixed.

Special-Purpose Computers--A special-purpose computer serves only one function. It is usually hardwired; i.e., no reprogramming is available. Computer memory is usually preallocated. The computers associated with the inertial navigators are usually of the special-purpose type.

C. On-Board Jet Transport Flight Instrumentation

1. General

It will be assumed throught this section that the output of all instruments may be converted into a digital signal and stored in the memory of a general-purpose computer. This does not imply that the outputs of all aircraft sensors will be digitally encoded but simply that the capability to convert analog to digital signals is generally available in the aircraft.

The definitions given above apply to the remainder of this report.

2. Flight Instruments

a. General Introduction

A minimum of twelve quantities are required to define the state of an aircraft: Position and velocity vectors of the aircraft center of gravity, and roll, pitch, and yaw, and their respective rates. Flight instruments provide the pilot with indications of the current state of his aircraft.

Flight instruments may also be described as those aircraft instruments required to maintain straight and level flight without external references. Although this definition is overly restrictive, it does represent a certain class of aircraft sensors.

b. Available Instrumentation

The flight instruments generally available in jet transport aircraft are briefly described below. Typical accuracies and ranges are also presented. Instruments are listed in order of decreasing utility for planar flight.

Airspeed--The airspeed indicator presents an indication of the difference between dynamic pressure and static pressure. A dynamic pressure probe is located in the free airstream of the aircraft--generally for jet transport type aircraft on the leading edge of the wing or on the aircraft nose. Range and accuracy are

Range	Accuracy
50 knots to 1000 knots	±2 kts > 200 kts; ±1 kts < 200 kts .

Altimeter--The altitude above a given reference is indicated by the barometric altimeter. The most common reference is sea level; however, for certain operations out of a single airport the altimeter is referenced to airport elevation. The altimeter then reads altitude above surface level (ASL). The basis of the instrument works is an aeronautical barometer; a bourdon tube is usually used. Range and accuracy of altimeters vary considerably. The range and accuracy quoted below are for the high-performance design specifications for the C-5 aircraft:

Range	Accuracy
-1000 to +120,000 feet	±10 ft .

Vertical Speed Indicator--The vertical speed indicator is similar to the altimeter in the sense that it senses a pressure variable. However, rate of change of pressure is sensed by measuring the absolute pressure in a chamber with a small orifice leading to the static pressure

source. An increase in altitude will cause air to flow from the chamber through the orifice to the static pressure source; hence the decrease in pressure in the chamber indicates the rate of climb of the aircraft. High-performance instruments have the following specifications:

Range	Accuracy
0 to ±40,000 ft/min	75 to 500 ft/min .

Pitch Indicator--The pitch angle of the aircraft is measured by the torque required to maintain a gyro in a given orientation. Presentation is generally through the artificial horizon. Range and accuracy are

Range	Accuracy
-15 to +15°	Variable .

Artificial Horizon--The artificial horizon is a consolidation of the pitch and bank angle instruments into a single pilot presentation. A fixed aircraft reference is attached to the instrument case, and pitch and bank angles are indicated by a rotating ball inside the instrument case. The amount of rotation is proportional to the current required torque to reposition the gyros to their referenced positions. Range and accuracies are identical to those indicated above for the pitch and bank angle measurements.

Angle of Attack--The angle of attack is defined as the angle between a reference line on the aircraft and the relative wind vector (also known as the flight-path vector). If the aircraft is not banked, the relation between the pitch angle and the angle of attack is given by

$$\theta_p = \gamma + \alpha \quad , \tag{17}$$

where θ_p represents pitch angle, γ flight-path angle, and α the angle of attack. If the flight-path angle is known, the angle of attack is easily computed, but at present no data exists on how angle of attack could be measured.

Mach--The mach number of the aircraft is related to the atmospheric characteristics through which the aircraft is flying. A mach number of 1.0 is the speed of sound at the particular atmospheric conditions, while Mach numbers less than 1.0 indicate speeds slower than that of sound. The equation for mach number is given by

$$M_n = v/\sqrt{\gamma R} \quad , \tag{18}$$

where M_n denotes mach number, v is true airspeed, γ is the ratio of specific heat for the atmosphere, R is the universal gas constant, and θ is absolute outside air temperature. Equation (18) may be approximated by the relation

$$M_n = K_m v/\sqrt{\theta} \quad , \tag{19}$$

where $K_m = 1/\sqrt{\gamma R}$. The mach meter simply uses the true airspeed signal and the outside air temperature to compute Mach number. The range and accuracy of this instrument vary depending on the application. The range and accuracy indicated below represent commercially available specifications:

Range	Accuracy
0.4 to 3.5 m	0.005 m .

Radio Altimeter--The radio altimeter, which presents altitude above surface level, is used for making precision landings. It uses timed radar pulses to determine range from the aircraft to surface level.

Since it is used primarily for instrument landings, its range is limited; however, it provides very accurate indications of altitude. Approximate range and accuracy are

Range	Accuracy
0-2500 ft	±0.5 ft

Turn Indicator--The turn indicator is a gyro-driven instrument that senses rate of turn or yaw rate in degrees per second or turns per minute. The basis of the instrument is the precession of a gyroscope. The instrument is calibrated in terms of standard rate turns (3°/s, 360° in 2 min) for light aircraft and ($1\text{-}1/2^\circ$/s, 360° turn in 4 min) for transport aircraft. The range and accuracy are

Range	Accuracy
3 standard rate of turn right or left	±0.25 turn

Slip Indicator--The slip indicator consists of a glass or metal ball in a curved glass tube, usually mounted on the face of the turn indicator. This instrument indicates the quality of the turn, and thus, enables the pilot to make coordinated turns. It senses the unbalance of centrifugal force caused by the turn and the inward force component of the lift vector. The slip indicator is usually not calibrated, but the ball width is often used as a reference. For example a turn one ball width from center is considered a poorly coordinated turn. Range and accuracy requirements are unspecified.

Bank Indicator--The bank angle of the aircraft is measured by a gyro located in the artificial horizon instrument case. Voltage and

torque commands required to maintain a given gyro orientation are used to measure bank angles. Range and accuracy are

Range	Accuracy
60° right and left	Variable .

Accelerometer--A simple linear accelerometer (a sliding mass and spring) is used to determine the forces acting on the aircraft during sudden or violent maneuvers. It is also used to indicate the degree of psychological stress on the passengers. Range and accuracy are

Range	Accuracy
-4.0 to +10.0 g	$\pm$0.05 g .

3. Flight Systems

A flight system is defined as any device or series of devices which transform elementary aircraft signals into forms more useful for the effective control of the aircraft. This definition includes all aircraft instruments processing at least two aircraft signals into two or more pilot displays. Note that the definition eliminates the artificial horizon from the class since no external measurements are processed.

The flight systems discussed below generally include a special-purpose digital computer which performs the data-processing functions required. The air data computer, flight director, and autopilot are discussed in the sections that follow.

a. Air Data Computer

The air data computer (10, 11), generally found on all large jet transport aircraft, acts as a buffer device between the sensor and

the pilot display. Its basic use is to provide a common storage location for general air data required of the different subsystems. With the air data computer, flight variables from several sources can be compared and logical tests established to verify received signals.

Outputs from the air data computer may include airspeed, mach numbers, vertical speed, outside air temperature, and other basic flight variables. One important function of the air data computer is to provide outputs to the relatively new vertical-scale instrumentation systems developed to provide a consolidated presentation to the pilot. The display provides a common horizontal reference line, defined by an extension of the wing tips of the flight-director's fixed airplane symbol, against which performance and command data are read. The direction of tape motion to display increasing and decreasing values of aircraft speed and altitude, for example, is related to stick and throttle movements to facilitate pilot recognition. The value of each display parameter, read against the horizontal reference, presents actual performance. Command markers are read against their respective tapes to provide a quantitative display of the difference between command and actual value and the direction to move to annul the error.

In general the air data computer may be considered as an analog-to-digital converter and storage device for signals related to the basic flight control of the aircraft.

b. Flight Director Systems

The basic flight director is simply an artificial horizon with command bars. These commands when satisfied put the aircraft in the desired attitude. In more sophisticated flight directors, altitude, airspeed, glide-slope and localizer deviations, initial flare, are all indicated by the flight director.

Electromechanical Flight Director Systems--The flight director is used extensively throughout the landing and cruise portions of subsonic flights. For supersonic flights, the flight director will also be used in the takeoff and descent portions of the flight. The attention of the pilot is directed almost completely to the flight director during an instrument landing. Not only does he pay little attention to other cockpit instruments, but also he does not use the information available on the periphery of the flight director. Current flight-director design pilosophy has been to develop retractable peripheral displays on the flight director; for example, during the final landing phase of an ILS approach the radar altitude, pitch and roll command, localizer and glide-slope deviations, speed commands, and crab angle roll-out indication are given from view. This immediately indicates a trend toward an electronic multifunction, attitude-director indicator display. A detailed description of a basic electromechanical flight director is given in Appendix B.

Electronic Attitude Director Indicator (EADI)--The Boeing[12] SST would include some type of electronic attitude-director indicator, which would present its flight information electronically on a cathode-ray tube.[13] The major advantage of an EADI is expected to be its flexibility. For example, during high-speed cruise the pitch sensitivity could be increased on an expanded scale. Furthermore, different types of flight information might be presented during the different portions of the SST flight. The EADI would probably include flight-path angle rather than pitch angle--a significant improvement since flight path is not solely dependent on pitch angle. Flight-path presentation should significantly improve the pilot's ability to maintain the aircraft on a fixed trajectory in space, an especially important improvement during instrument landings on an ILS system. Greater precision during climb and descent could also be maintained with flight-path angle presentation. From an economic point

of view, the climb portion of an SST trajectory may be the most costly phase of the flight, and precise control of the climb trajectory will be required.

Auto Pilot--An aircraft autopilot automatically performs the exacting tasks of precisely controlling the attitude and trajectory of the aircraft while the pilot retains complete control of the aircraft through the auto pilot command channels and the manual override capability.

A full three-axis auto pilot provides three basic modes of operation: (1) heading hold, (2) altitude hold, (3) and pitch attitude hold. The auto pilot may be extended to include a guidance coupler with ties to Doppler radar, VOR, and ILS systems. With the Doppler tie-in, navigation is completely automatic and independent of ground-based radio equipment, allowing direct control of ground track. VOR coupling provides automatic cross-country navigation, and ILS coupling provides automatic approach and landing.

The basic operational capabilities of an auto pilot system are as follows:

System Engagement

Attitude: roll--normal 0° capability
±30°
pitch--normal 0°, capability
± 10°

Manual Mode

Turn Knob--±30° of roll attitude change.
Pitch Wheel--±17° of pitch attitude change.
Turns--unlimited.

Altitude Hold

Engagement--at less than 2000 feet per minute of climb or dive, and a pitch attitude of less than 10°.

Preselect Heading

Engagement--with unlimited heading commands.
Heading Changes--unlimited changes in either direction.

VOR

Engagement--(normal) at intercept angles of less than 5° and a beam displacement of 15 μA (two-dot deflection) or greater. Engagement--(capability) all angles dependent upon aircraft position relative to beam, distance to station, aircraft speed, wind direction, and wind velocity. Crosswind--(capability) corrections for 25° of heading.

Localizer

Engagement--(normal) at capture angles of less than 90° and a beam displacement of 150 μA (two-dot deflection) or greater. Engagement--(capability) all angles dependent upon aircraft position relative to beam, distance to runway, aircraft speed, wind direction, and wind velocity. Crosswind--(capability) corretions for 25° of heading.

Glide Slope

Engagement--(normal) at intercept angles of less than 5° and a beam displacement of 15 μA (approximately one needle width) or less.
Engagement--(capability) dependent on beam geometry, aircraft position, and maneuverability.
Attitude Correction--(capability) 10° of pitch attitude.

D. Jet Transport Navigation Instruments

1. General Navigation Procedures

In the early days of cross-country flying, navigation was accomplished by pilotage; i.e. dead-reckoning. The basic approach was to estimate aircraft heading required to maintain a desired ground track. The inherent disadvantage in this approach is the uncertainty in the measurement and

prediction of the winds aloft. Although precise measurement of wind velocities are available at 6-hour intervals, winds often change rapidly both in direction and speed. Any change in altitude will also require a new computation of drift correction angle. With developments in the reliability of airborne radio receivers, cross-country navigation was simplified. Early low-frequency radio enabled pilots to fly to and from radio range stations on 3° airways. These ranges are rapidly being replaced by the more versatile VOR. Range information (DME) can also be obtained from ground-based radio transmitters.

Recent advances in electronic reliability and availability have led to the development of precise long-range navigation capability by inertial methods; i.e., no ground-based reference signals are required. In the near future, these inertial systems will become precise enough to permit instrument landings without ground-based radio aids. Further developments in long-range navigation include astro- and satellite-source methods.

2. Internal Navigation Systems

a. Doppler Systems

For long-range navigation, the Bendix DRA-12[14] Doppler radar with its associated computer is the most important noninertial navigation aid. The system uses the frequency shift of radar echoes to determine ground speed and drift, which is transferred by the computer into distance to the next check point and distance off track. This data may be fed into the auto pilot to automatically correct heading for zero drift.

This instrument is independent of external navigational aids; however, position fixes from external sources must be used at 30-minute intervals to compensate for the Doppler errors.

Doppler radar equipment has been standard with most airlines for several years. Current accuracy is approximately 1 to 2 percent of

the distance traveled and depends to a large extent on the accuracy of the reference data (gyro or magnetic compass).

b. Inertial Systems

Inertial navigation systems measure acceleration in all three axes and perform a double integration to obtain position. Inertial systems were originally developed for military applications, but have recently become available for commercial use. The accuracy of the commercial equipment is 1 to 2 nmi per hour. The system is easy to operate, since only departure position must be manually inserted.

A special-purpose digital computer is used in conjunction with the inertial measuring unit. A simplified block diagram for an inertial navigation system is shown in Fig. 24.

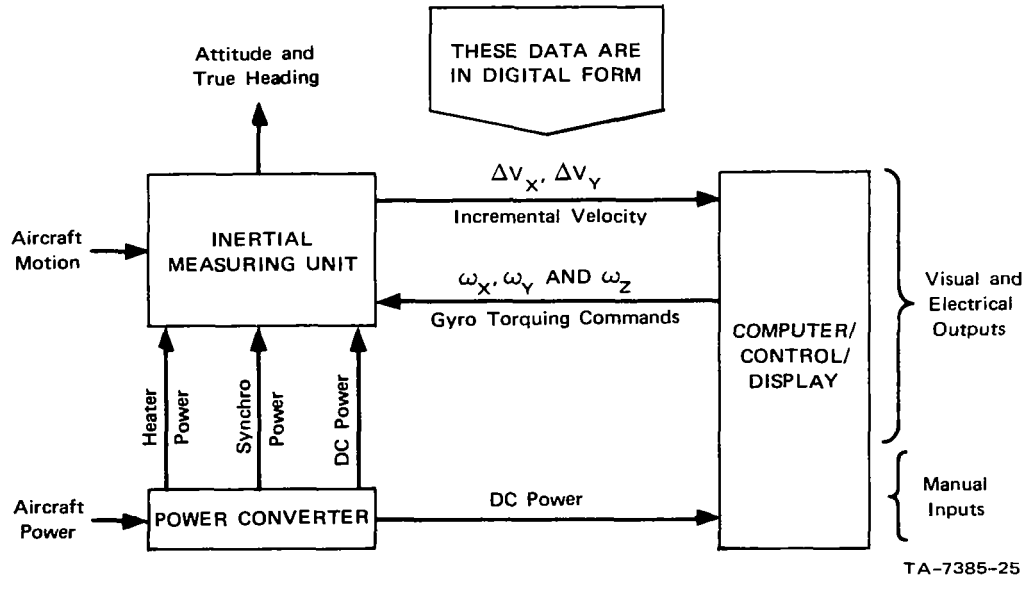

FIGURE 24 SIMPLIFIED BLOCK DIAGRAM FOR AN INERTIAL NAVIGATION SYSTEM

A complete list of the outputs from the Boeing Inertial Navigation System[15] is shown in Fig. 25. Included in this figure is a list of the tests to be evaluated using the outputs of the inertial platform.

The important variables for aircraft control and navigation are

(1) Pitch,

(2) Roll,

(3) Yaw,

(4) Flight-path vector,

(5) Position vector,

(6) Velocity vector.

Computers associated with the inertial measurement unit are generally wholly dedicated to the inertial navigation system and cannot be programmed. In the case of the C5-A[16] inertial navigation system, however, a general-purpose computer was used.

The characteristics of the C5-A inertial navigation computer are these:

General purpose

Parallel operation

28-bit word length
Core memory 12K for primary
8K for auxiliary

Memory Type

Random-access core
Nonvolatile DRO

Instructions

51, with two instructions per word and
half-word arithmetic capabilities

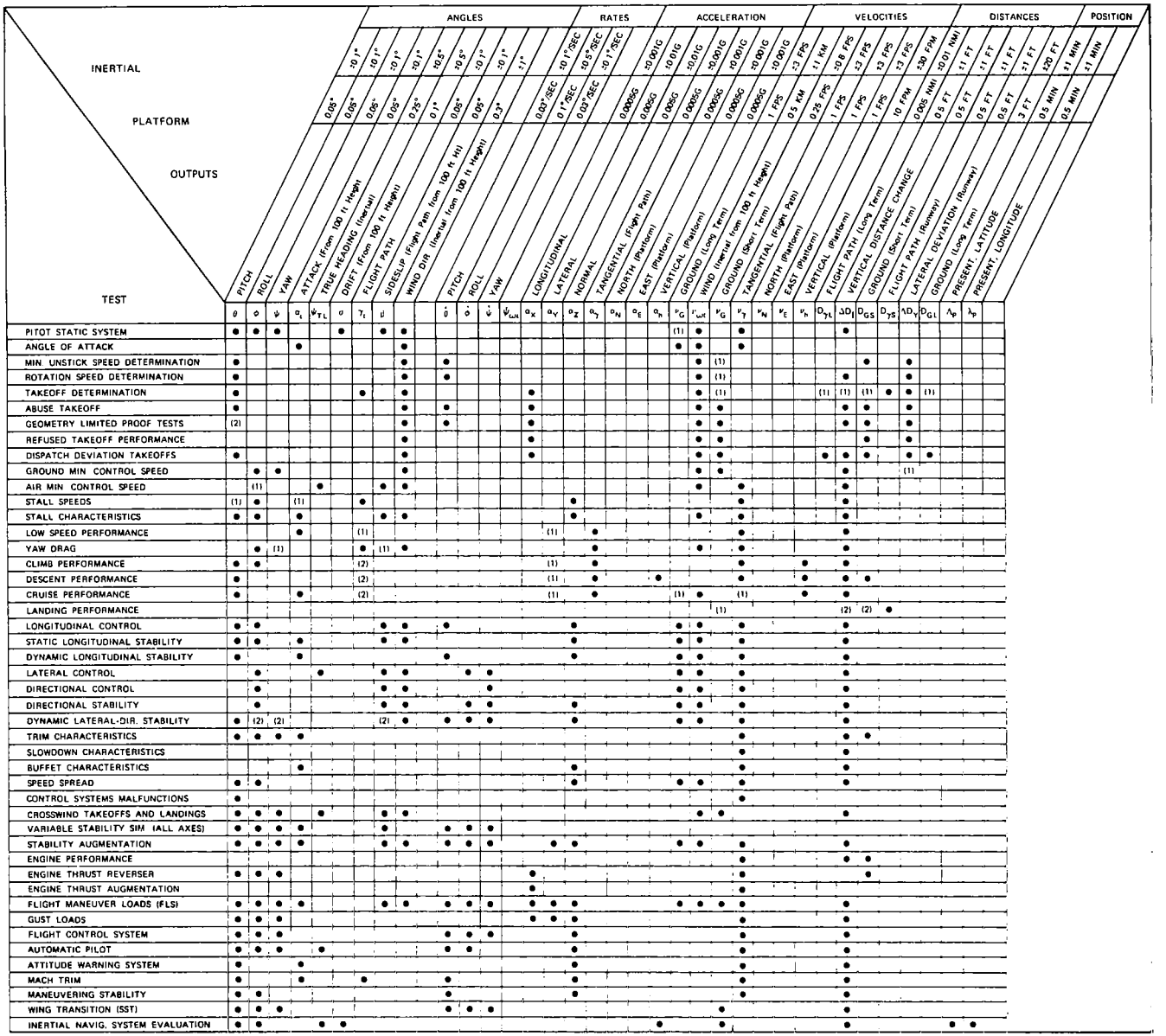

FIGURE 25 INERTIAL PLATFORM OUTPUTS VERSUS TEST TYPES, COURTESY OF THE BOEING COMPANY

Add time

Half word--6 μs
Full word--8 μs

Multiply time

Half word--28 μs
Full word--74 μs

Other features

Indexing
Indirect addressing
Roll table
Interrupt capability.

3. Basic Navigational Instrumentation

a. Magnetic Compass

The magnetic compass is used as a standby source of directional information in all aircraft. The basic instrument consists of float assembly on which are mounted two parallel magnetized needles, a compass card, and a float which is mounted on a pedestal; these are sealed in a chamber filled with acid-free white kerosene.

Several factors affect the accuracy of the magnetic compass in indicating true north. The most important factor affecting accuracy is the variation between magnetic north and true north, which is a function of the location on the earth's surface; for the U.S. alone, the variation is between 20° West and 20° East of true north. Other factors affecting the accuracy of the magnetic compass are magnetic dip, northerly turning error, acceleration error, oscillation error, and deviation. These errors relegate the magnetic compass to a role as a back-up instrument for navigation. Range and accuracy are

Range	Accuracy
0-360°	variable (±5° at best).

b. Directional Gyro

The directional gyro which entirely eliminates compass errors, is a significant improvement over the magnetic compass. This instrument is dependent on motionlessness in space of a universally mounted gyroscope; frictional forces on the gyro cause precession, which results in heading drift. The directional gyro must be referenced with a magnetic compass or some known magnetic reference point. The remote compass detects and transmits the magnetic heading information using an electronic amplifier to the directional gyro, which in turn controls the pointer on the instrument dial.

The remote compass transmitter is usually located in a wing where it is free from magnetic disturbances. The instrument is then slaved to magnetic north, and magnetic deviations and turn errors are negligible. Range and accuracy are

Range	Accuracy
0-360°	±2° magnetic .

c. Airspeed Indicator

True airspeed is used to compute ground speed, which is used to estimate time of arrival at a specific location. The functions of the airspeed indicator were discussed above in Sec. C-2-b.

d. Outside Air Temperature Indicator

Outside air temperature is used along with altitude to compute true airspeed. A description of the outside air temperature device may be found in Appendix C.

e. Altimeter

The altitude is also required to compute true airspeed. A discussion of the altimeter may be found in Sec. C-2-b.

4. External-Reference Navigation Instruments

The following paragraphs briefly describe the operation of ground-based radio navigation equipment.

a. L/MF Radio Range

In years past, the radio range was the only ground-based radio navigation system available. This system has largely been replaced by the VOR system; however, at times this method of navigation may be the only available operational facility.

Radio ranges transmit two signals in code. These signals overlap to form four distinct courses which are approximately 3° in width. The on-course signal is a solid aural tone.

Radio ranges are susceptible to irregularities in the terrain and atmospheric disturbances. Often multiple course beams, bent beams, and false cones are formed in irregular terrain.

L/MF radio ranges are gradually being phased out. These ranges, although not used extensively for navigation, are often used for transmitting scatter information to pilots.

b. MDF/ADF (Automatic Direction Finding)

The MDF/ADF navigational instruments receive signals from ground-based radio transmitters. Radio beacons (nondirectional L/MF transmitters), commercial broadcast stations, and compass locators may be received by the MDF/ADF receiver.

A directional or loop antenna provides information that is used to null the signals from the transmitter. The position of the loop antenna drives a pointer to the broadcast station. In the manual mode the antenna is manually slewed to the null position; however, in this mode a 180° ambiguity exists. In the automatic mode the needle always points directly to the station.

The MDF/ADF is used only as a back-up instrument in modern jet transports. It is also used to receive weather broadcasts from the L/MF facilities.

c. VOR (Variable Omnirange)

The VOR is the principal radio facility for navigation over land. The VOR operates in the frequency range 108 to 118 megahertz. The ground-based equipment transmits two signals: the reference, which is omnidirectional; and the measuring signals, which rotate through 360° at a rate of 30 revolutions per second. Phase difference between the two signals is measured by the receiver and used to determine relative position of the aircraft to the station.

The standard VOR receiver has a flight-path deviation indicator (FPDI) of ±10° from the course radial selected. A full deflection of the FPDI indicates that the aircraft is 10° to the right or left of the desired course. Some very high-quality VOR receivers have FPDI's of ±7.5°.

The VOR receivers must indicate magnetic courses to an accuracy of at least ±4° for instrument flight and are usually calibrated to within ±1°.

VOR stations are located throughout the U.S. and in many foreign countries. The FAA has based the Federal Airways System principally on the VOR navigation system.

d. TACAN

The Tactical Air Navigation system provides both azimuth and distance information. TACAN operates on the UHF band and is used primarily by military aircraft. The distance measuring (DME) capability of TACAN is used extensively by jet transport aircraft and other commercial aircraft. The TACAN and VOR facilities are often combined to form a VORTAC facility. In this case, for each VOR frequency a corresponding UHF channel is specified. This is known as frequency pairing. Current VORTAC equipment uses UHF channels for DME capability and VHF frequencies for azimuth information. Generally the UHF channel is not indicated on the receiver but is automatically tuned to the paired channel.

e. Loran

One of the most important long-range navigational aids is Loran. This type of navigation was introduced in 1942, and over eighty stations are now in operation. Normal operating frequencies are between 1.75 and 1.95 MHz in the low-frequency radio band. Range by day is approximately 550 nmi with maximum ranges of up to 1300 nmi at night with a sky wave.

A Loran fix is complex and time consuming. Signals from a master and slave station are superimposed on the screen of a cathode-ray tube, and the equipment then measures the distance from the stations in the form of a time difference in milliseconds. The Loran system is known as a pulsed hyperbolic navigation system. Time differences between pulses from remote stations define differences in distance from each pair of transmitters to the navigator. These distances define hyperbolae whose focii are pairs of transmitters and whose intersection with each other is the position fix. Hyperbolae, one set for each station, marked with corresponding time difference, are then used to plot lines of position. For an accurate fix a minimum of two position lines are required. Since

the lines cannot be determined simultaneously, navigators must transfer position lines along a track to the last position line.

Accuracy of Loran is dependent on distance from the transmitting stations and propagation conditions. Accuracies of up to ±1.5 nmi by day, and ±4.5 nmi by night are available.

An improved version of Loran was introduced in 1959. In this system, time and phase angle differences from two stations are used to determine position. There are now about 30 of these new or Loran C transmitting stations. Loran C systems use a frequency of about 100 kHz and have ranges up to 1600 nmi with an accuracy of ±550 yds.

f. Consol

The Consol system has been in operation since 1942. There are five stations in western Europe and two in the U.S.A. (Consolan in the U.S.). Operating frequencies are around 190 kHz for European stations and 300 kHz for U.S. stations. The Consol system operates on the principle of transmitting a rotating pattern of 20 useful lobes of 10° width. A bearing fix is obtained by counting the number of dots and dashes to the null line.

Maximum range by night is 1300 nmi.

g. Decca

The Decca system is similar to the Loran navigation system, except that phase differences are measured. The system operates in the low-frequency band around 70 kHz. The system uses an airborne computer for coordinate conversion. Continued presentation of position is available with this type of navigational system.

h. Omega

The Omega system is a hyperbolic system with phase difference measurement. This system operates in the very low frequency band, 10-30 kHz. Maximum range is 5000 nmi with an accuracy of ±110 yds by day and 2200 yds by night.

i. Astro-Navigation

Astro-navigation is based on knowing the substellar point of a particular star (i.e. the point on the earth's surface through which a line joining this star and the center of the earth would pass). To all observers on a circle centered on the substellar point, this star has the same altitude above the horizon although for each it has a different bearing or azimuth. Since the substellar point is normally outside the area covered by the chart, it is not possible to draw the circle of position. To overcome this the navigator chooses a position (assumed position) near the desired position. The navigator now consults an air almanac and the air navigation tables and extracts the altitude and azimuth of the star or other celestial body for this assumed position. By comparing the altitude measured by the sextant with the altitude from the tables, he calculates the intercept (difference in altitude converted to nautical miles) and plots this on the chart as a line of position at right angles to the azimuth. The intersection of three position lines obtained in this manner is the position of the aircraft at the time of the last observation, with the other two lines having been moved along the track to compensate for the difference of time of the observations. Swissair has modified all its sextants so that the observation of a star may be made in one minute instead of the usual two and uses a computer, developed with the company, to make a rapid calculation of the correction for time difference and speed. The air navigation tables have been modified to simplify selection of the stars that will give the best fix.

i. Satellite Navigation

Satellites have been used for navigational purposes for several years, and they provide greater accuracy than any other navigational system. Position fixes are possible every 60 minutes (4 satellites). Other systems have been proposed by various American companies. Westinghouse has proposed putting eight satellites in 6000-nmi orbit, with distance and direction measurement to be on the inferometer principle; data coordination, position transmission, and operations coordination would be by means of ground stations, and accuracy would be on the order of 1.5 to 2.5 nmi. Cubic proposes extending the SECOR satellite system to give direction information. General Electric has proposed four to five stationary satellites with a double distance measurement; evaluation and coordination would be by ground stations. Philco has proposed a rotating satellite that would transmit omnidirectional reference pulse signal and two fan-shaped RF energy beams; the position fix would be made by measuring the time interval between two signals, giving a passive system.

E. On Board Computer Systems

1. Special-Purpose Computers

There are several special-purpose digital computers on jet transport aircraft. Digital computers are associated with

(1) Inertial navigation
(2) Astro-navigation
(3) Doppler radar
(4) Autopilot
(5) Flight director
(6) Maintenance recorder
(7) Flight recorder

(8) Automatic throttle

(9) Vertical displays

(10) Air data computer.

These computers are usually hardwire-programmed and contain the absolute minimum in computational generality, e.g., fixed-point operation only. As solely dedicated computers they are unable to perform other computational tasks.

2. General-Purpose Computers

A general-purpose computer can be programmed for many different computational tasks. The computation logic is stored in reprogrammable memory. In multipurpose displays a general-purpose computer is usually required in order to use the inherent flexibility of the cathode-ray tube. The electronic attitude-direction indicator will also use a general-purpose digital computer.

Two general-purpose airborne computer systems are briefly described below.

EW-24 Computer System, TRW

8K word memory modules--24 bit two's complement

CPU

Independent IO (2 IO controller, 8 I/O processor)

Modular power supply

Direct address to 32K memory positions

49 instructions

4-μs add time

329-μs multiply time

55-μs divide time

Float subroutine

dbl processor Add--8 μs

Registers

Accumulator A req, Q

Data

3 hardware index registers

Control, 1, 2, 3

Interrupt capability

250-kHz clock

Direct and buffered I/O

System 4 π Computer, IBM

16K core memory two's complement

2.5-μs cycle

37 instructions

16 bits per word

5 output channels

8 input channels 67 digital input
32 digital output

3.8-μs add time 1 hardware index register

11.5-μs multiply time

46.3-μs divide time I/O rate 60,000 wd/s/channel.

The 4π computer is planned for installation in A7 fighter aircraft. Figure 26 shows the functions performed by the computer.

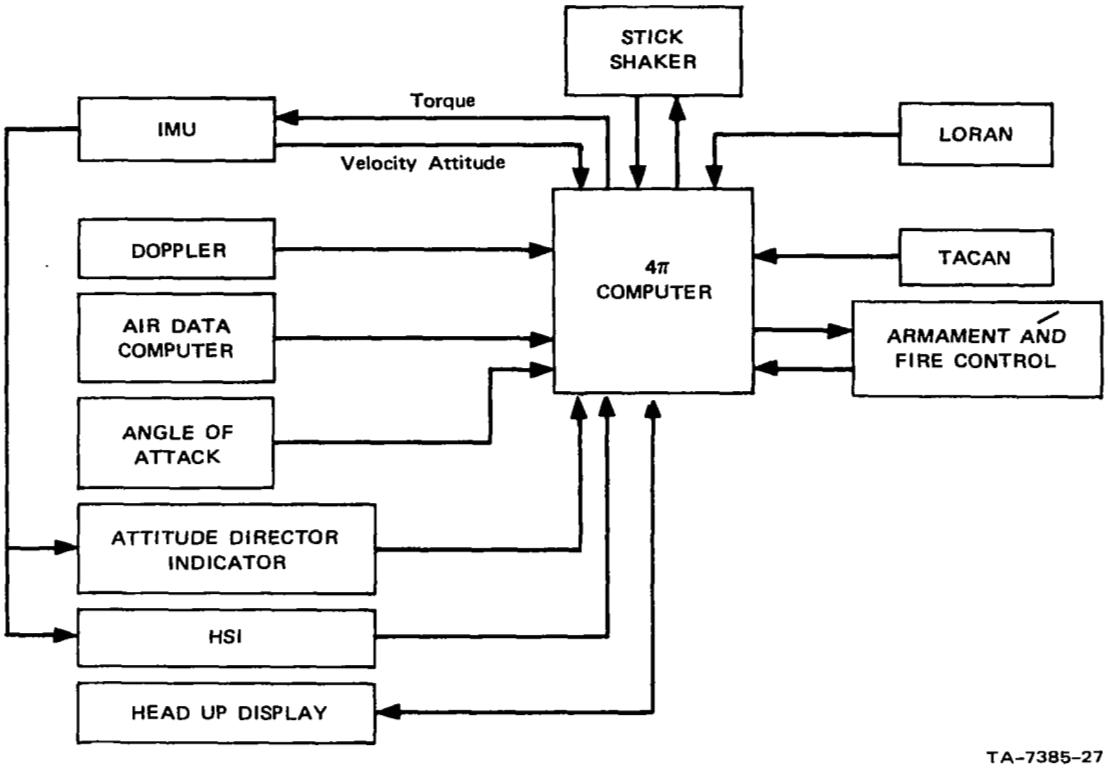

FIGURE 26 FUNCTIONS PERFORMED BY THE IBM 4π COMPUTER

Storage requirements for the A7 aircraft system are as follows:

	Words
Executive routine	500
Navigation	3,150
Initialization	200
Weapons delivery	2,950
Control panel	1,450
Ballistic tables	750
Self-test	900
Subroutines	600
Data	1,300
Scaling I/O	1,150
Total	12,950

In a commercial SST application, the Weapon Delivery and Ballistic Tables would not be required. It is conceivable that as many as 3,700 words could be allocated to an optimal control algorithm for the 4π system.

F. Engine Instrument

The engine measurement of greatest significance to the present study is the fuel flow meter. Fuel flow is measured by the use of a turbine meter, which is composed of a turbine with a magnetized blade placed in the fuel line. For each revolution of the turbine a constant volume of fuel is displaced, so that by counting the turbine revolutions, the flow may be measured. Revolutions are counted with a magnetic pick-up located outside the fuel line. The resulting pulses are accumulated and presented directly on digital readout devices. Range and accuracy are

Range	Accuracy
0-16,000 pounds/hour	±50 - ±200 pph .

In Appendix C the remainder of the engine instruments are discussed.

Part Two

THEORY NEEDED FOR THE OPTIMIZATION OF SST OPERATION

I SOME STOCHASTIC CONTROL THEORY

A. Introduction

The optimization of an SST trajectory can be formulated as a stochastic control problem; however, since the random effects are small in magnitude, it is reasonable to neglect terms of higher than second order in performance. In this section a theoretical development of stochastic control problems neglecting effects of higher than second order in performance is carried out. Application of this theory to the SST problem is presented later in this report. The most general controller that need be considered is a nominal control plus a linear function of the difference between the estimated and nominal state since higher order terms in the control are equivalent to second order in performance to changes of the nominal.

B. A Stochastic Control Problem

This problem is a generalization of the problem studied under Contract NAS2-3476.[2] The solution is similar to that obtained previously but is in a more informative form and is obtained more simply.

1. The State Equation

Consider a system described by

$$\dot{x} = f(x,u,t) + w(t), \tag{20}$$

where $E\{w(t)\} = 0$ and $E\{w(t)w^T(\tau)\} = \hat{Q}(t)\delta(t - \tau)$. The control is

$$u(t) = u^\circ(t) + K(t)[\hat{x}(t) - x^\circ(t)] + \Delta u(t) + \Delta K(t)[\hat{x}(t) - x^\circ(t)], \tag{21}$$

where $\hat{x}$ is an estimate of the state of the system and

$$\dot{x}^{\circ} = f(x^{\circ},u^{\circ},t). \tag{22}$$

Normally $\Delta u^{\circ}(t)$ and $\Delta K(t)$ are zero; however, for the purpose of optimization it is convenient to include them.

If

$$\Delta x(t) \triangleq x(t) - x^{\circ}(t) \tag{23}$$

and

$$\Delta\hat{x}(t) \triangleq \hat{x}(t) - x(t), \tag{24}$$

then

$$u(t) = u^{\circ}(t) + K(t)[\Delta\hat{x}(t) + \Delta x(t)] + \Delta u(t) + \Delta K(t)[\Delta\hat{x}(t) + \Delta x(t)]. \tag{25}$$

Furthermore, the derivatives of $\overline{\Delta x} \triangleq E\{\Delta x\}$ and $\bar{P} \triangleq E\{\Delta x\,\Delta x^{T}\}$ obey equations of the form

$$\dot{\overline{\Delta x}} = E\{\mathfrak{F}_1(x,x^{\circ},\hat{x},w,u^{\circ},\Delta u,K,\Delta K,t)\} \tag{26}$$

$$\dot{\bar{P}} = E\{\mathfrak{F}_2(x,x^{\circ},\hat{x},w,u^{\circ},\Delta u,K,\Delta K,\hat{Q},t)\}. \tag{27}$$

The exact forms of $\mathfrak{F}_1$ and $\mathfrak{F}_2$ are given in Appendix D. (Note that $\bar{P}$ is not the same as the $\bar{P}$ defined in Ref. 2.)

2. Performance

Consider the following performance index

$$J = E\left\{\int_0^T \mathcal{L}(x,u,t)\,dt + \Phi[x(T),T]\right\} \tag{28}$$

and make note of the following identity

$$\int_0^T [\lambda^T \dot{\overline{\Delta x}} + \dot{\lambda}^T \overline{\Delta x} + \mathrm{tr}(\dot{\bar{P}}\bar{P} + \bar{P}\dot{\bar{P}})]\,dt$$

$$= \lambda^T(T)\,\overline{\Delta x}(T) - \lambda^T(0)\,\overline{\Delta x}(0) + \mathrm{tr}[P(T)\bar{P}(T) - P(0)\bar{P}(0)], \tag{29}$$

where λ and P are as yet undefined. Let

$$\mathcal{H} \triangleq E\{\ell(x,u,t) + \lambda^T \mathfrak{F}_1 + \mathrm{tr}(P\,\mathfrak{F}_2)\}$$

$$\approx \ell(x^\circ,u^\circ,t) + \mathcal{H}_0 + \mathcal{H}_1 + \mathcal{H}_2\,\overline{\Delta x} + \mathcal{H}_3\,\overline{P}\,, \tag{30}$$

where (see Appendix D for details)

$$\mathcal{H}_0 = \mathrm{tr}\{P\hat{Q} + [2Pf_u(x^\circ,u^\circ,t) + H^\circ_{xu} + K^T H^\circ_{uu}]K\tilde{P} + \tfrac{1}{2}K^T H^\circ_{uu} K\hat{P}\} \tag{31}$$

$$\mathcal{H}_1 = \{H^\circ_u + \overline{\Delta x}^T[2Pf_u(x^\circ,u^\circ,t) + H^\circ_{xu} + K^T H^\circ_{uu}]\}\Delta u + \mathrm{tr}\Big(\{\overline{\Delta x}H^\circ_u + (\overline{P} + \tilde{P})[2Pf_u(x^\circ,u^\circ,t) + H^\circ_{xu} + K^T H^\circ_{uu}] + (\tilde{P}^T + \hat{P})K^T H^\circ_{uu}\}\Delta K + \tfrac{1}{2}H^\circ_{uu}\Delta K(\overline{P} + 2\tilde{P} + \hat{P})\Delta K^T\Big) + \tfrac{1}{2}\Delta u^T H^\circ_{uu}\Delta u + \Delta u^T H^\circ_{uu}\Delta K\overline{\Delta x} \tag{32}$$

$$\mathcal{H}_2 = H^\circ_x + H^\circ_u K \tag{33}$$

$$\mathcal{H}_3 = Pf_x(x^\circ,u^\circ,t) + f_x^T(x^\circ,u^\circ,t)P + \tfrac{1}{2}H^\circ_{xx} + [Pf_u(x^\circ,u^\circ,t) + \tfrac{1}{2}H^\circ_{xu}]K + K^T[Pf_u(x^\circ,u^\circ,t) + \tfrac{1}{2}H^\circ_{xu}]^T + \tfrac{1}{2}K^T H^\circ_{uu} K \tag{34}$$

$$H^\sigma(x^\circ,u^\circ,\lambda,t) = \lambda^T f(x^\circ,u^\circ,t) + \ell(x^\circ,u^\circ,t) \tag{35}$$

and $\tilde{P}$ and $\hat{P}$ are discussed below.

When Eqs. (28), (29), and (30) are combined,

$$J \approx \lambda^T(0)\Delta\bar{x}(0) + \mathrm{tr}[P(0)\bar{P}(0)] + \Phi[x^\circ(T),T]$$

$$+ \int_0^T \{\ell(x^\circ,u^\circ,t) + \mathcal{H}_0 + \mathcal{H}_1 + (\mathcal{H}_2 + \dot{\lambda}^T)\overline{\Delta x} + \mathrm{tr}[(\mathcal{H}_3 + \dot{P})\bar{P}]\}dt$$

$$+ \{\Phi_x[x^\circ(T),T] - \lambda^T(T)\}\bar{x}(T) + \mathrm{tr}\left(\{\Phi_{xx}[x^\circ(T),T] - P(T)\}\bar{P}(T)\right). \quad (36)$$

If the following definitions are made

$$\dot{\lambda} = -\mathcal{H}_2^T \qquad \lambda(T) = \Phi_x^T[x^\circ(T),T] \quad (37)$$

$$\dot{P} = -\mathcal{H}_3^T \qquad P(T) = \Phi_{xx}[x^\circ(T),T] \quad (38)$$

$$J^\circ = \int_0^T \ell(x^\circ,u^\circ,t) + \Phi[x^\circ(T),T]\,, \quad (39)$$

then Eq. (36) reduces to

$$J = J_0 + \lambda^T(0)\overline{\Delta x} + \mathrm{tr}[P(0)\bar{P}(0)] + \int_0^T(\mathcal{H}_0 + \mathcal{H}_1)dt\,. \quad (40)$$

The two quantities $\tilde{P}(t)$ and $\hat{P}(t)$ undefined above are defined as follows:

$$\tilde{P}(t) = E\{\Delta\hat{x}(t)\ \overline{\Delta x}^T(t)\} \quad (41)$$

$$\hat{P}(t) = E\{\Delta\hat{x}(t)\ \Delta\hat{x}^T(t)\}\,, \quad (42)$$

where it is assumed that $E\{\hat{\Delta x}(t)\} = 0$ (i.e., the estimate is unbiased). If a Kalman filter is used to estimate $x(t)$ from noisy measurements on the system, $\tilde{P}(t) = -\hat{P}(t)$ (this result is a consequence of the Wiener-Hopf equation) and $\hat{P}(t)$ is given by Eq. (III-10) of Ref. 2. Another case of interest occurs when all state variables are measured and corrupted by nonwhite noise--i.e.,

$$\dot{\hat{\Delta x}} = F_{noise}\hat{\Delta x} + w_{noise} , \tag{43}$$

where $E\{w_{noise}(t)\} = 0$ and $E\{w_{noise}(t)\, w^T_{noise}(t)\} = \hat{Q}_{noise}(t) \cdot \delta(t - \tau)$. In this situation,

$$\dot{\hat{P}} = F_{noise}\hat{P} + \hat{P}F^T_{noise} + \hat{Q}_{noise}$$

and (when $\Delta K = \Delta u = 0$)

$$\dot{\tilde{P}} = F_{noise}\tilde{P} + \tilde{P}[f_x(x^\circ,u^\circ,t) + f_u(x^\circ,u^\circ,t)K(t)]^T + \hat{P}[f_u(x^\circ,u^\circ,t)K(t)]^T . \tag{44}$$

3. Optimization

First consider the problem of finding the optimum K given $u^\circ(t)$. For this case set Δu equal to $-\Delta K \Delta x$; then

$$\mathcal{H}_1 = \mathrm{tr}\left((\bar{P} - \Delta x \bar{\Delta x}^T - \hat{P})\{[2P\, f_u(x^\circ,u^\circ,t) + H^\circ_{xu} + \left(K + \frac{1}{2}\Delta K\right)^T H^\circ_{uu}]\, \Delta K\}\right) , \tag{45}$$

where it is assumed that an optimal estimator (i.e., a Kalman filter) is used. If H°_{uu} is positive definite then a sufficient condition that K be optimal is

$$2P\, f_u(x^{\circ},u^{\circ},t) + H^{\circ}_{xu} + K^T H^{\circ}_{uu} = 0 . \tag{46}$$

Assume that K satisfies Eq. (46) and consider the problem of finding the optimal nominal trajectory. Now ΔK is zero and $\mathcal{H}_1$ becomes

$$\mathcal{H}_1 = H^{\circ}_u \Delta u + \Delta u^T H^{\circ}_{uu} \Delta u . \tag{47}$$

Thus, necessary conditions that $u^{\circ}(t)$ be optimal are that $H^{\circ}_u = 0$ and H°_{uu} be positive semidefinite. These conditions are the same conditions that exist for the deterministic problem found by setting $\hat{Q}(t) = \hat{\Delta x}(t) = \overline{\Delta x}(0) = 0$. If this deterministic problem has a unique solution, then its optimal control will be the optimal nominal control. In general, H°_{uu} will be positive definite; the exceptional cases are known as singular solutions.

C. The Effects of a State-Dependent Constraint on Control

In the above stochastic control problem no constraints were assumed on the control. In the present section the effects of the presence of such constraints are considered. For simplicity it is assumed that only one constraint and one control exists; multiple constraints and controls are easily handled in an analogous manner. The constraint takes the form

$$g(x,u) \leq 0 , \tag{48}$$

where it is assumed that g_u and g_x exist and g_u is positive.

1. With Perfect Information

First consider the situation in which $\hat{\Delta x}$ is zero. Assume that for a given t, u° is such that $g(x^\circ,u^\circ) = 0$. If

$$K = \frac{-1}{g_u(x^\circ,u^\circ)} g_x(x^\circ,u^\circ) , \tag{49}$$

and

$$\Delta K^T = -(H^\circ_u)^{-1} [2Pf_u(x^\circ,u^\circ,t) + H^\circ_{xu} + K^T H^\circ_{uu}]\Delta u , \tag{50}$$

then $g(x,u)$ will be less than or equal to zero to first order for $\Delta u \leq 0$ and (dropping terms of higher than second order)

$$\mathcal{H}_1 = H^\circ_u \Delta u + \frac{1}{2} \Delta u^T H^\circ_{uu} \Delta u . \tag{51}$$

Hence a necessary condition that u° be optimal for $g(x^\circ,u^\circ) = 0$ is that $H^\circ_u \leq 0$ with $H^\circ_{uu} \geq 0$ for $H^\circ_u = 0$. Furthermore, the appropriate adjoint equation to use is Eq. (37) with $\mathcal{H}^\circ_2$ as defined in Eq. (33) and K as defined in Eq. (49).

2. With Imperfect Information

If $\hat{\Delta x}$ is not zero then it is impossible to guarantee that the control chosen in Eq. (21) satisfies the constraint given by Eq. (48). Instead it may be required that the probability that for any given x the u chosen does not exceed the constraint be less than a fixed number, say α. If it is assumed that $\hat{\Delta x}$ is distributed normally (which is in keeping with the inclusion of terms to second order), then

$$\beta = \frac{K \hat{\Delta x}}{\sqrt{K \hat{P} K^T}} \tag{52}$$

is distributed normally with mean zero and variance one. Let γ be determined by

$$\alpha = \frac{1}{\sqrt{2\pi}} \int_{\gamma}^{\infty} e^{-\frac{1}{2}\beta^2} d\beta \ ; \tag{53}$$

then the probability that $\beta > \gamma$ is α. To first order (with Δu° and ΔK equal to zero),

$$g(x,u) = g(x^{\circ},u^{\circ}) + g_x(x^{\circ},u^{\circ})\ \Delta x + g_u(x^{\circ},u^{\circ})\ K\ (\Delta x + \hat{\Delta x}) \ . \tag{54}$$

If K is given by Eq. (49) and

$$g(x^{\circ},u^{\circ}) \leq g_u(x^{\circ},u^{\circ}) - \gamma\sqrt{\hat{KPT}} \quad , \tag{55}$$

$g(x,u)$ will be less than zero with probability α.

If Δu is set equal to $-\gamma\sqrt{\hat{KPK}^T}$ and ΔK as given by Eq. (50), Eq. (55) is satisfied to first order and

$$\mathcal{H}_0 + \mathcal{H}_1 = -H_u^{\circ} \cdot \gamma\ \hat{KPK}^T + \frac{1}{2} H_{uu}^{\circ}\ (1 + \gamma^2)\hat{KPK}^T \ . \tag{56}$$

Note that H_u° is negative on a constraint; hence the first term of Eq. (55) is positive. The term $\hat{KPK}^T$ is just the standard deviation σ_u in the estimate of the correct control u to be applied. In the absence of constraints, the lowest order term in the cost caused by measurement errors is a function of σ_u^2, but the presence of a constraint increases this cost and adds a term that is a function of σ_u. These additional costs depend upon how important it is that the constraint not be broken.

D. Discontinuities in the Derivative of the Hamiltonian

1. General Comments

The previous theory has assumed that H_x and H_u are continuous. It is possible to extend the theory to the situation in which H_x and H_u are not continuous on a finite number of surfaces in x-u space. Consider the control problem formulated in Sec. B-1 (with a scalar control u for simplicity). If $f(x,u,t)$ or $\ell(x,u,t)$ or both are discontinuous across the surface defined by $g(x,u,t) = 0$, where $g_u > 0$, then for any γ, $H^\circ(\lambda,x^\circ,u^\circ,t)$ defined by Eq. (35) will be discontinuous across the surface $g(x^\circ,u^\circ,t) = 0$. A control law of the form given by Eq. (25) will be assumed.

By use of the same procedure as that used above it can be shown that Eq. (31) and Eq. (33) to (39) hold when $g(x^\circ,u^\circ,t) = 0$, if

$$f_u^\circ \triangleq \frac{1}{2} \lim_{\epsilon \to 0} [f_u(x^\circ,u^\circ + \epsilon,t) + f_u(x^\circ,u^\circ - \epsilon,t)] \tag{57}$$

$$H_x \triangleq \frac{1}{2} \lim_{\epsilon \to 0} [H_x(\lambda,x^\circ + \epsilon,u^\circ,t) + H_x(\lambda,x^\circ - \epsilon,u^\circ,t)] \tag{58}$$

$$H_u \triangleq \frac{1}{2} \lim_{\epsilon \to 0} [H_u(\lambda,x^\circ,u^\circ + \epsilon,t) + H_u(\lambda,x,u^\circ - \epsilon,t)] \tag{59}$$

$$H_{xx} \triangleq \frac{1}{2} \lim_{\epsilon \to 0} [H_{xx}(\lambda,x^\circ + \epsilon,u^\circ,t) + H_{xx}(\lambda,x^\circ - \epsilon,u^\circ,t)] \tag{60}$$

$$H_{xu} \triangleq \frac{1}{2} \lim_{\epsilon \to 0} [H_{xu}(\lambda,x^\circ + \epsilon,u^\circ + \epsilon,t) + H_{xu}(\lambda,x^\circ - \epsilon,u^\circ - \epsilon,t)] \tag{61}$$

$$H_{uu} \overset{\Delta}{=} \frac{1}{2} \lim_{\epsilon \to 0} \left[H_{uu}(\lambda, x^\circ, u^\circ + \epsilon, t) + H_{uu}(\lambda, x^\circ, u^\circ - \epsilon, t) \right] . \tag{62}$$

The gain K is given by Eq. (49) and ΔK is given in Appendix E (which contains the detailed derivation) and

$$\mathcal{H}_1 = H_u^\circ \Delta u + \tilde{H}_u^\circ \tilde{\Delta u} + \frac{1}{2} H_{uu}^\circ \Delta u^2 + \frac{1}{2} \tilde{H}_{uu}^\circ \tilde{\Delta u^2} \tag{63}$$

$$\tilde{\Delta u} = \int_{-\infty}^{\infty} |\xi| \, N(\xi; \Delta u, \hat{KPK^T}) d\xi \tag{64}$$

$$\tilde{\Delta u^2} = \int_{-\infty}^{\infty} \xi |\xi| \, N(\xi; \Delta u, \hat{KPK^T}) d\xi \tag{65}$$

$$N(\xi; \Delta u, \hat{KPK^T}) \overset{\Delta}{=} \frac{1}{\sqrt{2\pi KPK^T}} e^{-\frac{1}{2} \frac{(\xi - \Delta u)^2}{\hat{KPK^T}}} \tag{66}$$

where $\tilde{H}_u$ and $\tilde{H}_{uu}$ are defined in Appendix E. The assumption has been made that the random variables are distributed normally, at least to second order.

2. Perfect Measurements

For perfect measurements, $\hat{P} = \tilde{P} = 0$; therefore $\tilde{\Delta u} = |\Delta u|$ and (to first order)

$$\mathcal{H}_1 = H_u^\circ \Delta u + \tilde{H}_u^\circ |\Delta u| . \tag{67}$$

If

$$\bar{H}_u^\circ + \tilde{H}_u^\circ < 0 \tag{68}$$

and

$$\bar{H}_u^\circ - \tilde{H}_u^\circ > 0 \tag{69}$$

then $\Delta u = 0$ minimizes $\mathcal{H}_1$. Therefore Eqs. (68) and (69) are necessary conditions for optimality of u° when $g(x^\circ, u^\circ, t) = 0$.

3. Imperfect Measurements

For imperfect measurements, make the assumption that

$$\Delta u = \alpha \sqrt{\hat{K} P \hat{K}^T} \; ; \tag{70}$$

then

$$\tilde{\Delta u} = \sqrt{\frac{\hat{K} P \hat{K}^T}{2\pi}} \int_{-\infty}^{\infty} |\xi| \, e^{-\frac{1}{2}(\xi-\alpha)^2} d\xi \, d\xi$$

$$\approx \sqrt{\frac{\hat{K} P \hat{K}^T}{2\pi}} \; (1 + \alpha)^2 \tag{71}$$

$$\tilde{\Delta u^2} = \frac{\hat{K} P \hat{K}^T}{\sqrt{2\pi}} \int_{-\infty}^{\infty} \xi |\xi| \, e^{-\frac{1}{2}(\xi-\alpha)^2} \, d\xi$$

$$\approx \frac{2\alpha \hat{K} P \hat{K}^T}{\sqrt{2\pi}} \tag{72}$$

Substitution of these results into Eq. (63) yields:

$$\mathcal{H}_1 = \left(H_u^\circ + \frac{1}{\sqrt{2\pi}} \tilde{H}_{uu}^\circ \sqrt{\hat{K} P \hat{K}^T} \right) \sqrt{\hat{K} P \hat{K}^T} \; \alpha$$

$$+ \left(\frac{1}{\sqrt{2\pi}} \tilde{H}_u^\circ + H_{uu}^\circ \sqrt{\hat{K} P \hat{K}^T} \right) \sqrt{\hat{K} P \hat{K}^T} \; \alpha^2 + \sqrt{\frac{\hat{K} P \hat{K}^T}{2\pi}} \; . \tag{73}$$

The optimum value of α found by differentiation of H_1 with respect to α is

$$\alpha = -\frac{H_u^o + \frac{1}{\sqrt{2\pi}} \tilde{H}_{uu}^o \sqrt{\hat{K}P\hat{K}^T}}{\frac{1}{\sqrt{2\pi}} \tilde{H}_u^o + H_{uu}^o \sqrt{\hat{K}P\hat{K}^T}} . \tag{74}$$

Note that for $\alpha = 0$ a term proportional to $\sqrt{\hat{K}P\hat{K}^T}$ has been added to the cost through the last term in Eq. (73). By use of an optimal α this cost may be partially offset.

E. Conclusions

In a stochastic control problem in which terms of higher than second order are neglected, the optimal controller consists of a nominal control plus a linear function of difference between the optimum estimate of the state of the system and the nominal state of the system. The optimum nominal control is found by solving the deterministic control problem resulting from ignoring all stochastic effects. The optimum linear gains are found by solving the linear quadratic problem in which the state equations are the original equations linearized about the nominal, and the cost functions are the second derivatives of the Hamiltonian for the nominal trajectory optimization problem. The stochastic effect and dual control effect mentioned in Ref. 2 are of higher than second order and thus do not appear. The presence of state-dependent constraints on control can be handled by a slight modification of the adjoint equations; if the state information is not exact the constraint used in determining the nominal trajectory must be tightened to

ensure that the actual constraint is violated with low probability. The presence of discontinuities in the derivatives of the Hamiltonian may also be handled; the nominal trajectory will under proper conditions lie on the surface of discontinuity.

In the absence of constraints and discontinuities in the derivatives of the Hamiltonian, the lowest order term in the cost caused by imperfect measurements is proportional to σ^2, where σ is the standard deviation of the error in control caused by the imperfect measurements. The presence of constraints on the nominal adds a term proportional to σ and increases the term proportional to σ^2 because of the necessity of tightening the constraint. The presence of discontinuity in the derivatives of the Hamiltonian along the nominal also adds a term proportional to σ because of the rectifying effect of the discontinuity. This latter cost may be minimized by slightly offsetting the nominal trajectory.

II SOME OPTIMIZATION THEORY

A. Introduction

In this section the focus is on the problem of determining the optimum control history for a deterministic control problem. Such a problem is, for example, encountered in trying to find the nominal control history for the stochastic control scheme discussed in Sec. I of Part Two.

B. Necessary Conditions

Focus now on the problem of determining the nominal trajectory. For ease of presentation the $^{\circ}$'s will be dropped. The problem is to select $u(t)$ to minimize

$$J = \int_0^T \mathcal{L}(\mathbf{x},u,t) + \varphi[\mathbf{x}(T),T]$$

subject to

$$\dot{\mathbf{x}} = \mathbf{f}(\mathbf{x},u,t) \qquad \mathbf{x}(0) = \mathbf{x}_0 \tag{75}$$

$$\mathbf{g}(\mathbf{x},u,t) \leq 0 \quad . \tag{76}$$

It is expedient to add a state variable x' defined by

$$\dot{x}' = 1 \qquad x'(0) = 0 \tag{77}$$

and replace t by x'. The necessary conditions for a solution (derived in the previous section) can be stated:

$$H_u \mathbf{g}(\mathbf{x},u,x') = 0 \quad , \tag{78}$$

$$H_u \leq 0 \quad , \tag{79}$$

and

$$H_{uu} \geq 0 \quad , \tag{80}$$

if $H_u = 0$ where

$$H(x,x',\lambda,\lambda',u) = \lambda^T f + \lambda' + \ell \tag{81}$$

$$-\dot{\lambda}^T = H_x + H_u g_x \qquad \lambda^T(T) = \varphi_x[x(T),T] \tag{82}$$

$$-\dot{\lambda}' = H_{x'} + H_u g_{x'} \qquad \lambda'(T) = 0 \quad . \tag{83}$$

C. A Useful Identity

Make note of the following result:

$$\begin{aligned} \dot{H} &= H_x \dot{x} + H_\lambda \dot{\lambda} + H_{x'} \dot{x}' + H_{\lambda'} \dot{\lambda}' + H_u \dot{u} \\ &= -(\dot{\lambda}^T + H_u g_x) f + f^T \dot{\lambda} - (\dot{\lambda}' + H_u g_{x'}) + \dot{\lambda}' + H_u \dot{u} \\ &= 0 \end{aligned} \tag{84}$$

since

$$\dot{u} = g_x f + g_{x'} \tag{85}$$

when $H_u \neq 0$. Adding a constant to λ' will in no way change the necessary conditions. In particular, if the final condition on λ' is made $-\lambda^T f - \ell$ rather than zero, H will be identically equal to zero along an optimal trajectory.

D. A Change in Independent Variable

Consider now a change in independent variable defined by

$$\frac{dt}{dt^{\dagger}} = h(x,x',u), \qquad t^{\dagger}(0) = 0 \tag{86}$$

where $h > 0$. In terms of $t^{\dagger}$ the optimization problem becomes:

$$J = \int_0^{t^{\dagger}(T)} \ell(x,x',u)\ h(x,x',u)\ dt^{\dagger} \tag{87}$$

subject to

$$\overset{\circ}{x} = f(x_1,x',u)\ h(x,x',u) \qquad x(0) = x_0 \tag{88}$$

$$g(x_1,x',u) \leq 0 \tag{89}$$

$$\overset{\circ}{x}' = h(x,x',u) \qquad x'(0) = 0\ , \tag{90}$$

where $^{\circ}$ indicates derivative with respect to $t^{\dagger}$. In terms of the new independent variable, necessary conditions are given by Eqs. (78), (79), and (80) with H replaced by $H^{\dagger}$, where

$$H^{\dagger} = \lambda^{\dagger T} fh + \lambda^{\dagger'} h + \ell h \tag{91}$$

$$-\dot{\lambda}^{\dagger T} = -\frac{\overset{\circ}{\lambda} t^{T}}{h} = \frac{(H_x^{\dagger} + H_u^{\dagger} g_x)}{h}$$

$$= H_x^{\star} + H_u^{\star} g_x + H^{\star}(h_x + h_u g_x)x/h\ ,$$

$$\lambda^{\dagger}(T) = \lambda(T) \tag{92}$$

$$
\begin{aligned}
-\dot{\lambda}^{\dagger\prime} &= -\frac{\overset{\circ}{\lambda}{}^{\dagger\prime}}{h} = \frac{(H_x^{\dagger\prime} + H_u g_x')}{h} \\
&= H_x^{\star\prime} + H_u^{\star} g_x' + H^{\star}(h_x' + h_u g_x')/h \quad , \\
\lambda^{\dagger\prime}(T) &= -\lambda^{T}(T) f(T) - \ell(T) \quad , \qquad (93)
\end{aligned}
$$

where $H^{\star}$ is H with λ replaced by $\lambda^{\dagger}$ and λ' by $\lambda^{\dagger\prime}$.

Along an optimal trajectory $H \equiv 0$ and, from comparison of Eqs. (91), (92), and (93) with Eqs. (81), (82), and (83), $\lambda^{\dagger} = \lambda$, $\lambda^{\dagger\prime} = \lambda'$, and $H^{\star} = H^{\dagger} = 0$. Thus by the use of this change of independent variable, the dynamics of the adjoint variable can be modified along nonoptimal trajectories with no effect on the adjoint equation along the optimal trajectories. This change is useful in applying numerical techniques to find optimal trajectories.

E. Conclusion

It is possible to change the dynamics of the adjoint equation for nonoptimal trajectories by a change in independent variable--a change that will subsequently prove useful in the numerical determination of the optimum nominal for the SST problem.

PART THREE

FORMULATION OF THE SUPERSONIC TRANSPORT VERTICAL CONTROL PROBLEM

I THE PATH AND COMPONENT EQUATIONS

A. Introduction

In this section the equations of motion of the center of mass of an aircraft are derived by the use of flat-earth and small-angle approximation to simplify the exact equations, which follow from Newton's laws. In addition, the equations used in describing the aerodynamics, atmosphere, and engine are developed. The standard model is used for the aerodynamics, while the atomospheric and engine models are those presented in Secs. I and II of Part One.

B. Equations of Motion

In this section approximate aircraft equations of motion are derived step by step from the exact equations found by application of Newton's laws.

1. Exact Equations

If the aircraft is considered to be a point mass in three-dimensional space, then six variables (the velocity vector and the position vector) are needed to describe its motion. It is common practice to use for these six variables the following: β the latitude, λ the longitude, h the geometric altitude, v the speed, γ the flight-path angle, and ψ the heading. To complete the equations, it is necessary to specify the forces acting on the aircraft: gravity, centrifugal and Coriolis forces, lift and drag, and thrust. If it is assumed that engines are aligned with the aircraft, then the direction of the thrust is determined

by the angle of attack α and the roll angle φ. All eight of these variables are defined by Fig. 27.

By use of Newton's laws, a system of six coupled differential equations can be written:

$$m\dot{v} = T \cos \alpha - D - mg \sin \gamma$$

$$+ m\omega^2 r \cos \beta \, (\cos \beta \sin \gamma - \sin \beta \cos \gamma \sin \psi) \qquad (94)$$

$$mv\dot{\gamma} = (T \sin \alpha + L) \cos \varphi - m\left(g - \frac{v^2}{r}\right) \cos \gamma$$

$$+ 2 mv\omega \cos \beta \cos \psi$$

$$+ m\omega^2 r \cos \beta \, (\cos \beta \cos \gamma + \sin \beta \sin \gamma \sin \psi) \qquad (95)$$

$$-mv \cos \gamma \dot{\psi} = (T \sin \alpha + L) \sin \varphi + mv \cos \gamma$$

$$\cdot\left[\frac{v}{r} \tan \beta \cos \gamma \cos \psi + 2\omega \, (\sin \beta - \tan \gamma \sin \psi \cos \beta)\right]$$

$$+ m\omega^2 r \sin \beta \cos \beta \cos \psi \qquad (96)$$

$$\dot{h} = v \sin \gamma \qquad (97)$$

$$r\dot{\beta} = v \cos \gamma \sin \psi \qquad (98)$$

$$r \cos \beta \dot{\lambda} = v \cos \gamma \cos \psi \quad , \qquad (99)$$

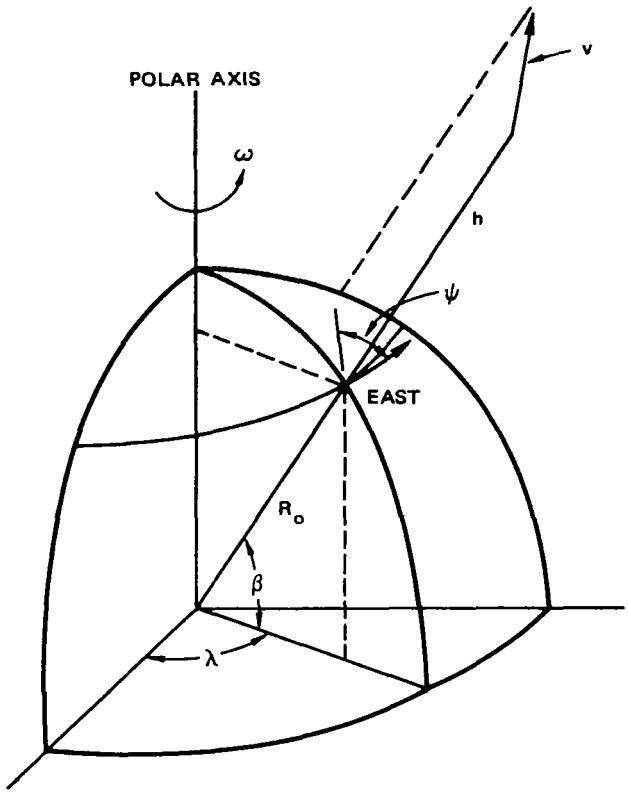

(a) Basic Coordinate System

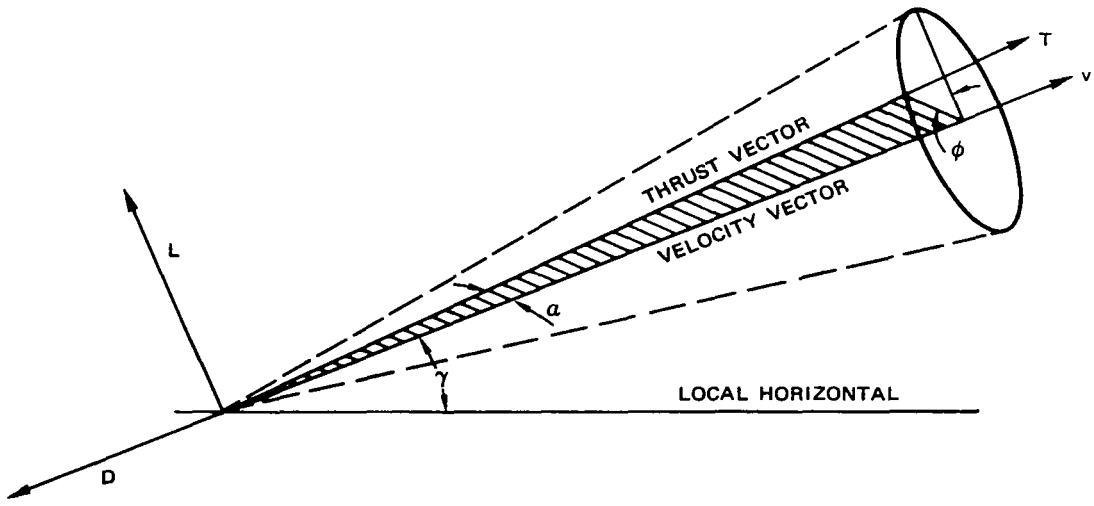

(b) Vehicle Orientation

FIGURE 27 DEFINITION OF VARIABLES

where ω is the rate of rotation of the earth, g is the acceleration of gravity, r is $R_0 + h$, R_0 is the radius of the earth, m is the mass of the aircraft, T is Thrust, L is lift, and D is drag.

2. Approximate Equations

Make note of the following values:

$$g_0 = 9.80665 \text{ m/s}^2 ,$$

$$R_0 \approx 7 \times 10^6 \text{ m} ,$$

$$v < 10^3 \text{ m/s} ,$$

$$\omega \approx 7 \times 10^{-5} \text{ rads} , \text{ and}$$

$$h < 3 \times 10^4 \text{ m} .$$

Therefore:

$$r = R_0 + h \approx R_0 ,$$

$$g = \frac{R_0^2}{r^2} g_0 \approx g_0 ,$$

$$\omega^2 r \approx 3.5 \times 10^{-2} \ll g_0 ,$$

$$v\omega \approx 7 \times 10^{-2} \ll g_0 , \text{ and}$$

$$\frac{v^2}{r} \approx 0.14 \ll g_0 .$$

For passenger comfort, γ will be constrained; certainly it is reasonable to assume that $\cos\gamma > \sin\gamma$ (i.e., $\gamma < 45^\circ$). Hence from the above, Eqs. (94) and (95) may be rewritten

$$\dot{mv} = T\cos\alpha - D - mg_0 \sin\gamma - m\omega^2 R_0 \cos\beta \sin\beta \cos\gamma \sin\psi \quad (100)$$

$$mv\dot{\gamma} = (T\sin\alpha + L)\cos\varphi - mg_0 \cos\gamma \quad . \quad (101)$$

3. Alternate Equations

a. Energy

The energy (per unit mass) is the sum of potential and kinetic energy

$$E = g_0 h + \frac{1}{2} v^2 \quad . \quad (102)$$

A differential equation for E may be written by combining Eqs. (94) and (97):

$$\dot{E} = \frac{(T\cos\alpha - D)v}{m} + \omega^2 r \cos\beta\,(\cos\beta \sin\gamma - \sin\beta \cos\gamma \sin\psi)v \quad .(103)$$

Equation (97) can be replaced by Eq. (103) and h by E as a state variable.

b. Range

For any ground path, β and λ can be taken to be known functions of x, the range (distance traveled on earth's surface), which obeys

$$\dot{x} = \frac{R_0}{r} v\cos\gamma \approx v\cos\gamma \quad . \quad (104)$$

Furthermore, with knowledge of β and λ as functions of x, Eqs. (98), (99), and (104) can be solved to yield

$$\sin \psi = \frac{\partial \beta}{\partial x} R_0 \tag{105}$$

$$\cos \psi = \frac{\partial \lambda}{\partial x} R_0 \cos \beta \tag{106}$$

$$\cos \psi \dot{\psi} = \frac{\partial^2 \beta}{\partial x^2} R_0^2 \frac{v}{r} \cos \gamma \approx \frac{\partial^2 \beta}{\partial x^2} R_0 v \cos \gamma \quad . \tag{107}$$

These three equations may be substituted into Eq. (96) to give φ. Hence for a specified ground path the behavior of the airplane can be described by four state variables: v, γ, x, and E.

4. Straight-Flight Equations

It will be assumed in the sequel that the ground path is a straight line; i.e., turns will not be considered. To consider turns properly, it is necessary to consider attitude control of the airplane as well as guidance. If the ground path is straight, then φ will be quite small and hence cos φ will be very close to one. Furthermore, the last term on the right-hand side of Eqs. (100) and (103) is in effect an additional drag caused by centrifugal force and will be ignored in the sequel. Hence, in straight flight the equations of motion are

$$\dot{E} = \frac{(T \cos \alpha - D)v}{m} \tag{108}$$

$$\dot{v} = \frac{T \cos \alpha - D}{m} - g_0 \sin \gamma \tag{109}$$

$$v\dot{\gamma} = \frac{T \sin \alpha + L}{m} - g_0 \cos \gamma \tag{110}$$

$$\dot{x} = v \cos \gamma \quad . \tag{111}$$

C. Component Equations

1. Aerodynamics

a. Drag

A standard quadratic polar is assumed for the drag:[17]

$$D = \frac{S}{2} \rho v^2 \left[f_D^0(M_n) + f_D^L(M_n) C_L^2(M_n, \alpha) \right] \quad , \tag{112}$$

where S is a reference area, $(1/2)\rho v^2$ is the dynamic pressure, ρ is the air density, f_D^0 and f_D^L are drag coefficients, which depend upon M_n the Mach number, and C_L is the lift coefficient.

b. Lift

Lift is given by

$$L = \frac{S}{2} \rho v^2 C_L(M_n, \alpha) \quad . \tag{113}$$

It is assumed that C_L is linear in α:

$$C_L(M_n,\alpha) = f_L(M_n)\alpha \quad . \tag{114}$$

c. Lift and Drag Coefficients

In the above equations for lift and drag there appear three functions of the Mach number. For a typical SST they might take the form shown in Fig. 28. Note that below $M_n = C_1$ all three are constants. Because the plane diverts the flow of air, portions of the flow will attain Mach one before the plane reaches Mach one; C_1 is the Mach number at which this starts. The drag and lift coefficients are constant below this value because the flow is completely subsonic.

Consider the following models for the drag coefficients:

$$f_D^0(M_n) = \begin{cases} C_2 , & M_n \le C_1 \\ C_3 + (C_4 M_n^2 + C_5 M_n + C_6) e^{C_7 M_n} + C_8 e^{C_9 M_n} , & M_n > C_1 \end{cases} \tag{115}$$

$$f_D^L(M_n) = \begin{cases} C_{10} , & M_n \le C_1 \\ (C_{11} M_n^2 + C_{12} M_n + C_{13}) e^{C_{14} M_n} + C_{15} e^{C_{16} M_n} , & M_n > C_1 \end{cases} . \tag{116}$$

In a similar manner f_L can be modeled by

$$f_L(M_n) = \begin{cases} C_{17} , & M_n \le C_1 \\ C_{17} + C_{18}(M_n - C_1)^2 e^{C_{19} M_n} , & M_n > C_1 \end{cases} . \tag{117}$$

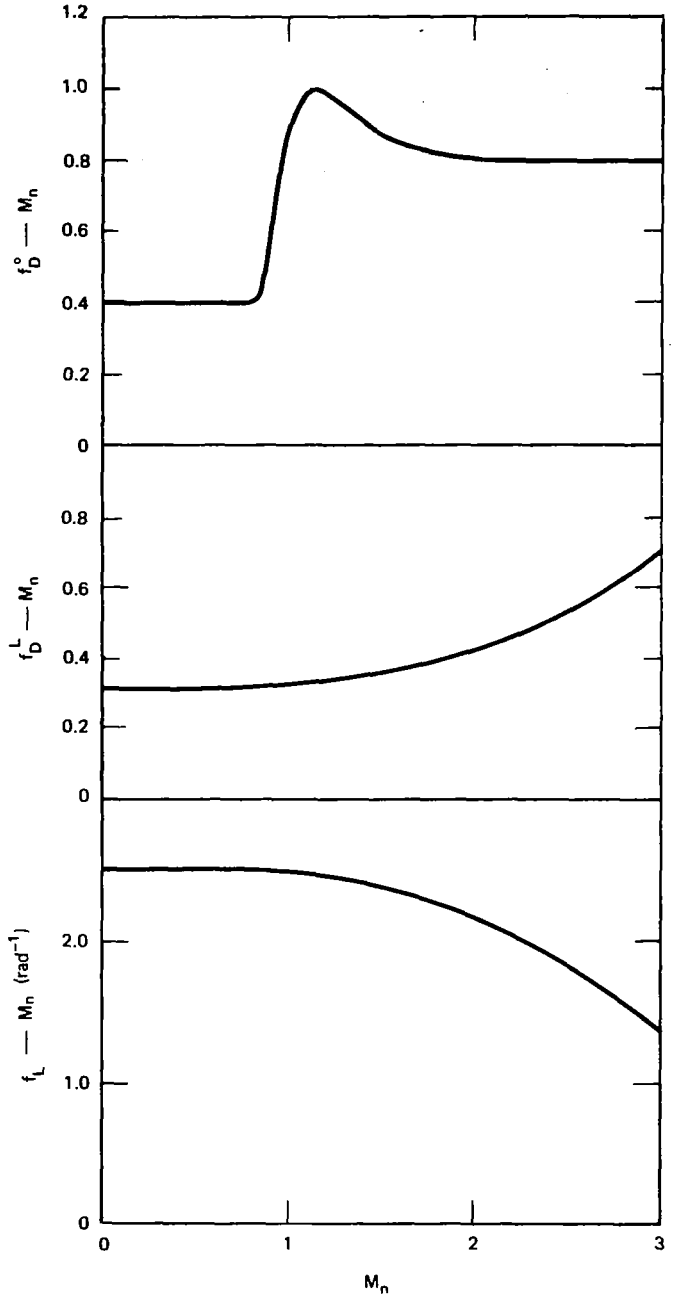

FIGURE 28 TYPICAL AERODYNAMICS

Figure 28 gives a set of typical aerodynamics modeled by these equations.

2. Atmosphere

a. The Basic Equation

The change of air pressure $\Delta\rho$ in a change in altitude of Δh is given by

$$\Delta p = -\Delta h \cdot \rho g \quad , \tag{118}$$

where ρ is the density of air. The truth of this statement is easily verified by noting that the right-hand side is the weight of air in a volume Δh high with unit cross-sectional area. But from the perfect gas law

$$\rho = \frac{p}{R\theta} \quad , \tag{119}$$

where p is the air pressure and θ the absolute air temperature. Substitution of Eq. (119) in Eq. (118) and passage to the limit yields

$$\frac{dp}{dh} = -\frac{g}{R} \cdot \frac{p}{\theta} \quad . \tag{120}$$

Given a temperature profile $\theta = \theta(h)$, one can integrate Eq. (120) to yield a pressure profile $p(h)$. An atmosphere obeying Eq. (120) is commonly called an exponential atmosphere.

b. The Temperature Profile

The model of the temperature used is

$$\theta(h) = \begin{cases} \theta_{TROP} + k_{LPS}(h_{TROP} - h) & h < h_{TROP} \\ \theta_{TROP} & h \geq h_{TROP} \end{cases} \qquad (121)$$

where θ_{TROP} is the temperature at the tropopause, h_{TROP} is the altitude of the tropopause, and k_{LPS} is the lapse rate.

c. The Pressure Profile

If the temperature profile of Eq. (121) is substituted into Eq. (120) and Eq. (120) is integrated, the following pressure profile results:

$$p = \begin{cases} p_{TROP}\left[1 + \frac{k_{LPS}}{\theta_{TROP}}(h_{TROP} - h)\right]^{-\frac{g_0}{Rk_{LPS}}} & h < h_{TROP} \\ p_{TROP}\, e^{-\frac{g}{R\theta_{TROP}}(h - h_{TROP})} & h \geq h_{TROP} \end{cases} , \qquad (122)$$

where p_{TROP} is the pressure at the tropopause.

3. Engine

a. Basic Model

The trust T and fuel flow W_f depend upon outside pressure p, the outside (absolute) temperature θ, the Mach number M_n, and the power setting Π. In Sec. I of Part One a very good simple model of these dependencies was presented. Translated into equation form, this model is

$$T = p^{\star} g_1(M_n) g_2(\pi, \theta^{\star}) \quad , \tag{123}$$

and

$$W_f = p^{\star} g_1(M_n) g_3(\pi, \theta^{\star}) \quad , \tag{124}$$

where

$$\theta^{\star} = \theta\left(1 + \frac{\gamma-1}{2} M_n^2\right) \quad , \tag{125}$$

and

$$p^{\star} = p\left(1 + \frac{\gamma-1}{2} M_n^2\right)^{\gamma-1} \quad . \tag{126}$$

The function g_1 contains the information in Fig. 5, and g_2 and g_3 contain the information from Figs. 15 and 16. The power setting Π has been replaced by a related variable π, defined below.

---

* The γ in these equations is not the flight-path angle but rather the ratio of specific heats (see Appendix A).

b. Functional Equations

As approximate fits to the curves given in Sec. I of Part One, the functions g_1, g_2, and g_3 may be parameterized in the following manner:

$$g_1(M_n) = \begin{cases} k_{g_1} \cdot a_1 & M_n \leq 1 \\ k_{g_1} \cdot (a_2 + a_3 M_n) & M_n > 1 \end{cases} , \tag{127}$$

where k_{g_1} is a constant equal to the number of engines times a conversion factor between units (e.g. pressure might be in millibars and thrust in newtons/m^2).

$$g_2(\pi,\theta^\star) = \begin{cases} (a_4 + a_5\pi + a_6\pi^2)\theta^{\star 2} + (a_7 + a_8\pi + a_9\pi^2)\theta^\star \\ \qquad + (a_{10} + a_{11}\pi + a_{12}\pi^2) & , \quad \theta^\star \geq k_{g_2 g_3} \\ (a_{13} + a_{14}\pi + a_{15}\pi^2)\theta^\star + a_{16} + a_{17}\pi + a_{18}\pi^2 & , \quad \theta^\star < k_{g_2 g_3} \end{cases} \tag{128}$$

$$g_3(\pi,\theta^\star) = \begin{cases} \pi(a_{19}\theta^{\star 2} + a_{20}\theta^\star + a_{21}) & , \quad \theta^\star \geq k_{g_2 g_3} \\ \pi(a_{22}\theta^\star + a_{23}) & , \quad \theta^\star < k_{g_2 g_3} \end{cases} , \tag{129}$$

where $k_{g_2 g_3}$ is the outside total temperature at which the engine total temperature first reaches its constraint for maximum power setting. If a_{19} to a_{23} are chosen so that $g_3(1,\theta^{\star})$ models the fuel flow for maximum power setting, then π is just the fraction of the maximum possible fuel flow possible at a given temperature. Furthermore, for each $\theta^{\star}$ there is a one-to-one correspondence between π and the power setting Π. Figure 29 gives typical g_2 and g_3 modeled by these equations.

$a_4 = 0$, $a_9 = 4{,}030.1$, $a_{14} = 41.9917 \times 10^3$, $a_{19} = 1.6398 \times 10^4$,

$a_5 = 6.4799$, $a_{10} = 0$, $a_{15} = 1.6774 \times 10^3$, $a_{20} = -0.17178$

$a_6 = -4.2418$, $a_{11} = 1.8159 \times 10^6$, $a_{16} = 0$, $a_{21} = 50.077$,

$a_7 = 0$, $a_{12} = -1.0033 \times 10^6$, $a_{17} = 1.0314 \times 10^6$ $a_{22} = 0.0013571$,

$a_8 = -6{,}574.4$ $a_{13} = 0$ $a_{18} = -6.7776 \times 10^5$, $a_{23} = 10.114$

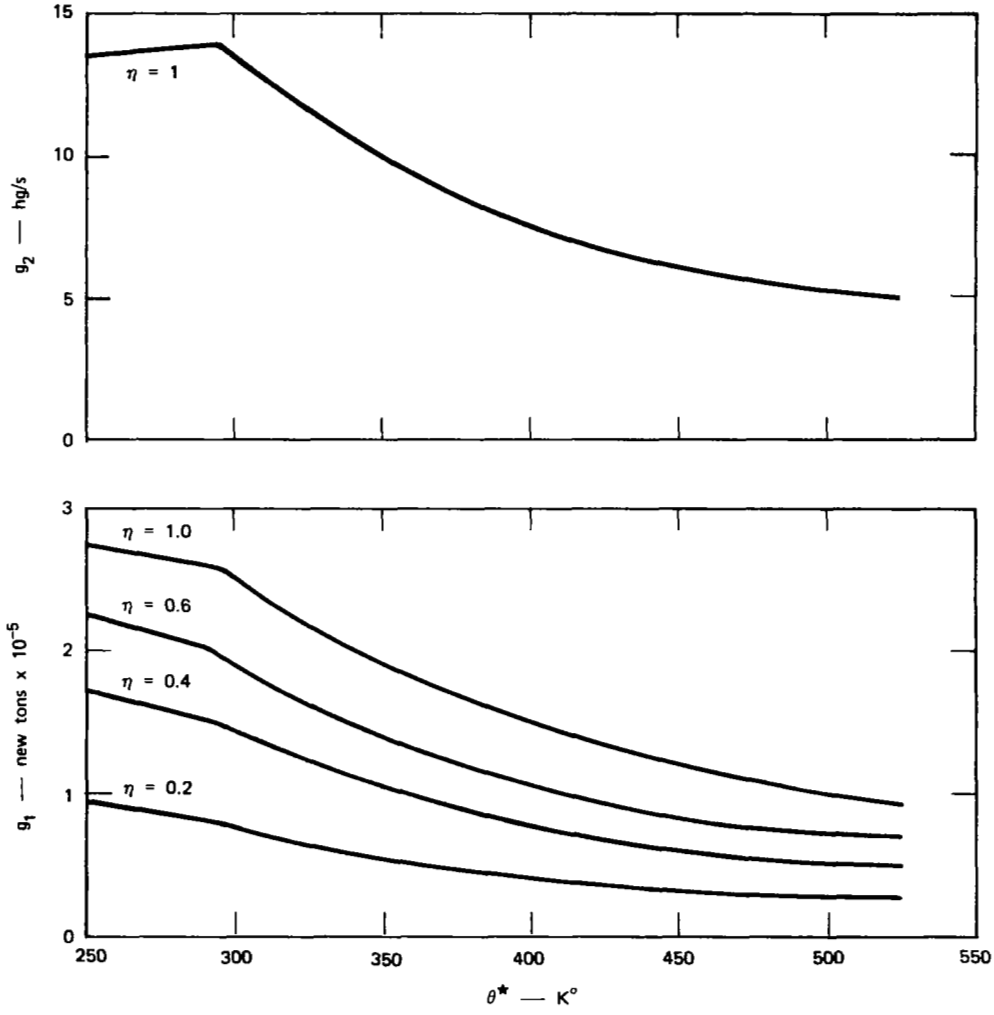

FIGURE 29 TYPICAL ENGINE

II THE VERTICAL CONTROL PROBLEM

A. Introduction

In this section the vertical control problem posed in the Introduction is formulated mathematically. The state equations to be used are based upon the equations of motion derived in the previous section. To formulate the control problem, it is necessary to change the independent variable and to reduce the number of state equations to one.

B. Problem Formulation

1. Basic Equations

Equations (108) to (111) are the equations of motion for straight flight. They form the basis of the optimization problem for determining the nominal trajectory.

a. Fuel Equations

The above-mentioned equations use time as the independent variable; it is more convenient to use fuel used μ as an independent variable. In this situation the mass of the SST is a function of μ:

$$m = m_0 - \mu \quad , \tag{130}$$

where m_0 is the initial mass. To convert the equations of the previous section from time-dependent differential equations to fuel-used-dependent

differential equations, the relation between fuel used and time is needed:

$$\dot{\mu} = W_f \quad . \tag{131}$$

b. State Equations

The basic state variables needed for trajectory optimization are E, v, and γ. In terms of fuel used, they obey the following differential equations:

$$\frac{dE}{d\mu} = \frac{(T \cos \alpha - D)v}{(m_0 - \mu)W_f} \tag{132}$$

$$\frac{dv}{d\mu} = \frac{T \cos \alpha - D}{(m_0 - \mu)W_f} - \frac{g_0}{W_f} \sin \gamma \tag{133}$$

$$v\frac{d\gamma}{d\mu} = \frac{T \sin \alpha + L}{(m_0 - \mu)W_f} - \frac{g_0}{W_f} \cos \gamma \quad . \tag{134}$$

c. Performance Index

The following performance index is used:

$$J = x(\mu_f) - a\, t(\mu_f)$$

$$= \int_0^{\mu_f} \frac{v \cos \gamma - a}{W_f} \, d\mu \quad , \tag{135}$$

where J is to be maximized and a determines the trade-off between maximizing range and minimizing time.

d. Constraints

Two constraints limit the velocity at which an SST can travel: sonic boom constraints and structural constraints. Simple forms were assumed for these constraints in the optimizations described as follows: The sonic boom constraint prohibits the SST from exceeding the speed of sound below a given altitude, and the structural constraint prohibits the total temperature $\theta^{\star}$ from exceeding a given limit. Both these constraints can be stated as constraints on velocity that are functions of the energy and atmospheric parameters; details are given in Appendix F.

A constraint exists on the total acceleration that a passenger in the SST may experience. In particular it is assumed that the total g's felt by the passenger including gravity do not vary from 1 g by more than 0.1 g:

$$\left|\sqrt{(\dot{v} + g \sin \gamma)^2 + (v\dot{\gamma} + g \cos \gamma)^2} - g\right| \leq 0.1\ g \quad . \tag{136}$$

Finally, a buffeting constraint exists on the permissible angle of attack that the airplane can take at a given velocity and energy level.

2. The Elimination of γ as a State Variable

In the state equations given above, the control variable is α. If α is the control variable, some aspects of attitude control are included in the trajectory optimization program. The amount of time taken for (or equivalently, the amount of fuel used in) changing γ is very small; hence it is much more reasonable to take γ to be the control variable.

a. Elimination of α

To make γ the control variable it is necessary to eliminate Eq. (134). This task is accomplished by setting $\dot{\gamma}$ equal to zero, which in turn implies that

$$T \sin \alpha + L = (m_0 - \mu) g_0 \cos \gamma \quad , \tag{137}$$

or with the aid of Eqs. (113) and (114) and a small-angle approximation,

$$\alpha = \frac{(m_0 - \mu) g_0 \cos \gamma}{T + \Gamma f_L(M_n)} \quad , \tag{138}$$

where

$$\Gamma \triangleq \frac{S}{2} \rho v^2 \quad . \tag{139}$$

b. Computation of Lift and Drag

To compute the drag it is necessary to know the lift, which may be found by substitution of Eqs. (138) and (113) into Eq. (114):

$$L = \frac{1}{1 + \Xi} (m_0 - \mu) g_0 \cos \gamma \quad , \tag{140}$$

where

$$\Xi = \frac{T}{\Gamma f_L(M_n)} \quad . \tag{141}$$

Drag is computed by substitution of Eqs. (113) and (137) into Eq. (112):

$$D = \Gamma f_D^o(M_n) + \frac{L^2}{\Gamma} \quad . \tag{142}$$

Note that both L and D are functions of γ and T.

c. Modification of the Acceleration Constraint

If $\dot{\gamma}$ is taken equal to zero, Eq. (136) may be simplified as follows: Eq. (136) implies that

$$0.9\ g \leq \sqrt{\dot{v}^2 + 2\dot{v}g \sin\gamma + g^2} \leq 1.1\ g$$

or

$$0.81g^2 \leq \dot{v}^2 + 2\dot{v}g \sin\gamma + g^2 \leq 1.21\ g^2$$

or approximately that

$$\left| \frac{\dot{v}}{g}\left(\frac{\dot{v}}{g} + 2 \sin\gamma\right)\right| \leq 0.2 \quad . \tag{143}$$

3. The Elimination of v as a State Variable

Just as above γ was eliminated as a state variable and made a control variable with α being replaced with a nominal value, v will be eliminated as a state variable and made a control variable with γ being replaced by a nominal value. It is not possible to determine the nominal γ by setting $\dot{v}$ equal to zero in analogy to the determination of the nominal α by setting $\dot{\gamma} = 0$. Instead the nominal γ will be chosen in

the course of numerical integration of Eq. (132) during the actual optimization discussed in Sec. II of Part Four.

From Eqs. (132) and (133) with small-angle approximations on α,

$$\sin \gamma = \frac{W_f}{g_0}\left[\frac{1}{v}\frac{dE}{d\mu} - \frac{dv}{d\mu}\right] \quad . \tag{144}$$

Suppose μ_{i-1} and μ_{i-2} are the fuels used at the two previous integration steps, v_{i-1} and v_{i-2} are the corresponding optimal velocities, and $(dE/d\mu)_{i-1}$ and $(W_f)_{i-1}$ are the values of $(dE/d\mu)$ and W_f computed at μ_{i-1}. Then γ_{i-1}, the value of γ at μ_{i-1}, is given approximately by

$$\sin \gamma_{i-1} \approx \frac{(W_f)_i}{g_0}\left[\frac{1}{v_i}\left(\frac{dE}{d\mu}\right)_i - \frac{v_i - v_{i-1}}{\mu_i - \mu_{i-1}}\right] \quad . \tag{145}$$

When performing the optimization at μ_i, the value of cos γ needed is computed from

$$\cos \gamma = \sqrt{1 - \sin^2 \gamma_{i-1}}$$

$$\approx \sqrt{\frac{1}{1 + \sin^2 \gamma_{i-1}}} \quad . \tag{146}$$

The final formula is used to ensure that the value under the radical is positive.

PART FOUR

SOLUTION OF THE VERTICAL CONTROL PROBLEM

I THE NOMINAL CONTROL

A. Introduction

The nominal control history for the vertical control problem posed in Sec. I of Part Three and formulated mathematically in Sec. II of Part Three can be found using the technique described in Sec. II of Part Two. There exists a maximum velocity at which the SST can fly. When at this maximum, the only optimization that can be performed is to pick the altitude at which fuel consumption is minimum. This altitude, which may depend upon the weight of the airplane, determines the optimum cruise. The remainder of the trajectory can be broken down into an optimum climbout to get to cruise and an optimum letdown to get back to the ground. The problem of determining optimum cruise is purely algebraic while that of determining optimum letdown and climbout are variational problems.

B. Cruise

In cruise, the SST is traveling at maximum velocity, and since cruise is above the tropopause, this maximum velocity is independent of the energy. Furthermore, the flight-path angle γ is small during cruise; therefore performance will be optimized if W_f is minimized by choice of cruise energy (or equivalently since v is known, cruise altitude). This minimization must be performed subject to the constraint that $\dot{v}$ be zero; therefore, with a small-angle approximation for cos α, π must be chosen so that

$$T - D - (m_0 - \mu)g_0 \sin \gamma = 0 \quad , \tag{147}$$

or since γ is quite small,

$$T - D = 0 \quad . \tag{148}$$

Since $L \approx (m_0 - \mu)g_0$ and $W_f \overset{\Delta}{=} SFC\ T$, where SFC is the specific fuel consumption,

$$W_f \approx \frac{SFC}{L/D} \cdot (m_0 - \mu) \cdot g_0 \tag{149}$$

Then W_f will be minimized if L/D divided by SFC is maximized. A cruise in which L/D divided by SFC is maximized as a function of altitude is known as a Breuget cruise. Because L/D is a much stronger function of altitude than SFC, this optimization is essentially a trade-off between zero lift drag, which decreases with altitude, and induced drag, which increases with altitude. As the SST flies it becomes lighter, and hence the induced drag becomes less and the cruise altitude higher.

The optimization can be performed by adjoining Eq. (148) to W_f:

$$\mathcal{L} = \nu W_f + T - D \quad . \tag{150}$$

Necessary conditions for optimization are then

$$\frac{\partial \mathcal{L}}{\partial h} = \nu \frac{\partial W_f}{\partial h} + \frac{\partial T}{\partial h} - \frac{\partial D}{\partial h} = 0 \tag{151}$$

$$\frac{\partial \mathcal{L}}{\partial \pi} = \nu \frac{\partial W_f}{\partial \pi} + \frac{\partial T}{\partial \pi} - \frac{\partial D}{\partial \pi} = 0 \quad . \tag{152}$$

C. Climbout and Letdown

1. Separation of the Problem

The performance index given in the previous section, Eq. (135), can be rewritten

$$J = J_1 + J_2 + J_3 \quad , \tag{153}$$

where

$$J_1 = \int_0^{\mu_f} \frac{v_{max} - a}{W_f^*} \, d\mu \tag{154}$$

$$J_2 = \int_0^{\mu_1} \left(\frac{v \cos \gamma - a}{W_f} - \frac{v_{max} - a}{W_f^*} \right) d\mu \tag{155}$$

$$J_3 = \int_{\mu_2}^{\mu_f} \left(\frac{v \cos \gamma - a}{W_f} - \frac{v_{max} - a}{W_f^*} \right) d\mu \tag{156}$$

and where W_f^* is the fuel consumption along an optimum cruise, μ_1 is the fuel used at the end of climbout, and μ_2 is the fuel used at the start of descent.

With a small-angle approximation on α, Eq. (132) becomes:

$$\frac{dE}{d\mu} = \frac{(T - D)v}{(m_0 - \mu)W_f} \quad . \tag{157}$$

The problem of finding the optimal climbout is thus maximization of J_2 subject to Eq. (157) and the constraint that $v \leq v_c(E)$, where v_c is given in Appendix F. The problem of finding the optimal letdown is the same except that J_3 replaces J_2.

The optimal climbout is a fixed initial point, free final point problem whereas the optimal letdown is a free initial point, fixed final point problem (since μ_1 and μ_2 are not specified a priori). Furthermore, it will be assumed that the power setting π is set to 1 in climbout and to its minimum value in letdown. Hence energy increases with fuel used in climbout and decreases with fuel used in letdown. For these two reasons, it is convenient to solve letdown in reverse time. Below, the climbout problem only will be treated, in general, since the letdown problem is mathematically equivalent.

2. Hamiltonian and Adjoint Equations

In Sec. II of Part Two general equations are given for the Hamiltonian and adjoints for a general control problem. For the SST climbout problem these equations take the form

$$H = \frac{\lambda_1 \left(\frac{T - D}{m_0 - \mu}\right) v + \lambda_2 W_f}{W_f - b(v \cos \gamma - a)} - \frac{1}{b} \tag{158}$$

$$-\frac{d\lambda_1}{d\mu} = B\lambda_1 - C\lambda_2 \tag{159}$$

$$-\frac{d\lambda_2}{d\mu} = A\lambda_1 \quad , \tag{160}$$

where

$$b = \frac{W_f^{\bigstar}}{v_{max} - a} \tag{161}$$

$$A = \frac{v}{(m_0 - \mu)W_f}\left\{\frac{T - D}{m_0 - \mu} - \frac{\partial D}{\partial \mu}\right\} \tag{162}$$

$$B = \frac{v}{(m_0 - \mu)W_f}\left\{\frac{\partial T}{\partial E} - \frac{\partial D}{\partial E} - (T - D)\,\frac{\frac{\partial W_f}{\partial E}}{W_f - b(v\cos\gamma - a)}\right.$$
$$\left. + \left[\frac{\partial T}{\partial v} - \frac{\partial D}{\partial v} + (T - D)\left(\frac{1}{v} - \frac{\frac{\partial W_f}{\partial v} - b\cos\gamma}{W_f - b(v\cos\gamma - a)}\right)\right]\frac{\partial v_c}{\partial E}\right\} \tag{163}$$

$$C = \frac{-1}{W_f}\left\{\frac{\partial W_f}{\partial E} - W_f \cdot \frac{\frac{\partial W_f}{\partial E}}{W_f - b(v\cos\gamma - a)}\right.$$
$$\left. + \left[\frac{\partial W_f}{\partial v} - W_f\left(\frac{\frac{\partial W_f}{\partial v} - b\cos\gamma}{W_f - b(v\cos\gamma - a)}\right)\right]\frac{\partial v_c}{\partial E}\right\} \quad . \tag{164}$$

In obtaining these equations the theory of Sec. II , Part Two, was applied with

$$d\mu' = \frac{W_f}{W_f - b(v\cos\gamma - a)}\,d\mu \quad . \tag{165}$$

For climbout $W_f > b(v \cos \gamma - a)$ so that this change is legitimate. For letdown $W_f < b(v \cos \gamma - a)$; hence $d\mu'$ and H must be taken as the negatives of the value given in Eqs. (158) and (165). Similar considerations apply in the sequel, but will not be noted.

Final conditions on λ_1 and λ_2 are determined as follows. Since μ_1 is free

$$\lambda_2(\mu_1) = 0 \tag{166}$$

and from the requirement $H(\mu_1) = 0$

$$\lambda_1(\mu_1) = \frac{(m_0 - \mu)}{(T - D)v} \cdot \frac{W_f - b(v \cos \gamma - a)}{b} \quad . \tag{167}$$

3. Modification of the Hamiltonian and Adjoint Equations

Only the first terms of the Hamiltonian [Eq. (158)] affect the optimization; in addition, from physical considerations λ_1 is positive; hence H may be replaced by

$$H' = \frac{(T - D)v + \lambda W_f(M_0 - \mu)}{W_f - b(v \cos \gamma - a)} \quad , \tag{168}$$

where $\lambda \triangleq \lambda_2/\lambda_1$. Necessary conditions for optimality are

$$H'_v v_c = 0 \tag{169}$$

with $H_v' > 0$ for $v_c = 0$ and where

$$H_v' = \frac{1}{W_f - b(v\cos\gamma - a)}\left\{\frac{\partial T}{\partial v} - \frac{\partial D}{\partial v} + (T - D)\left(\frac{1}{v} - \frac{\frac{\partial W_f}{\partial v} - b\cos\gamma}{W_f - b(v\cos\gamma - a)}\right)\right.$$

$$\left. + \lambda(m_0 - \mu)\left[\frac{\partial W_f}{\partial v} - W_f\left(\frac{\frac{\partial W_f}{\partial v} - b\cos\gamma}{W_f - b(v\cos\gamma - a)}\right)\right]\right\}. \tag{170}$$

From Eqs. (159) and (160)

$$\frac{d\lambda}{d\mu} = \frac{1}{\lambda_1}\frac{d\lambda_2}{d\mu} - \frac{\lambda_2}{\lambda_1^2}\frac{d\lambda_1}{d\mu}$$

$$= -A + B\frac{\lambda_2}{\lambda_1} - C\frac{\lambda_2^2}{\lambda_1^2} \tag{171}$$

$$= -A + B\lambda - C\lambda^2 \quad ,$$

and from Eqs. (166) and (167)

$$\lambda(\mu_1) = 0 \quad . \tag{172}$$

4. Discontinuities in Derivatives of the Hamiltonian

For a given E, at v such that $h = h_{TROP}$ and $\theta^{\star} = k_{g_2 g_3}$, H_v and H_E are not continuous (which in turn implies that B, C, and H'_v are not continuous). The theory of Sec. I of Part Two may be applied to accommodate this circumstance. Let $\tilde{v}(E)$ be a v such that the discontinuous derivatives occur. Then if $\partial v_c/\partial E$ is set equal to $\partial\tilde{v}/\partial E$ in Eqs. (163) and (164) A and B will be continuous at $\tilde{v}$. The necessary conditions become

$$H'_v \cdot \tilde{v}(E) = 0 \tag{173}$$

with H'_v positive for v approaching $\tilde{v}$ from below and negative for v approaching $\tilde{v}$ from above.

The necessary conditions taking into account both constraints and discontinuities may be summarized as follows: When $v = v_c(E)$ set $\partial v_c/\partial E = \partial v_c/\partial E$ in Eqs. (163) and (164) for B and C; when $v = \tilde{v}(E)$ set $\partial v_c/\partial E = \partial\tilde{v}/\partial E$, and when v does not equal $v_c(E)$ or $\tilde{v}(E)$ set $\partial v_c/\partial E$ equal to zero. A necessary condition that v be optimal is that it maximize H'.

5. The Optimization Procedure

The following technique may be used to find the optimum climbout trajectory. An initial guess is found by setting λ in Eq. (168) for H' equal to zero. The state equation, Eq. (157), is integrated forward with v selected at each integration step so as to maximize H'; integration proceeds until the energy $E(\mu)$ equals the energy $E^*(\mu)$ for the optimum

cruise.† A, B, and C are computed and stored at each integration step and then used to integrate the adjoint equation, Eq. (171), backward with $\lambda = 0$ as the final condition. The state equation may now be integrated forward a second time, maximizing H' with the newly computed values of λ. The process of forward integration of the state equation and backward integration of the adjoint equation is repeated until the values of v converge. The same technique may be used for optimizing letdown, except that the state equation is integrated backward, the adjoint equation forward, and $-H'$ is maximized rather than H'.

† It is desirable to constrain $v \geq \sqrt{v_{max}^2 - 2(E-E^*)}$ so that altitude in climbout or letdown never exceeds cruise altitude. This prevents jumps in v in the transition to and from cruise.

II THE SENSITIVITY OF VERTICAL CONTROL TO MEASUREMENT ERRORS

A. Introduction

The topic of this section is the application of the theory of Sec. I of Part Two to the vertical control problem formulated in Sec. II of Part Three. It will be assumed that all measurements are made independently and that no filtering takes place; therefore, each measurement may be characterized by its standard deviation. The sensitivities to be obtained are the coefficients of the first two terms of the series expansion of the cost in terms of the standard deviation, i.e., the cost proportional to the standard deviation and the standard deviation squared.

B. Transformation of Variables

The optimization is carried out in terms of a set of variables including the states variables, the control variables, and variable parameters. To realize the optimal control without filtering, it is necessary to have as many measurements as optimization variables. In general the measurements will not correspond one for one with the optimization variables. Let x_M be the vector of measurements, x_O be the vector of optimization variables, and T the Jacobian of the transformation from x_O to x_M.

The expressions for the costs due to measurements errors derived in Sec. I of Part Two may be summarized (for a scalar control u) by

$$\Delta J = \int_0^T \left(S_1 \sqrt{K_O \hat{P}_O K_O^T} + S_2 K_O \hat{P}_O K_O^T \right) dt \quad , \qquad (174)$$

where ΔJ is the increase in cost, $\hat{P}$ is the covariance of the error in estimate of the values of the optimization variables, where

$$K_0 = -\frac{g_{x_0}}{g_u} \quad , \quad S_1 = 3H^\circ_u \quad , \quad S_2 = 5H^\circ_{uu} \tag{175}$$

for a part of the nominal trajectory on a constraint given by $g(x) < 0$ that is tightened by three standard deviations, where

$$K_0 = -\frac{g_{x_0}}{g_u} \quad , \quad S_1 = \frac{1}{\sqrt{2\pi}} \tilde{H}^\circ_u \quad , \quad S_2 = \frac{1}{2} H^\circ_{uu} \tag{176}$$

for a part of the nominal trajectory on a surface of discontinuity in H°_u given by $g(x) = 0$, that is not displaced to minimize sensitivity, and where

$$K_0 = -\frac{\lambda^T_{x_0} f^\circ_u + H^\circ_{x_0}}{H^\circ_{uu}} \quad , \quad S_1 = H^\circ_u \quad , \quad S_2 = \frac{1}{2} H^\circ_{uu} \tag{177}$$

for other parts of the nominal trajectory. The derivatives of the adjoint obey

$$-\dot{\lambda}_{x_0} = T_{xx_0}\left[\lambda^T_{x_0}\left(f^\circ_{x_0} + f^\circ_u K_0\right) + \left(f^\circ_{x_0} + f^\circ_u K_0\right)^T \lambda_{x_0} + K_0^T\left(H^\circ_{ux_0} + H^\circ_{uu} K_0\right)\right] + H^\circ_{xx_0} + H^\circ_{xu} K_0 \tag{178}$$

where x is that part of x_0 corresponding to the state of the system and is related to x_0 by $x = T_{xx_0} x_0$.

Let σ_M be the vector of standard deviations in the measurements and σ_M^2 the vector of standard deviations squared. Then

$$\sqrt{\hat{KPK}^T} = KT\sigma_M \tag{179}$$

and

$$\hat{KPK}^T = (KT)^2\sigma_M^2 \quad , \tag{180}$$

where $(KT)^2$ is the vector found by squaring the vector KT componentwise. Equation (174) may be rewritten.

$$\Delta J = \int_0^T \left[(S_1 KT)\sigma_M + S_2(KT)^2\sigma_M^2\right] \, dt \tag{181}$$

But on a constraint or surface of discontinuity

$$KT = -\frac{g_{x_0}^T}{g_u} = -\frac{g_{x_M}}{g_u} \triangleq K_M \tag{182}$$

and otherwise

$$KT = -\left(\frac{\lambda_{x_0} f_u^\circ + H_{x_0 u}^\circ}{H_{uu}^\circ}\right)^T = -\left(\frac{\lambda_{x_M} f_u^\circ + H_{x_M u}^\circ}{H_{uu}^\circ}\right) \triangleq K_M \quad . \tag{183}$$

The derivatives of the adjoint, λ_{x_M}, obey

$$-\dot{\lambda}_{x_M} = T_{xx_M}\left[\lambda_{x_M}^T\left(f_{x_M}^\circ + f_u^\circ K_M\right) + \left(f_{x_M}^\circ + f_u^\circ K_M\right)^T\lambda_{x_M}\right.$$

$$\left. + K_M^T\left(H_{ux_M}^\circ + H_{uu}^\circ K_M\right)\right] + H_{xx_M}^\circ + H_{xu}^\circ K_0 \quad . \tag{184}$$

The required sensitivities are just the vectors $S_1 K_M$ and $S_2 K_M^2$. The remainder of this section presents the algebra necessary to compute S_1, S_2, and K_M.

C. General Relationships Among Variables

1. Measurements

The measurements made on board the SST for use in making control decisions are measurements of fuel used μ, the temperature θ, the pressure p, and the dynamic pressure q. In addition it is necessary to know at least two of the three conditions at the tropopause--θ_{TROP} the temperature, P_{TROP} the pressure, and h_{TROP} the altitude. It will be assumed that measurements of p_{TROP} and h_{TROP} are made available to the SST. Note that with knowledge of θ, p, p_{TROP}, and h_{TROP}, the geometric altitude of the aircraft can be determined.

2. Primary Variables

The thrust T and the fuel consumption W_f are modeled as functions of θ, p, and the Mach number M_n. The drag is modeled as a function of the density ρ, the velocity v, μ, and M_n. Some constraints depend upon the altitude h in addition to selected ones of μ, θ, p, ρ, v, and M_n. Similar comments apply to the surface of discontinuous partials in the Hamiltonian. The optimum cost during cruise (1/b) is a function of only

θ_{TROP} and μ. The relationship between these eight primary variables (μ, θ p, ρ, v, M_n, h, θ_{TROP}) and the measurements (μ, θ, p, q, p_{TROP}, h_{TROP}) are given in Table VI.

3. Optimization Variables

During climbout and letdown the variables used in the optimization were the control v, the state variable E (the energy), the independent variable μ, and the variable atmospheric parameters θ_{TROP}, h_{TROP}, and p_{TROP}. During cruise the optimization can be assumed to be performed with p as the control variable, with a requirement that v be maintained less than v_{max} (the constant value of $v_c(E)$ that holds during cruise) and with μ and θ as variable parameters. The power setting π is set to 1.0 during climbout, to its minimum value during letdown, and to maintain T = D during cruise. It will be assumed that π is controlled perfectly in all three phases. The relationship between the two sets of optimization variables (μ, E, v, θ_{TROP}, p_{TROP}, h_{TROP}) and (μ, θ, p, v) and the primary variables is given in Table VI.

4. Partial Derivatives

The partial derivatives of the primary variables with respect to the measurements are needed to determine the sensitivity in the three phases; these partials are given in Table VII. During climbout and letdown, it is also necessary to know the partial of the primary variables with respect to the control variable v. And during cruise, it is necessary to know the partials of the primary variables with respect to the controls v and p. These three sets of partial derivatives are given in Table VII; v_c is used to distinguish v in cruise from v in climbout and letdown, while p_c is to distinguish p as a control in cruise from p as a measurement.

Table VI

RELATIONSHIP BETWEEN PRIMARY VARIABLES AND MEASUREMENTS

Primary Variables	Function of $(\mu, \theta, p, q, p_{TROP}, h_{TROP})$	Function of $(\mu, E, v, \theta_{TROP}, p_{TROP}, h_{TROP})$	Function of (μ, θ, p, v)
μ	μ	μ	μ
θ	θ	$\theta(h)$	θ
p	p	$p(h)$	p
ρ	$\frac{p}{R\theta}$	$\frac{p(h)}{R\theta(h)}$	$p/R\theta$
v	$\sqrt{\frac{2qR\theta}{p}}$	v	v
M_n	$\sqrt{\frac{2q}{\gamma p}}$	$\frac{v}{\sqrt{\gamma R\theta(h)}}$	$v/\sqrt{\gamma R\theta}$
h	$h_{TROP} + \frac{R\theta}{g_0} \ell n\left(\frac{p}{p_{TROP}}\right)$ for $p \le p_{TROP}$ $h_{TROP} + \frac{\theta}{k_{LPS}}\left[1 - \left(\frac{p}{p_{TROP}}\right)^{\frac{Rk_{LPS}}{g_0}}\right]$ for $p > p_{TROP}$	$\frac{E - \frac{1}{2}v^2}{g_0}$	--
θ_{TROP}	θ for $p \le p_{TROP}$ $\theta\left(\frac{p}{p_{TROP}}\right)^{\frac{Rk_{LPS}}{g_0}}$ for $p > p_{TROP}$	θ_{TROP}	--

Error

An error occurred while processing this page. See the system log for more details.

5. Constraints and Discontinuities

Two constraints exist (see Appendix F): a noise constraint defined by $g_1(M_n,h) \leq 0$, where

$$g_1(M_n,h) = \begin{cases} h_0 - h & \text{if} \quad M_n \leq 1 \\ h_s - h & \text{if} \quad M_n > 1 \\ 1 - M_n & \text{if} \quad h_0 < h < h_s \end{cases} \tag{185}$$

and a structural constraint defined by $g_2(\theta,v)$, where

$$g_2(\theta,v) = \theta_{max} - \theta - \frac{\gamma - 1}{2\gamma R} v^2 \quad . \tag{186}$$

Two surfaces of discontinuity in derivatives of H exist defined by $g_3(h) = 0$ and $g_4(\theta) = 0$, where

$$g_3(h) = h_{TROP} - h \tag{187}$$

$$g_4(\theta) = k_{g_2 g_3} - \theta \quad . \tag{188}$$

Partial derivatives of g_1, g_2, g_3, and g_4 with respect to the primary variables are given in Table VIII (note that these g_1, g_2, and g_3 are not the same g_1, g_2, and g_3 used in the engine model). Total derivatives of g_1, g_2, g_3, and g_4 with respect to the measurements and controls can be determined from Tables VII and VIII through use of the chain rule; results are presented in Table IX.

Table VIII

PARTIAL DERIVATIVES OF g_1, g_2, g_3, AND g_4 WITH RESPECT TO PRIMARY VARIABLES

	$/\partial\theta$	$/\partial v$	$/\partial M_n$	$/\partial h$
$\partial g_1/$	0	0	1 if $m_n = 1$, $h_0 < h < h_s$ 0 otherwise	1 if $h = h_0$, $M_n < 1$ or $h = h_s$, $M_n > 1$ 0 otherwise
$\partial g_2 1$	-1	$-\frac{\gamma - 1}{\gamma R} v$	0	0
$\partial g_3/$	0	0	0	-1
$\partial g_4/$	-1	0	0	0

Table IX

PARTIAL DERIVATIVES OF g_1, g_2, g_3, AND g_4

$g_{1_\mu} = 0$	$g_{2_\mu} = 0$	$g_{3_\mu} = 0$	$g_{4_\mu} = 0$
$g_{1_\theta} = \frac{\partial g_1}{\partial h}\frac{\partial h}{\partial \theta}$	$g_{2_\theta} = -1 + \frac{\partial g_2}{\partial v}\frac{\partial v}{\partial \theta}$	$g_{3_\theta} = -\frac{\partial h}{\partial \theta}$	$g_{4_\theta} = -1$
$g_{1_p} = \frac{\partial g_1}{\partial M_n}\frac{\partial M_n}{\partial p} + \frac{\partial g_1}{\partial h}\frac{\partial h}{\partial p}$	$g_{2_p} = \frac{\partial g_2}{\partial v}\frac{\partial v}{\partial p}$	$g_{3_p} = -\frac{\partial h}{\partial p}$	$g_{4_p} = 0$
$g_{1_q} = \frac{\partial g_1}{\partial M_n}\frac{\partial M_n}{\partial q}$	$g_{2_q} = \frac{\partial g_2}{\partial q}\frac{\partial q}{\partial p}$	$g_{3_q} = 0$	$g_{4_q} = 0$
$g_{1_{p_{TROP}}} = \frac{\partial g_1}{\partial h}\frac{\partial h}{\partial p_{TROP}}$	$g_{2_{p_{TROP}}} = 0$	$g_{3_{p_{TROP}}} = -\frac{\partial h}{\partial p_{TROP}}$	$g_{4_{p_{TROP}}} = 0$
$g_{1_{h_{TROP}}} = \frac{\partial g_1}{\partial h}\frac{\partial h}{\partial h_{TROP}}$	$g_{2_{h_{TROP}}} = 0$	$g_{3_{h_{TROP}}} = 0$	$g_{4_{h_{TROP}}} = 0$
$g_{1_v} = \frac{\partial g_1}{\partial M_n}\frac{\partial M_n}{\partial v} + \frac{\partial g_1}{\partial h}\frac{\partial h}{\partial v}$	$g_{2_v} = -\frac{\partial \theta}{\partial v} + \frac{\partial g_2}{\partial v}$	$g_{3_v} = -\frac{\partial h}{\partial v}$	$g_{4_v} = -\frac{\partial \theta}{\partial v}$
--	$g_{2_{v_c}} = \frac{\partial g_2}{\partial v}$	--	$g_{4_{v_c}} = 0$
--	$g_{2_{p_c}} = 0$	--	$g_{4_{p_c}} = 0$

D. Climbout and Letdown

1. The State and Hamiltonian

For climbout and letdown the state is E and the Hamiltonian is given by

$$H = \lambda_1 \frac{[T(\mu,\theta,M_n) - D(\mu,\rho,v,M_n)]}{(m_0 - \mu)W_f(p,\theta,M_n)} + \frac{v\cos\gamma + a}{W_f(p,\theta,M_n)} - \frac{1}{b(\mu,\theta_{TROP})} + \lambda_2 \tag{189}$$

2. Partial Derivatives with Respect to Primary Variables

The partial derivatives of H with respect to the primary variables $(\mu,\theta,p,\rho,v,M_n,h,\theta_{TROP})$ are

$$\frac{\partial H}{\partial \mu} = \frac{\lambda_1}{(m_0 - \mu)W_f}\left[\frac{1}{m_0 - \mu} - \frac{\partial D}{\partial \mu}\right] + \frac{1}{b^2}\frac{\partial b}{\partial \mu} \tag{190}$$

$$\frac{\partial H}{\partial \theta} = \frac{\lambda_1}{(m_0 - \mu)W_f}\left[\frac{\partial T}{\partial \theta} - (T - D)\frac{1}{W_f}\frac{\partial W_f}{\partial \theta}\right] - \frac{v\cos\gamma - a}{W_f^2}\frac{\partial W_f}{\partial \theta} \tag{191}$$

$$\frac{\partial H}{\partial p} = \frac{\lambda_1}{(m_0 - \mu)W_f}\left[\frac{\partial T}{\partial p} - (T - D)\frac{1}{W_f}\frac{\partial W_f}{\partial p}\right] - \frac{v\cos\gamma - a}{W_f^2}\frac{\partial W_f}{\partial p} \tag{192}$$

$$\frac{\partial H}{\partial \rho} = -\frac{\lambda_1}{(m_0 - \mu)W_f}\frac{\partial D}{\partial \rho} \tag{193}$$

$$\frac{\partial H}{\partial v} = -\frac{\lambda_1}{(m_0 - \mu)W_f}\frac{\partial D}{\partial v} \tag{194}$$

$$\frac{\partial H}{\partial M_n} = \frac{\lambda_1}{(m_0 - \mu)W_f}\left[\frac{\partial T}{\partial M_n} - \frac{\partial D}{\partial M_n} - (T - D)\frac{1}{W_f}\frac{\partial W_f}{\partial M_n}\right] - \frac{v\cos\gamma - a}{W_f^2}\frac{\partial W_f}{\partial M_n} \tag{195}$$

$$\frac{\partial H}{\partial h} = 0 \tag{196}$$

$$\frac{\partial H}{\partial \theta_{TROP}} = +\frac{1}{b^2}\frac{\partial b}{\partial \theta_{TROP}} \quad . \tag{197}$$

The partial derivatives of the state E with respect to the primary variables are

$$\frac{\partial E}{\partial h} = g \tag{198}$$

and

$$\frac{\partial E}{\partial v} = \frac{1}{2}v \tag{199}$$

with all other partials equal to zero.

3. Partial Derivatives with Respect to Measurements and Controls

The partial derivatives with respect to the measurements may be obtained by use of chain rule. They are

$$H_\mu = \frac{\partial H}{\partial \mu} \tag{200}$$

$$H_\theta = \frac{\partial H}{\partial \theta} + \frac{\partial H}{\partial \rho}\frac{\partial \rho}{\partial \theta} + \frac{\partial H}{\partial v}\frac{\partial v}{\partial \theta} + \frac{\partial H}{\partial \theta_{TROP}}\frac{\partial \theta_{TROP}}{\partial \theta} \tag{201}$$

$$H_p = \frac{\partial H}{\partial p} + \frac{\partial H}{\partial \rho}\frac{\partial \rho}{\partial p} + \frac{\partial H}{\partial v}\frac{\partial v}{\partial p} + \frac{\partial H}{\partial M_n}\frac{\partial M_n}{\partial p} - \frac{\partial H}{\partial \theta_{TROP}}\frac{\partial \theta_{TROP}}{\partial p} \tag{202}$$

$$H_q = \frac{\partial H}{\partial v}\frac{\partial v}{\partial q} + \frac{\partial H}{\partial M_n}\frac{\partial M_n}{\partial q} \tag{203}$$

$$H_{p_{TROP}} = \frac{\partial H}{\partial \theta_{TROP}}\frac{\partial \theta_{TROP}}{\partial p_{TROP}} \tag{204}$$

$$H_{h_{TROP}} = 0 \quad . \tag{205}$$

The partial derivative of H with respect to the control v may also be found by use of the chain rule and is given by

$$H_v = \frac{\partial H}{\partial \theta}\frac{\partial \theta}{\partial v} + \frac{\partial H}{\partial p}\frac{\partial p}{\partial v} + \frac{\partial H}{\partial \rho}\frac{\partial p}{\partial v} + \frac{\partial H}{\partial v} + \frac{\partial H}{\partial M_n}\frac{\partial M_n}{\partial v} \quad . \tag{206}$$

Finally the partial derivatives of E with respect to the measurements can be computed in the same way

$$E_\mu = 0 \tag{207}$$

$$E_\theta = \frac{\partial E}{\partial v}\frac{\partial v}{\partial \theta} + \frac{\partial E}{\partial h}\frac{\partial h}{\partial \theta} \tag{208}$$

$$E_p = \frac{\partial E}{\partial v}\frac{\partial v}{\partial p} + \frac{\partial E}{\partial h}\frac{\partial h}{\partial p} \tag{209}$$

$$E_q = \frac{\partial E}{\partial v}\frac{\partial v}{\partial q} \tag{210}$$

$$E_{p_{TROP}} = \frac{\partial E}{\partial h}\frac{\partial h}{\partial h_{TROP}} \tag{211}$$

$$E_{h_{TROP}} = \frac{\partial E}{\partial h}\frac{\partial h}{\partial h_{TROP}} \quad . \tag{212}$$

4. Second Derivatives

Derivatives with respect to E and h of the above derivatives of H are needed. They may be determined numerically by

$$H_{zv} = \frac{H_z(v + \Delta v) - H_z(v)}{\Delta v} \tag{213}$$

$$H_{zE} = \frac{H_z(E + \Delta E) - H_z(E)}{\Delta E} \quad , \tag{214}$$

where z may be any of the measurement variables or v. Care must be taken not to cross a surface of discontinuity in determining these second derivatives.

E. Cruise

1. The Hamiltonian

There is no state variable in the cruise optimization since it is an algebraic optimization. However, equivalent formulas may be used if H is defined by

$$H = \lambda_1 \frac{(T - D)}{(m_0 - \mu)W_f} + \frac{v + a}{W_f} + \lambda_2 \tag{215}$$

Minimization of $\mathcal{L}$ given by Eq. (150) is equivalent to maximization of H if

$$\lambda_1 \stackrel{\Delta}{=} - \frac{(v + a)(m_0 - \mu)}{W_f v} \tag{216}$$

2. Partial Derivatives with Respect to Primary Variables

The partial derivatives of H with respect to the primary variables $(\mu, \theta, p, \rho, v, M_n, h)$ are given by Eqs. (190) to (196) with $\cos \gamma = 1$ and the terms involving b deleted.

3. Partial Derivatives with Respect to Measurements and Controls

Equations (200) to (209) hold with the terms involving θ_{TROP} deleted. Controls are v_c and p_c (v is always on a constraint); the partial derivatives with respect to these variables are

$$H_{p_c} = \frac{\partial H}{\partial p} + \frac{\rho H}{\partial \rho} \frac{\partial \rho}{\partial p_c} \tag{217}$$

$$H_{v_c} = \frac{\partial H}{\partial v} + \frac{\partial H}{\partial M_n} \frac{\partial M_n}{\partial v_c} \quad . \tag{218}$$

4. Partial Derivative of b

The partial derivatives of b with respect to μ and θ_{TROP} needed by the climbout and letdown sensitivity analyses are given by

$$-\frac{1}{b^2} \frac{\partial b}{\partial \theta_{TROP}} = H_\theta \tag{219}$$

$$-\frac{1}{b^2} \frac{\partial b}{\partial \mu} = H_\mu \quad . \tag{220}$$

These two quantities are computed at cruise conditions.

PART FIVE--PROGRAM DESCRIPTION

I THE OPTIMIZATION PROGRAM

A. General Comments

This section is broken into two parts: a description of each subroutine giving inputs, outputs, and relevant equations; and the results of running the program for selected cases. In the description the correspondence between program variables and the variables used in the remainder of the report is given. For example, in FUNCTION ALT (E,V) the inputs are E and v, which take the form E and V in the program.

In general the notation agrees with the rest of the report with these three exceptions: s is used for W_f, b is used for -b, and the following notation is used for derivatives. Consider the thrust T. Thrust is a function directly of pressure p, temperature θ, Mach number M_n, and power setting π. But ultimately p, θ, and M_n are functions of the velocity v and energy E; hence thrust may be considered a function of v and E. Derivatives of T with respect to p, θ, and M_n are denoted with the ordinary partial symbol, whereas derivatives with respect to E and v are represented with the total derivative symbol. Similar comments apply to fuel flow s (W_f) and drag D. In particular $\partial D/\partial v$ refers to the effect of v on D directly, whereas dD/dv refers to the effect of v on D directly and indirectly through changes in ρ and M_n.

Note that the drag depends upon thrust. Since the derivatives of T-D are required rather than the partials of T and D separately, it is convenient to place those derivatives of D that result from D's dependence on T in the equations for the derivatives of T. This fact explains the presence of the FAC2 terms in SUBROUTINE PARST.

B. Subroutine Descriptions

1. Executive Routine

Name: SST

Input: Below is listed the common list (Table X). The following key applies:

* means the quantity is read as an input.

‡ means the quantity is set in SST.

θ means the quantity is computed in SST.

N means the quantity is not used.

Formula(s): Given in common list.

Remarks: This is the executive program which reads inputs, computes constants, and calls JOVERMU and BAKN4TH.

Table X

COMMON LIST

1	G	$g_0 = 9.80665$	‡	7	B6	$b_6 = \frac{-b_1}{b_{15} + b_3}$	θ
2	B1	$b_1 = k_{LPS}$	*	8	B7	$b_7 = -b_6 b_9 b_{10}$	θ
3	B2	$b_2 = -202.0$	‡	9	B8	$b_8 = b_9 - 1$	θ
4	B3	$b_3 = 273.0$	‡	10	B9	$b_9 = \frac{0.0342}{b_1}$	θ
5	B4	$b_4 = h_{TROP}$	*	11	B10	$b_{10} = b_{11}$	θ
6	B5	$b_5 = \frac{-0.0342}{b_{15} + b_3}$	θ	12	B11	$b_{11} = P_{TROP}$	*

Table X (Continued)

13	B12	$b_{12} = -b_5 \cdot b_4$	θ	35	C16	c_{16}	*
14	B13	$b_{13} = 0.348$	‡	36	B17	$b_{17} = \frac{b_{16}^2}{b_{15} + b_3}$	θ
15	B14	$b_{14} = b_{15} - b_1 b_4$	θ				
16	B15	$b_{15} = \theta_{TROP}$	*	37	B18	$b_{18} = b_1/g$	θ
17	B16	$b_{16} = 20.1$	‡	38	B19	$b_{19} = \frac{b_{16}^2}{1 + 0.5 \cdot b_{16}^2 b_{18}}$	θ
18	EMO	m_0	*				
19	GSQ	g_0^2	‡	39	B20	$b_{20} = b_{14} + b_3$	θ
20	C1	c_1	*	40	ETEST	$= 0.5 b_{17} + b_4 g$	θ
21	C2	c_2	*	41	HOG	$= h_0 g$	θ
22	C_3	c_3	*	42	HSG	$= h_s g$	θ
23	C_4	c_4	*				
24	C5	c_5	*	43	VMAX	$v_{max} = b_{16}\sqrt{\frac{2.0(\theta max - b_{15})}{\gamma - 1}}$	θ
25	C6	c_6	*	44	IDOUBL	used by CHKCONV, JOVERMU, JANDE	
26	C7	c_7	*	45	IHALVE	used by CHKCONV, JOVERMU, JANDE	
27	C8	c_8	*	46	IXFR	used by CHKCONV, JOVERMU, JANDE	
28	C9	c_9	*	47-56	PE(10)	used by CHKCONV, JOVERMU, JANDE	
29	C10	c_{10}	*				
30	C11	c_{11}	*	57-66	CE(10)	used by CHKCONV, JOVERMU, JANDE	
31	C12	c_{12}	*	67-76	PH(10)	used by CHKCONV, JOVERMU, JANDE	
32	C13	c_{13}	*	77-86	CH(10)	used by CHKCONV, JOVERMU JANDE	
33	C14	c_{14}	*				
34	C15	c_{15}	*	87-96	DP(10)	used by CHKCONV, JOVERMU, JANDE	

Table X (Continued)

97-106	DC(10)	used by CHCONV, JOVERMU, JANDE		125	A	a	*
107	DMINI	(minimum difference allowed between predictor and corrector)	*	126	HAFUMSQ	$= 0.5\ v_{max}^2$	θ
				127	HPINU(1)	$= h$	
108	DMAXI	(maximum difference allowed between predictor and corrector)	*	128	HPINU(2)	$= \pi$ } set in HSTAR	
				129	HPINU(3)	$= \nu$	
109	EPSI	(relative error criterion for convergence)	*				
				130	W(1)	$W_1 = v_{max}$	θ
110	JO	(output unit, set = 6)	‡				
				131	W(2)	$W_2 = b_{15}$	θ
111	DELMU1	(initial interval for cruise)	*				
112	DELMU2	(initial interval for letdown)	*	132	W(3)	$W_3 = \frac{v_{max}}{W_4}$	θ
113	DELMU3	(initial interval for climbout)	*	133	W(4)	$W_4 = \sqrt{b_{17}}$	θ
114	EMU0	$\mu_o = 0$	‡	134	W(5)	$W_5 = \mu$(set by HSTAR)	
				135	W(6)		N
115	EMUF	μ_f	*	136	W(7)	$W_7 = \Delta_\pi$	θ
116	ESTART	$= h_o g + \frac{1}{2} v_o^2$	θ	137	W(8)	$W_8 = \Delta_h$	θ
				138	W(9)		N
117	IH	(used in HSTAR)		139	W(10)		N
118	V1S	(initial guess for v in VSTAR)	*	140-142	R(3)	$= R$ } set in RP123 $= (VR)^{-1}$	
119	EPSV1	(relative error criterion for convergence VSTAR)	*	143-151	PP(3,3)	$= \overline{VR}$ } set in HSTAR	
120	DELV1	(These inputs	N	152	EPS3	(relative error criterion for convergence HSTAR)	*
121	V2S	not used	N	153	GAM	γ (thermodynamic)	*
122	EPSV2	in present	N	154-163	U(10)	(set by TANDS for use in PARST)	
123	DELV2	program)	N				
124	PIMIN	π_{min}	*	164	G1K	$k_{g_1} = \frac{4.0}{1013.3}$	‡

Table X (Concluded)

165	G2G3K	$k_{g_1 g_2}$	*	210	BB(2)		N
				211	BB(3)		N
166-190	AG(25)	a_i i = 1...25	*	212	BB(4)		N
191	G1A1K	$= k_{g_1} a_1$	θ	213	BB(5)		N
192	G1A2K	$= k_{g_1} a_2$	θ	214	BB(6)		N
				215	BB(7)	$= 0.5\ b_{18} b_{19}$	θ
193	G1A3K	$= k_{g_1} a_3$	θ	216	BB(8)	$= 0.5\ b_{21} b_{18}$	θ
194	G1MINT	$g_1 T = 1$	‡	217	BB(9)		N
195	HALFS	$= \frac{1}{2} S$	θ	218	BB(10)		N
196	DJNUM	$= v_{max} - a$	θ	219	BB(11)		N
				220	BB(12)		N
197	SLAMB	λ^* (set in VSELECT)		221	BB(13)	THTMAX-B_{14}	θ
198	XLAMD	λ_o (set by CHKSTAR)		222	BB(14)		N
199	LTOG	(set by CHKSTAR)		223	BB(15)		N
200	NEEDLE	(used by CHKSTAR)		224	BB(16)		N
				225	BB(17)		N
201	EPSJR	(used by BAKN4TH to determine convergence)	*	226	BB(18)		N
202	THTMAX	θ_{max}	*	227	BB(19)		N
203	B21	$b_{21} = \frac{2b_{16}^2}{\gamma - 1 - b_{16}^2 b_{18}}$	θ	228-233	BB(20-25)		N
				234	GAMDRAG	cos γ (set by JANDE)	
204-205	TAU(2)	(used by BAKN4TH to determine convergence)	*	235	BLNK(1)	ESTAR	
				236	BLNK(2)	BT	
206	C17	c_{17}	*	237	XI	Ξ	
207	C18	c_{18}	*	238	CAPL	L	
208	C19	c_{19}	*	239	CAPGAM	Γ (set by DRAG)	
				240	W1	w_1	
209	BB(1)		N	241	TT	T	

2. Differential Equation Routines

Name: SUBROUTINE JOVERMU (ZMU,ZPT,ZEE,ZJJ,MXPT,KPTS,LPRNT)

Input: MXPT,LPRNT: MXPT is the dimension of the actual arrays (defined in the main program) which are represented by the formal array parameters ZMU,ZPI,ZEE,ZJJ.

Output: The values of μ ($0 \leq \mu \leq \mu_F$) are stored in array ZMU; corresponding values of π, E, and J are stored in ZPI, ZEE, and ZJJ, respectively. The total number of points thus stored in each of these arrays is KPTS.

Remarks: This subroutine integrates the J equation over the entire μ interval, from μ=0 to $\mu=\mu_F$. Values at μ_F are found by interpolation. Calls SUBROUTINE DJDMU to obtain $dJ/d\mu$. Integration is by means of Clippinger-Dimsdale formulas. Test for convergence at each integration step is made by SUBROUTINE CHKCONV.

Usage: Called by MAIN PROGRAM SST

Name: SUBROUTINE BAKN4TH (MXPT,ZMU,ZEE,ZPI,ZJJ,MXPO,YMU,YBB, YCC,YLAM,KPTS,LPRNT)

Input: ϵ_{RJ} : EPSRJ (in COMMON)

τ_1 : TAU(1) (in COMMON)

Formula(s): RJ = (ENDJX - ENDJ)/TAU(1)

Remarks: The entire integration scheme (described below) is executed for J=1 (letdown) first, and then with J=2 (climbout). At various places in this subroutine (see flow chart, Fig. 30) a quantity K is set either to 1, 2, or 3. These quantities J and K are tested by FUNCTION VSELECT in order to determine how v is to be computed. (See write-up of FUNCTION VSELECT.)

Usage: This is the principal executive subroutine, called by MAIN PROGRAM SST, which causes the integrations of the several systems of differential equations to be performed. The J and E equations (i.e., the performance and state

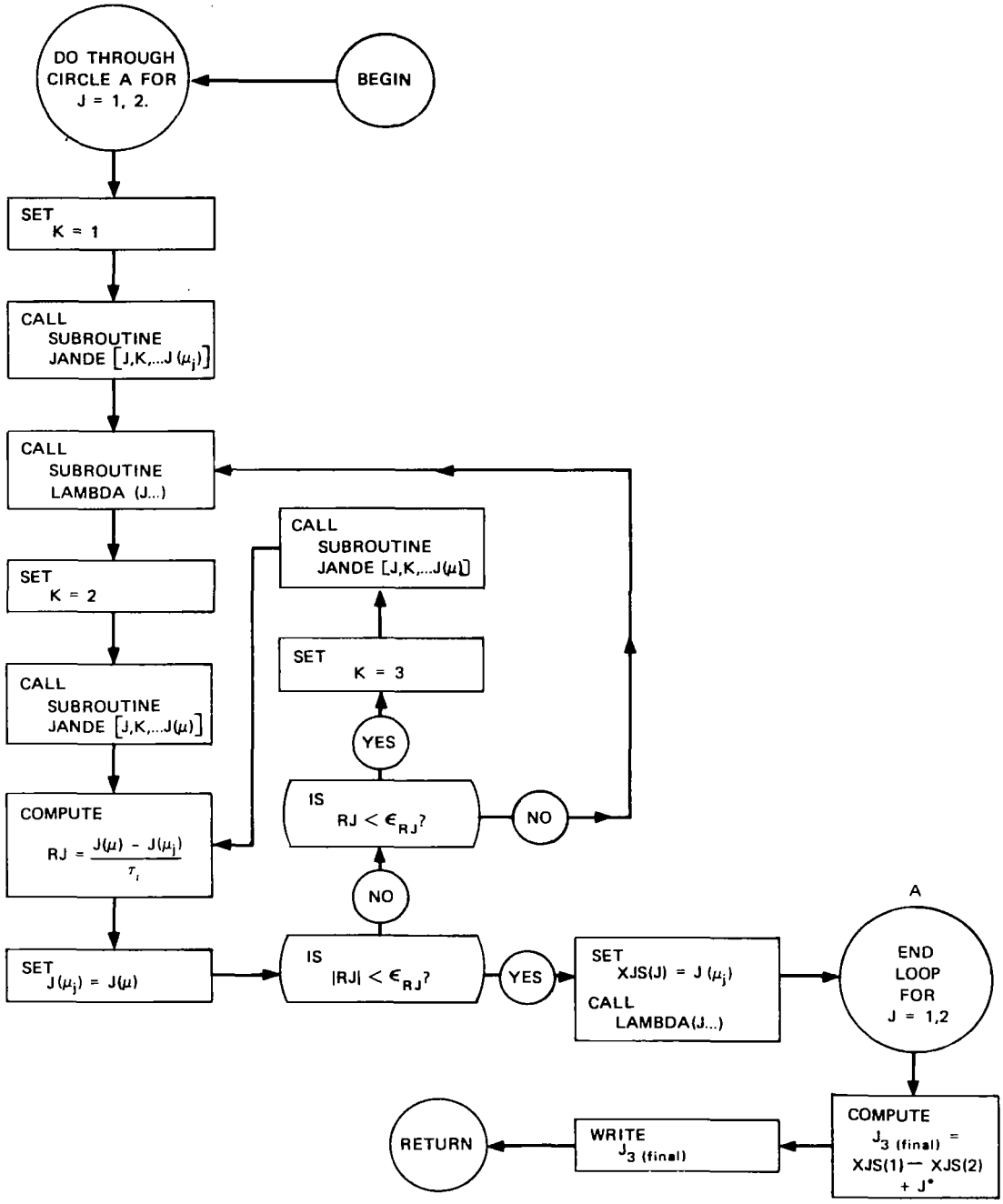

FIGURE 30 FLOW CHART FOR SUBROUTINE BAKN4TH

equations, respectively) are integrated by calling SUBROUTINE JANDE, and the λ-equation (adjoint) is integrated via SUBROUTINE LAMBDA. Each time (except the very first time) that the J and E system is integrated, a test is made to determine whether $|RJ| < \epsilon_{RJ}$. When this test is passed, the current phase--i.e., either "letdown" or "climbout"--is finished. (The formula for RJ is given above; ϵ_{RJ} is an input.)

Name: SUBROUTINE JANDE (J,K,MXPT,KPTS,ZMU,ZEE,ZPI,ZJJ,LPRNT, YLAM,MXPO,JPTS,YMU,YAA,YBB,YCC,ENDMU,ENDJ)

Input: J,K,MXPT,LPRNT (see JOVERMU for description of MXPT, LPRNT,ZMU,ZEE,ZPI,ZJJ).

Formula(s): This subroutine executes the integration of the J and E equations (performance and state equations, respectively) over the interval $\mu_2 \leq \mu \leq \mu_f$ = for "letdown," where μ_2 is determined by SUBROUTINE CHKSTAR--integration here is backwards, with $\Delta\mu$ negative. For "climbout" the integration is over the interval $\mu_0 \leq \mu \leq \mu_1$, where $\mu_0 = 0$ and μ_1 is determined by CHKSTAR and $\Delta\mu$ is positive here for forward integration.

Remarks: Calls FUNCTION CRUISE to set BT and ESTAR in COMMON. Calls FUNCTION VSELECT (L,J,K...) which uses K to determine manner of computing v. Calls SUBROUTINE DEDJ to obtain $dE/d\mu$ and $dJ/d\mu$. Integration is by means of Clippinger-Dimsdale method. Calls SUBROUTINE CHKSTAR to test for "cutoff" of integration in each phase (i.e., J = 1,2).

Usage: Called by SUBROUTINE BAKN4TH with J=1 and 2 (i.e., "letdown" and "climbout") and with K = 1, 2 or 3.

Name: SUBROUTINE LAMBDA (J,MXPO,YMU,YAA,YBB,YCC,JPTS,YLAM,LPRNT)

Input: J,μ_i,A_i,B_i,C_i (i = 1,...,JPTS): J,YMU( ), YAA( ), YBB( ), YCC( ). Also LPRNT--printing frequency; i.e., every LPRNTth integration step has results printed.

Output: λ_i(i = 1 ,...,JPTS) : YLAM( )

Formula(s): $\frac{d\lambda}{d\mu} = \lambda(B - C\lambda) - A$

Usage: Called by SUBROUTINE BAKN4TH. Employs Clippinger-Dimsdale integration scheme to solve $d\lambda/d\mu$ equation. Values of μ_i, A_i, B_i, C_i are furnished by previous integration of J and E equations. Hence the interval $\Delta\mu$ is predetermined and there is no convergence-checking, nor halving or doubling of the interval. The values of λ corresponding to the μ values are stored in order in the array YLAM(I). I = 1,...JPTS.

Name: SUBROUTINE CHKCONV (N,DELTA,DMIN,DMAX,CONV)

Input: N = the number of differential equations in the system; DELTA = the size of the interval at entry time; DMIN = the minimum difference allowed between predictor and corrector; DMAX = the maximum difference allowed between predictor and corrector; CONV = relative error tolerance.

Output:

Found in COMMON:

IDOUBL = toggle set to 1 when interval is doubled; otherwise, set to 0. (preset by calling routine)

IHALVE = toggle set to 1 when interval is halved; otherwise set to 0. (preset by calling routine)

IXFR = transfer switch set by CHKCONV to 1,2,or 3. (See REMARKS below)

Formula(s): $RE_i = \left| \frac{(CE_i - PE_i)}{\tau_i} \right|$, i = 1,...,N and PE, CE defined below.* If, for all i, $RE_i \leq$ CONV, then convergence is accepted at the present point. RE_i = relative error.

Remarks: (Figure 31 is the flow chart for this subroutine.) The following are found in COMMON:

IDOUBL, IHALVE (defined above); IXFR, defined above, which becomes the index of a "computed go to" statement in the calling routine, immediately upon reentry thereto;

---

* τ_i, i = 1,2 in COMMON as TAU(1), TAU(2).

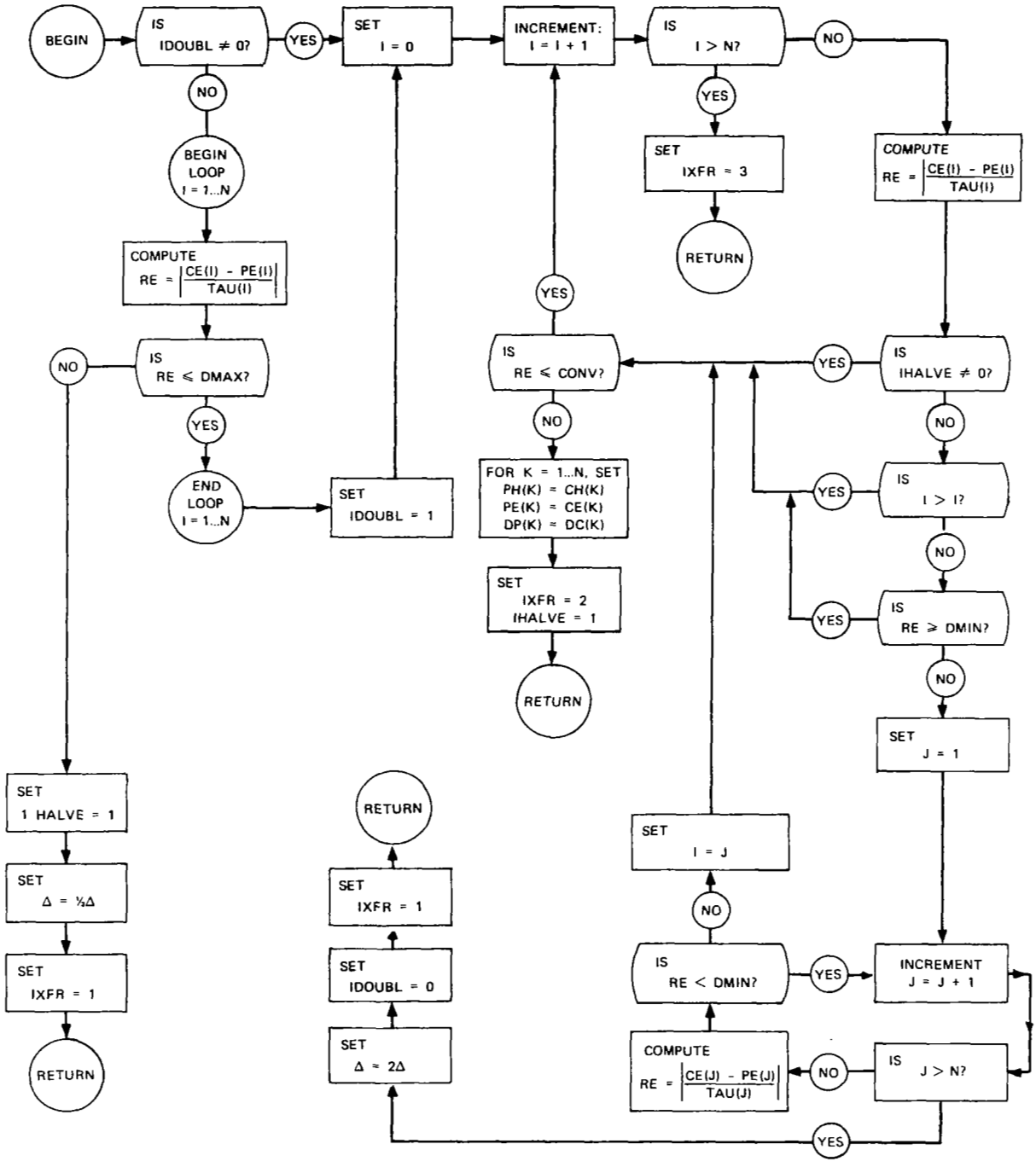

FIGURE 31 FLOW CHART FOR **SUBROUTINE CHKCONV, N, DELTA, DMIN, DMAX, CONV**

PE( ) contains predicted values at endpoint of the interval.
CE( ) contains corrected values at endpoint of the interval.
PH( ) contains predicted values at midpoint of the interval.
CH( ) contains corrected values at midpoint of the interval.
DP( ) contains derivatives at the endpoint, using predictors.
DC( ) contains derivatives at the endpoint, using correctors.

} These arrays are all prefilled by the calling subroutine.

PE, CE, PH, CH, DP, DC all dimensioned 10.

Usage: This is a convergence-checking (CHKCONV) subroutine, used in conjunction with and called by JANDE and JOVERMU, which solve systems of differential equations by the method of Clippinger-Dimsdale. This subroutine (CHKCONV) is used only when the interval (called h or Δ), i.e., DELTA, is permitted to be altered by halving or doubling.

3. Optimization Routines

Name: SUBROUTINE HSTAR (EMU,H,PI)

Input: μ: EMU
COMMON v_{max}, θ, M_n, v_s : W(1), W(2), W(3), W(4)

Output: h, π : H, PI
COMMON μ : W(5)

Formula(s): $R_1 (h, \pi, \nu) = D - T$

$$R_2 (h, \pi, \nu) = \frac{\partial T}{\partial p} + \frac{\partial s}{\partial p} \nu - \frac{\partial D}{\partial \rho} \frac{\partial \rho}{\partial p}$$

$$R_3 (h, \pi, \nu) = \frac{\partial T}{\partial \pi} + \frac{\partial s}{\partial \pi} \nu$$

Remarks: HSTAR solves the system $R_1 = R_2 = R_3 = 0$ for h, π, and ν using Newton's method. The following subroutines are called by HSTAR:

SETHPN, which computes an initial guess of h, π, and ν the first time HSTAR is called.

RP123, which computes R_1, R_2, R_3 and the Jacobian matrix for the system.

Usage: HSTAR is called by DJDMU

Name: SUBROUTINE RP123

Input: (all in COMMON)

$W(1) = v$, $W(2) = \theta$, $W(3) = M_n$, $W(4) = v_s$, $W(5) = \pi$
$W(7) = \Delta\pi$, $W(8) = \Delta h$, $HPINU(1) = h$, $HPINU(2) = \pi$, $HPINU(3) = \nu$, and also the constants G, B3, B5, B11, B12, B13, $EMO(m_o)$

Output:

$$R = \begin{pmatrix} R_1(h,\pi,\nu) \\ R_2(h,\pi,\nu) \\ R_3(h,\pi,\nu) \end{pmatrix} \text{ and } \nabla R \begin{pmatrix} \frac{\partial R_1}{\partial h} & \frac{\partial R_1}{\partial \pi} & \frac{\partial R_1}{\partial \nu} \\ \frac{\partial R_2}{\partial h} & \frac{\partial R_2}{\partial \pi} & \frac{\partial R_2}{\partial \nu} \\ \frac{\partial R_3}{\partial h} & \frac{\partial R_3}{\partial \pi} & \frac{\partial R_3}{\partial \nu} \end{pmatrix}$$

R is stored in R(1), R(2), R(3); ∇R is stored in RP(3,3). R(3) and RP(3,3) are in COMMON.

Formula(s):

$$\frac{\partial R_1}{\partial h} = \frac{\partial D}{\partial \rho}\frac{\partial \rho}{\partial p} - \frac{\partial T}{\partial p}\frac{dp}{dh}\ ;\ \frac{\partial R_1}{\partial \pi} = -\frac{\partial T}{\partial \pi}\ ;\ \frac{\partial R_1}{\partial \nu} = 0\ ;$$

$$\frac{\partial R_2}{\partial h} = \frac{R_2(h+\Delta h,\pi,\nu) - R_2(h,\pi,\nu)}{\Delta h};\ \frac{\partial R_2}{\partial \pi} = \frac{R_2(h,\pi+\Delta\pi,\nu) - R_2(h,\pi,\nu)}{\Delta\pi};\ \frac{\partial R_2}{\partial \nu} = \frac{\partial s}{\partial p};$$

$$\frac{\partial R_3}{\partial h} = \frac{R_3(h+\Delta h,\pi,\nu) - R_3(h,\pi,\nu)}{\Delta h};\ \frac{\partial R_3}{\partial \pi} = \frac{R_3(h,\pi+\Delta\pi,\nu) - R_3(h,\pi,\nu)}{\Delta\pi};\ \frac{\partial R_3}{\partial \nu} = \frac{\partial s}{\partial \pi}$$

Remarks: This subroutine uses the following subprograms:

(1) FUNCTION DRAG to obtain D

(2) FUNCTION PRHOP to obtain $\partial\rho/\partial p$

(3) FUNCTION DPH to obtain dp/dh

(4) SUBROUTINE PARD(J,...), with J=0, to obtain $\partial D/\partial\rho$

(5) SUBROUTINE TANDS to obtain T and s

(6) SUBROUTINE PARST (J,...), with J=1, to obtain

$$\frac{\partial T}{\partial p},\ \frac{\partial s}{\partial p},\ \frac{\partial T}{\partial \pi} \text{ and } \frac{\partial s}{\partial \pi} \ .$$

Usage: This subroutine is called by SUBROUTINE HSTAR (EMU,H,PI) in order to obtain the function vector R (see HSTAR for equations) and its Jacobian matrix ∇R for the Newton-Raphson iterative solution for h, π, and ν.

Name: SUBROUTINE SETHPN

Input: (all in COMMON): W(1) = v, W(2) = θ, W(3) = M_n, W(5) = μ. G=g, B3 , B5 , B11, B12, B13, EMO=m_o, G2G3K=kg_2g_3, G1A1K=$kg_1 \cdot a_1$, G1A2K=$kg_1 \cdot a_2$, G1A3K=$kg_1 \cdot a_3$, GIMNT= g_1T and coefficients a_i in AG( ) and HALFS = S/2.

h, π, v : HPINU(1), HPINU(2), HPINU(3)

Formula(s):

$$h = \frac{-10^4}{1.57}\left[\ell n\ \frac{p}{194} - 1.884\right] \text{ , where } p = \frac{\rho(\theta + 273)}{0.348}$$

$$\text{and } p = \frac{(m_o - \mu)g}{\frac{S}{2}v^2}\sqrt{\frac{f_D^L(M_n)}{f_D^o(M_n)}} \ .$$

$$\pi = -\frac{q_2}{2q_1} - \sqrt{\left(\frac{q_2}{2q_1}\right)^2 + \frac{1}{q_1}\left[\frac{D}{p\left(1 + \frac{\gamma-1}{2} M_n^2\right)^{\frac{\gamma}{\gamma-1}} \cdot g_1(M_n)} - q_3\right]},$$

where

$$q_1 = \begin{cases} a_6 \theta T^2 + a_9 \theta T + a_{12} & , \text{ if } \theta T \geq k g_2 g_3 \\ a_{15} \theta T + a_{18} & , \text{ if } \theta T < k g_2 g_3 \end{cases}$$

$$q_2 = \begin{cases} a_5 \theta T^2 + a_8 \theta T + a_{11} & , \text{ if } \theta T \geq k g_2 g_3 \\ a_{14} \theta T + a_{17} & , \text{ if } \theta T < k g_2 g_3 \end{cases}$$

$$q_3 = \begin{cases} a_4 \theta T^2 + a_7 \theta T + a_{10} & , \text{ if } \theta T \geq k g_2 g_3 \\ a_{13} \theta T + a_{16} & , \text{ if } \theta T < k g_2 g_3 \end{cases}$$

Usage: Called only once during any given program run by SUBROUTINE HSTAR in order to yield initial guesses for h, π, and v to start off the Newton-Raphson solution of (R_1, R_2, R_3). These initial guesses are:

(1) h such that $\partial D/\partial p = 0$;

(2) π such that $T = D$;

(3) $v = 0$.

Name: FUNCTION VSTAR (J,E,EMU,PI,VIN,EPS)

Input: $E, \mu, \pi, v_{in}, \epsilon$: E,EMU,PI,VIN,EPS

COMMON g, b_1, b_3, b_4, b_{14}, b_{15}, b_{16}, a, $k_{g_2g_3}$, λ^*, cos γ, E^*, b : G, B1, B3, VOID2(1), B14, B15, B16, A, G2G3K, SLAMB, GAMDRAG, ESTAR,-BT

Output: $v^*(E,\mu)$

Formula(s):

$$QQ = \pm \frac{v(T-D) + \lambda^*(v \cos\gamma - a)}{s + b(v \cos\gamma - a)}$$

$$Q = \pm \frac{v\left(\frac{dT}{dv} - \frac{dD}{dv}\right) + (T-D)\left(\frac{1}{v} - \frac{b\cos\gamma + \frac{ds}{dv}}{s + b(v\cos\gamma - a)}\right) + \lambda^*\left[\cos\gamma - (v\cos\gamma - a)\frac{b\cos\gamma + \frac{ds}{dv}}{s + b(v\cos\gamma - a)}\right]}{s + b(v\cos\gamma - a)}$$

+ used for climbout, - used for letdown

$$\frac{dQ}{dv} \approx \frac{Q[v + 0.001v\ \mathrm{sgn}(Q)] - Q(v)}{0.001v\ \mathrm{sgn}(Q)}$$

Remarks: This routine finds the v that maximizes QQ for fixed E and μ as follows: Q, the derivative of QQ with respect to v, is continuous except for v such that $\theta + 273 = kg_2g_3$ and v such that $h = b_1$ (i.e., $h = h_{TROP}$). The routine first computes QQ for these two values of v and for v_{in}, the previous value of v^* and sets $\tilde{v}$ (VT) equal to the one for which QQ is greatest. Next the routine checks to see whether $\tilde{v}$ is the maximizing v by computing $\tilde{v} + 0.001\tilde{v}$ and $\tilde{v} - 0.001v$. If $\tilde{v}$ is not the maximizing v then v is found by solution of Q = 0 by Newton's method, where $d\theta/dv$ is approximated as above and the maximum step in v is limited to 0.1 v.

Usage: Performed by VSELECT

4. Atmosphere

Name: SUBROUTINE PTRVSM (H,V,P,THETA,RHO,VS,EMN)

Input: h,v: H,V

Output: $p, \theta, \rho, v_s, M_n$: P,THETA,RHO,VS,EMN

Formula(s):

$$p = \begin{cases} B10[1 - B6(h - B4)]^{B9} & \text{if } h \leq B4 \\ B11 \exp(B12 + h \cdot B5) & \text{if } h > B4 \end{cases}$$

$$\theta = \begin{cases} h \cdot B1 + B14 & \text{if } h \leq B4 \\ B15 & \text{if } h > B4 \end{cases}$$

$$\rho = \frac{p \cdot B13}{\theta + B3}$$

$$Vs = B16\sqrt{\theta + B3}$$

$$M_n = \frac{v}{Vs}$$

Remarks: The following constants are found in COMMON: B1, B3, B4, B5, B6, B9, B10, B11, B12, B13, B14, B15, B16.

Usage: Called frequently throughout program. Calls made by DJDMU, STANDD.

Name: FUNCTION DTHH(H)

Input: h: H

Output: $\frac{d\theta}{dh}$

Formula(s):

$$\frac{d\theta}{dh} = \begin{cases} B1 & \text{if } h \leq B4 \\ 0 & \text{if } h > B4 \end{cases}$$

Remarks: B1 and B4 are found in COMMON

Usage: Referenced by DDV, DDE, DSTE, DSTV

Name: FUNCTION DPH (H,P)

Input: h,p: H,P

Output: $\frac{dp}{dh}$

Formula(s):

$$\frac{dp}{dh} = \begin{cases} B7[1 - B6(h - B4)]^{B8} & \text{if } h \leq B4 \\ p \cdot B5 & \text{if } h > B4 \end{cases}$$

Remarks: The following constants are found in COMMON: B4, B5, B6, B7, B8.

Usage: Frequent use throughout program. Referenced by DDV, DDE, DSTE, DSTV, RP123.

Name: FUNCTION PRHOP (RHO,P)

Input: ρ,p: RHO,P

Output: $\frac{\partial \rho}{\partial p}$

Formula(s): $\frac{\partial \rho}{\partial p} = \frac{\rho}{p}$

Usage: Referenced by DDV, DDE, and RP123

Name: FUNCTION PRHOTH (RHO,THETA)

Input: ρ, θ: RHO,THETA

Output: $\frac{\partial \rho}{\partial \theta} = -\frac{\rho}{\theta + B3}$

Remarks: B3 found in COMMON

Usage: Referenced by DDV and DDE

Name: SUBROUTINE PMNVTH (V,VS,PMNV,PMNTH)

Input: v, v_s : V,VS

Output: $\frac{\partial M_n}{\partial v}$, $\frac{\partial M_n}{\partial \theta}$: PMNV,PMNTH

Formula(s): $$\frac{\partial M_n}{\partial v} = \frac{B2}{v_s}$$

$$\frac{\partial M_n}{\partial \theta} = \frac{B2}{v_s^3} \cdot v$$

Remarks: B2 found in COMMON

Usage: Called by DDV, DDE, DSTE, DSTV

Name: SUBROUTINE GAMMA(GAMM)

Input: Uses the constant GAM in COMMON

Output: γ : GAMM

Formula(s): γ is set equal to the input constant GAM

GAMM = GAM

Remarks: Although at present (i.e., as of October 1969) γ is simply set equal to an input constant, this is done by means of a subroutine in order that a more complicated expression may, if desired, by substituted at a later date.

Usage: Called by SUBROUTINE TANDS

5. Aerodynamics

Name: SUBROUTINE DRAG (RHO,V,EMN,EMU,T,D)

Input: ρ, v, M_n, μ, T : RHO,V,EMN,EMU
COMMON T, cos γ, $\frac{s}{2}$: T, GRAMDRAG, HALFS

Output: $D(\rho, v, M_n, \mu, T)$
COMMON Ξ, L, Γ, w_1, T : XI,CAPL,CAPGAM,W1,TT

Formula(s): $w_1 = m_o\ g \cos\gamma \qquad \Gamma = \frac{s}{2}\rho v^2 \qquad \Xi = T/\Gamma\ f_L(M_n)$

$$L = w_1/(1 + \Xi)$$

$$D = \Gamma\ f_D^{\circ}(M_n) + \frac{L^2}{\Gamma} f_D^{L}(M_n)$$

Remarks: This subroutine must be preceded by TANDS; g and m_o are found in COMMON as G and EMO. $f_D^{\circ}(M_n)$, $f_D^{L}(M_n)$, and $f_L(M_n)$ are obtained by calling FDOL and FLMN with J = 0.

Usage: Called by RP123 and STANDD

Name: SUBROUTINE PARD (J,RHO,V,EMN,EMU,PDRHO,PDV,PDMN)

Input: J, ρ, v, M_n, μ: J,RHO,V,EMN,EMU
COMMON L, Ξ, Γ: CAPL,XI,CAPGAM

Output: If J = 0 then $\frac{\partial D}{\partial \rho}$ only; PDRHO

If J $\neq$ 0 then in addition $\frac{\partial D}{\partial v}$ and $\frac{\partial D}{\partial M_n}$; PDV,PDMN

Formula(s):

$$\frac{\partial D}{\partial \rho} = \frac{1}{\rho}\left[\Gamma\ f_D^{\circ} - \frac{L^2}{\Gamma} f_D^{L}\left(1 - \frac{2\ \Xi}{1 + \Xi}\right)\right]$$

$$\frac{\partial D}{\partial v} = \frac{2}{v}\left[\Gamma\ f_D^{\circ} - \frac{L^2}{\Gamma} f_D^{L}\left(1 - \frac{2\ \Xi}{1 + \Xi}\right)\right]$$

$$\frac{\partial D}{\partial M_n} = \Gamma\ \frac{df_D^{\circ}}{dM_n} + \frac{L^2}{\Gamma}\left(\frac{df_D^2}{dM_n} + \frac{f_D^2}{f_L} \cdot \frac{2\ \Xi}{1 + \Xi}\ \frac{df_L}{dM_n}\right)$$

Remarks: **This subroutine must be preceded by TANDS and DRAG.**

FDOL is called for f_D° , f_D^L and $\frac{df_L}{dM_n}$ if needed.

FLMN is called for f_L and $\frac{df_L}{dM_n}$ if needed.

Usage: Called with J ≠ 0 by DDV and DDE and with J = 0 by RP123

Name: FUNCTION PARDMU (EMN,EMDMMU,T,D)

Input: $m_o - \mu$, M_n : EMOMMU,EMN
COMMON Ξ, L, Γ, w_1 : XI,CAPL,CAPGAM,W1

Output: $\frac{\partial D}{\partial \mu}$: PARDMU

Formula(s):

$$\frac{\partial D}{\partial \mu} = -2L\, f_D^L \frac{g^2(m_o - \mu)}{w_1 \Gamma(1 + \Xi)}$$

Remarks: Must be preceded by TANDS and DRAG. Uses FDOL with j = 0 to compute f_D^L .

Usage: Called by ABANDC

Name: FUNCTION DDV (H,V,P,RHO,THETA,VS,EMN,EMU)

Input: $h, v, p, \rho, \theta, v_s, M_n, \mu$: H,V,P,RHO,THETA,VS,EMN,EMU

Output: $\frac{dD}{dv}$

Formula(s):

$$\frac{dD}{dv} = \frac{\partial D}{\partial \rho}\left[\frac{\partial \rho}{\partial p}\frac{dp}{dh} + \frac{\partial \rho}{\partial \theta}\frac{d\theta}{dh}\right]\frac{\partial h}{\partial v} + \frac{\partial D}{\partial v} + \frac{\partial D}{\partial M_n}\left[\frac{\partial M_n}{\partial v} + \frac{\partial M_n}{\partial \theta}\frac{d\theta}{dh}\frac{\partial h}{\partial v}\right]$$

Remarks: Uses SUBROUTINE PARD to obtain $\frac{\partial D}{\partial \rho}$, $\frac{\partial D}{\partial v}$ and $\frac{\partial D}{\partial M_n}$; uses FUNCTION PHV to obtain $\frac{\partial h}{\partial v}$; uses FUNCTION DTHH to obtain $\frac{d\theta}{dh}$; uses SUBROUTINE PMNVTH to obtain $\frac{\partial M_n}{\partial v}$ and $\frac{\partial M_n}{\partial \theta}$; uses FUNCTION PRHOP to obtain $\frac{\partial \rho}{\partial p}$; uses FUNCTION DPH to obtain $\frac{dp}{dh}$; uses FUNCTION PRHOTH to obtain $\frac{\partial \rho}{\partial \theta}$.

Usage: Called by VSTAR, ABANDC

Name: FUNCTION DDE(H,V,P,RHO,THETA,VS,EMN,EMU)

Input: $h, v, p, \rho, \theta, v_s, M_n, \mu$: H,V,P,RHO,THETA,VS,EMN,EMU

Output: $\frac{dD}{dE}$

Formula(s): $$\frac{dD}{dE} = \frac{1}{g}\left[\frac{\partial D}{\partial \rho}\left(\frac{\partial \rho}{\partial p}\frac{dp}{dh} + \frac{\partial \rho}{\partial \theta}\frac{d\theta}{dh}\right) + \frac{\partial D}{\partial M_n}\frac{\partial M_n}{\partial \theta}\frac{d\theta}{dh}\right]$$

Remarks: G(g) found in COMMON. Calls SUBROUTINE PARD (1,RHO...) to obtain $\frac{\partial D}{\partial \rho}$ and $\frac{\partial D}{\partial M_n}$; calls SUBROUTINE DMNVTH to obtain $\frac{\partial M_n}{\partial \theta}$; references FUNCTION DTHH for $\frac{d\theta}{dh}$; FUNCTION PRHOP for $\frac{\partial \rho}{\partial p}$; FUNCTION DPH for $\frac{dp}{dh}$; FUNCTION PRHOTH for $\frac{\partial \rho}{\partial \theta}$

Usage: Referenced by SUBROUTINE ABANDC

Name: SUBROUTINE FDOL (J,EMN,FDO,FDL,DFDO,DFDL)

Input: J, M_n : J,EMN

Output: If $J = 0$, $f_D^\circ(M_n)$ and $f_D^L(M_n)$ only: FDO, FDL

If $J \neq 0$, then in addition $\frac{df_D^\circ}{dM_n}$ and $\frac{df_D^\circ}{dM_n}$: DFDO,DFDL

Formula(s):

$$f_D^{\circ}(M_n) = \begin{cases} C_2 & \text{if } M_n \le C_1 \\ \left(C_4 M_n^2 + C_5 M_n + C_6\right) e^{C_7 M_n} + C_8 e^{C_9 M_n} + C_3 , & \text{if } M_n > C_1 \end{cases}$$

$$f_D^{L}(M_n) = \begin{cases} C_{10} & \text{if } M_n \le C_1 \\ \left(C_{11} M_n^2 + C_{12} M_n + C_{13}\right) e^{C_{14} M_n} + C_{15} e^{C_{16} M_n} , & \text{if } M_n > C_1 \end{cases}$$

$$\frac{df_D^{\circ}(M_n)}{dM_n} = \begin{cases} 0 , & \text{if } M_n \le C_1 \\ \left[C_7\left(M_n^2 + C_5 M_n + C_6\right) + 2C_4 M_n + C_5\right] e^{C_7 M_n} + C_8 C_9 e^{C_9 M_n} , & \text{if } M_n > C_1 \end{cases}$$

$$\frac{df_D^{L}(M_n)}{dM_n} = \begin{cases} 0 & \text{if } M_n \le C_1 \\ \left[C_{14}\left(C_{11} M_n^2 + C_{12} M_n + C_{13}\right) + 2C_{11} M_n + C_{12}\right] e^{C_{16} M_n} + C_{14} C_{16} e^{C_{16} M_n} , & \text{if } M_n > C_1 \end{cases}$$

Remarks: Constants C_1 through C_{16} are found in COMMON

Usage: Called by DRAG, PARD, PARST, SETHPN, PARDMU

Name: SUBROUTINE FLMN(J,EMN,FL,DFL)

Input: j, M_n : J,EMN

Output: for $j = 0$ $f_L(M_n)$: FL

for $j \neq 0$ $f_L(M_n)$, $\frac{df_L}{dM_n}$: FL,DFL

Formula(s):

$$f_L(M_n) = \begin{cases} C_{17} & \text{if } M_n \leq C_1 \\ C_{17} + C_{18}(M_n - C_1)^2 e^{C_{17}M_n} & \text{if } M_n > C_1 \end{cases}$$

$$\frac{df_L}{dM_n}(M_n) = \begin{cases} 0 & \text{if } M_n \leq C_1 \\ C_{18}\left[(M_n - C_1)^2 C_{19} + 2(M_n - C_1)\right] e^{C_{19}M_n} & \text{if } M_n > C_1 \end{cases}$$

Remarks: Constants C_1 and C_{17}, to C_{19} found in COMMON

Usage: Called by PARD,DRAG

6. Engine

Name: SUBROUTINE TANDS (PI,THETA,EMN,P,S,T)

Input: π, θ, M_n, p : PI,THETA,EMN,P and also B3 in COMMON

Output: s,T : S,T

Formula(s):

$$s = p\left(1 + \frac{\gamma - 1}{2} M_n^2\right)^{\frac{\gamma}{\gamma - 1}} g_1(M_n) g_3(\pi, \theta_T)$$

$$T = p\left(1 + \frac{\gamma - 1}{2} M_n^2\right)^{\frac{\gamma}{\gamma - 1}} g_1(M_n) g_2(\pi, \theta_T) \quad ,$$

where

$$\theta_T = \left(1 + \frac{\gamma - 1}{2} M_n^2\right)(\theta + 273)$$

Remarks: SUBROUTINE GAMMA (GAMM) is called to obtain γ (GAMM). SUBROUTINE G1G2G3 (EMN, PI, THETAT, G1, G2, G3) is called to obtain $g_1(M_n)$, $g_2(\pi, \theta_T)$ and $g_3(\pi, \theta_T)$.

Usage: Frequent use during program

N.B. Since all calls upon SUBROUTINE PARST are immediately preceded by a call upon this subroutine (TANDS), certain quantities computed during TANDS are saved in COMMON in array U ( ), for subsequent (possible) use by PARST.

These are:

$U(1) = \gamma$

$U(2) = \gamma - 1$

$U(3) = \theta + 273$

$U(4) = g_1(M_n)$

$U(5) = g_2(\pi, \theta_T)$

$U(6) = g_3(\pi, \theta_T)$

$$U(7) = 1 + \frac{\gamma - 1}{2} M_n^2$$

$$U(8) = \left(1 + \frac{\gamma - 1}{2} M_n^2\right)^{\frac{\gamma}{\gamma - 1}}$$

$$U(9) = p\left(1 + \frac{\gamma - 1}{2} M_n^2\right)^{\frac{\gamma}{\gamma - 1}}$$

$$\nu(10) = p\left(1 + \frac{\gamma - 1}{2} M_n^2\right)^{\frac{\gamma}{\gamma - 1}} g_1(M_n)$$

Name: SUBROUTINE PARST (J,P,PI,THETA,EMN,PTTH,PSTH, PTMN,PSMN,PTP,PSP,PTPI,PSPI) No. 25

Input: J, p, π, θ, M_n : J,P,PI,THETA,EMN and also U(i),I = 1-10, in COMMON, COMMON (see Remarks below).

Output: If $J \neq 0$: $\frac{\partial T}{\partial p}$, $\frac{\partial s}{\partial p}$, $\frac{\partial T}{\partial \pi}$, $\frac{\partial s}{\partial \pi}$: PTP, PSP, PTPI, PSPI

If $J = 0$: $\frac{\partial T}{\partial \theta}$, $\frac{\partial s}{\partial \theta}$, $\frac{\partial T}{\partial M_n}$, $\frac{\partial s}{\partial M_n}$, $\frac{\partial T}{\partial p}$, $\frac{\partial s}{\partial p}$: PTTH, PSTH, PTMN,PSMN, PTP, PSP

Formula(s): $\frac{\partial T}{\partial p} = \text{FAC } 2\left(1 + \frac{\gamma - 1}{2} M_n^2\right)^{\frac{\gamma}{\gamma - 1}} \cdot g_1 \cdot g_2$;

$$\frac{\partial s}{\partial p} = \left(1 + \frac{\gamma - 1}{2} M_n^2\right)^{\frac{\gamma}{\gamma - 1}} \cdot g_1 \cdot g_3 \quad ;$$

$$\frac{\partial T}{\partial \pi} = \text{FAC } 2 \cdot p\left(1 + \frac{\gamma - 1}{2} M_n^2\right)^{\frac{\gamma}{\gamma - 1}} \cdot g_1 \cdot \frac{\partial g_2}{\partial \pi} \quad ;$$

$$\frac{\partial s}{\partial \pi} = p\left(1 + \frac{\gamma - 1}{2} M_n^2\right)^{\frac{\gamma}{\gamma - 1}} \cdot g_1 \cdot \frac{\partial g_3}{\partial \pi} \quad ;$$

$$\frac{\partial T}{\partial \theta} = \text{FAC } 2 \cdot p\left(1 + \frac{\gamma - 1}{2} M_n^2\right)^{\frac{2\gamma - 1}{\gamma - 1}} \cdot g_1 \cdot \frac{\partial g_2}{\partial \theta_T} \quad ;$$

$$\frac{\partial s}{\partial \theta} = p\left(1 + \frac{\gamma - 1}{2} M_n^2\right)^{\frac{2\gamma - 1}{\gamma - 1}} \cdot g_1 \cdot \frac{\partial g_3}{\partial \theta_T}$$

$$\frac{\partial T}{\partial M_n} = \text{FAC 2} \cdot p\left(1 + \frac{\gamma - 1}{2} M_n^2\right)^{\frac{\gamma}{\gamma - 1}} \left[g_2 \cdot \frac{dg_1}{dM_n} + g_1(\gamma - 1)M_n(\theta + 273) \frac{\partial g_2}{\partial \theta_T} \right]$$

$$+ p\gamma M_n g_1 g_2 \left(1 + \frac{\gamma - 1}{2} M_n^2\right)^{\frac{1}{\gamma - 1}}$$

$$\frac{\partial s}{\partial M_n} = p\left(1 + \frac{\gamma - 1}{2} M_n^2\right)^{\frac{\gamma}{\gamma - 1}} \left[g_3 \cdot \frac{dg_1}{dM_n} + g_1(\gamma - 1)M_n(\theta + 273) \frac{\partial g_3}{\partial \theta_T} \right]$$

$$+ p\gamma M_n g_1 g_3 \left(1 + \frac{\gamma - 1}{2} M_n^2\right)^{\frac{1}{\gamma - 1}}$$

$$\text{FAC 2} = 1 - = f_D^L \cdot \Xi \cdot \frac{L^2}{T\Gamma(1 + \Xi)}$$

Remarks: This subroutine must be preceded by TANDS and DRAG. The following subprograms are used by this subroutine:

(1) SUBROUTINE PΘ23PI to obtain $\frac{\partial g_2}{\partial \pi}$ and $\frac{\partial g_3}{\partial \pi}$

(2) SUBROUTINE PΘ23TH to obtain $\frac{\partial g_2}{\partial \theta_T}$ and $\frac{\partial g_3}{\partial \theta_T}$

(3) FUNCTION DGIMN to obtain $\frac{dg_1}{dM_n}$

(4) SUBROUTINE FDOL to obtain FDL.

Usage: Called with J = 0 by SUBROUTINE DSTV, and with J ≠ 0 by SUBROUTINE RP123

Name: SUBROUTINE G1G2G3(EMN,PI,THETAT,G1,G2,G3)

Input: M_n, π, θ_T : EMN,PI,THETAT

Output: $g_1(M_n)$, $g_2(\pi,\theta_T)$, $g_3(\pi,\theta_T)$: G1, G2, G3

Formula(s):

$$g_1(M_n)=\begin{cases} kg_1 \cdot a_1 & \text{if } M_n \le g_1^T \\ kg_1(a_2 + a_3 M_n) & \text{if } M_n > g_1^T \end{cases}$$

$$g_2(\pi,\theta_T) = \begin{cases} \theta_T^2(a_4 + a_5\pi + a_6\pi^2) + \theta_T(a_7 + a_8\pi + a_9\pi^2) + a_{10} + a_{11}\pi + a_{12}\pi^2, & \text{if } \theta_T \ge kg_2g_3 \\ \theta_T(a_{13} + a_{14}\pi + a_{15}\pi^2) + a_{16} + a_{17}\pi + a_{18}\pi^2, & \text{if } \theta_T < kg_2g_3 \end{cases}$$

$$g_3(\pi,\theta_T) = \begin{cases} \pi(a_{19}\theta_T^2 + a_{20}\theta_T + a_{21}), & \text{if } \theta_T \ge kg_2g_3 \\ \pi(a_{22}\theta_T + a_{23}), & \text{if } \theta_T < kg_2g_3 \end{cases}$$

Remarks: g_1^T = GIMNT (in COMMON); $kg_1 \cdot a_1$ = G1A1K (in COMMON); $kg_1 \cdot a_2$ = G1A2K (in COMMON); $kg_1 \cdot a_3$ = G1A3K (in COMMON); kg_2g_3 = G2G3K (in COMMON); the coefficients a_i in array AG( ) in COMMON

Usage: Called by SUBROUTINE TANDS

Name: FUNCTION DGIMN (EMN)

Input: M_n : EMN

Output: $\dfrac{dg_1}{dM_n}$

Formula(s): $$\frac{dg_1}{dM_n} = \begin{cases} 0 & M_n \le g_1T \\ kg_1 \cdot a_3 & M_n > g_1T \end{cases}$$

Remarks: g_1T = G1MNT in COMMON

$kg_1 \cdot a_3$ = G1A3K in COMMON

Usage: Called by SUBROUTINE PARST

Name: SUBROUTINE PG23PI(PI,THETAT,G2PI,G3PI)

Input: π, θ_T : PI,THETAT

Output: $\frac{\partial g_2}{\partial \pi}$, $\frac{\partial g_3}{\partial \pi}$: G2PI, G3PI

Formula(s): $$\frac{\partial g_2}{\partial \pi} = \begin{cases} \theta_T^2(a_5 + 2\pi a_6) + \theta_T(a_8 + 2\pi a_9) + a_{11} + 2\pi a_{12} , & \text{if } \theta_T \ge kg_2g_3 \\ \theta_T(a_{14} + 2\pi a_{15}) + a_{17} + 2\pi a_{18} , & \text{if } \theta_T < kg_2g_3 \end{cases}$$

$$\frac{\partial g_3}{\partial \pi} = \begin{cases} a_{19}\theta_T^2 + a_{20}\theta_T + a_{21} , & \text{if } \theta_T \ge kg_2g_3 \\ a_{22}\theta_T + a_{23} , & \text{if } \theta_T < kg_2g_3 \end{cases}$$

Remarks: kg_2g_3 = G2G3K (in COMMON); the coefficients a_i in array AG ( ) in COMMON

Usage: Called by SUBROUTINE PARST

Name: SUBROUTINE PG23TH(PI,THETAT,G2TH,G3TH)

Input: π, θ_T : PI,THETAT

Output: $\frac{\partial g_2}{\partial \theta_T}$, $\frac{\partial g_3}{\partial \theta_T}$: G2TH, G3TH

Formula(s):

$$\frac{\partial g_2}{\partial \theta_T} \begin{cases} 2\theta_T(a_4 + a_5\pi + a_6\pi^2) + a_7 + a_8\pi + a_9\pi^2, & \text{if } \theta_T \geq kg_2g_3 \\ a_{13} + a_{14}\pi + a_{15}\pi^2, & \text{if } \theta_T < kg_2g_3 \end{cases}$$

$$\frac{\partial g_3}{\partial \theta_T} \begin{cases} \pi(2a_{19}\theta_T + a_{20}), & \text{if } \theta_T \geq kg_2g_3 \\ a_{22}\pi, & \text{if } \theta_T < kg_2g_3 \end{cases}$$

Remarks: kg_3g_3 = G2G3K (in COMMON); the coefficients a_i in array AG ( ) in COMMON

Usage: Called by SUBROUTINE PARST

Name: SUBROUTINE DSTV(H,P,V,VS,THETA,PI,EMN,DSV,DTV)

Input: $h, p, v, v_s, \theta, \pi, M_n$: H,P,V,VS,THETA,PI,EMN

Output: $\frac{ds}{dv}$, $\frac{dT}{dv}$: DSV, DTV

Formula(s):

$$\frac{dT}{dv} = \left[\frac{\partial T}{\partial p}\frac{dp}{dh} + \frac{\partial T}{\partial \theta}\frac{d\theta}{dh}\right]\frac{\partial h}{\partial v} + \frac{\partial T}{\partial M_n}\left[\frac{\partial M_n}{\partial v} + \frac{\partial M_n}{\partial \theta}\frac{d\theta}{dh}\frac{\partial h}{\partial v}\right]$$

$$\frac{ds}{dv} = \left[\frac{\partial s}{\partial p}\frac{dp}{dh} + \frac{\partial s}{\partial \theta}\frac{d\theta}{dh}\right]\frac{\partial h}{\partial v} + \frac{\partial s}{\partial M_n}\left[\frac{\partial M_n}{\partial v} + \frac{\partial M_n}{\partial \theta}\frac{d\theta}{dh}\frac{\partial h}{\partial v}\right]$$

Remarks: This subroutine uses the following subprograms:

(1) FUNCTION DPH to obtain $\frac{dp}{dh}$

(2) FUNCTION DTHH to obtain $\frac{d\theta}{dh}$

(3) FUNCTION PHV to obtain $\frac{\partial h}{\partial v}$

(4) SUBROUTINE PMNVTH to obtain $\frac{\partial M_n}{\partial v}$ and $\frac{\partial M_n}{\partial \theta}$

(5) SUBROUTINE PARST(j,...), with J = 0, to obtain

$$\frac{\partial T}{\partial p}\ ,\ \frac{\partial T}{\partial \theta}\ ,\ \frac{\partial T}{\partial M_n}\ ,\ \frac{\partial s}{\partial p}\ ,\ \frac{\partial s}{\partial \theta}\ ,\ \text{and}\ \frac{\partial s}{\partial M_n}\ .$$

Usage: Called by VSTAR and ABANDC

Name: SUBROUTINE DSTE(H,P,V,VS,THETA,PI,EMN,DSE,DTE)

Input: $h,p,v,v_s,\theta,\pi,\ M_n$: H,P,V,VS,THETA,PI,EMN

Output: $\frac{ds}{dE}\ ,\ \frac{dT}{dE}$: DSE, DTE

Formula(s):

$$\frac{ds}{dE} = \frac{1}{g}\left[\frac{\partial s}{\partial p}\frac{dp}{dh} + \left(\frac{\partial s}{\partial \theta} + \frac{\partial s}{\partial M_n}\frac{\partial M_n}{\partial \theta}\right)\frac{d\theta}{dh}\right]$$

$$\frac{dT}{dE} = \frac{1}{g}\left[\frac{\partial T}{\partial p}\frac{dp}{dh} + \left(\frac{\partial T}{\partial \theta} + \frac{\partial T}{\partial M_n}\frac{\partial M_n}{\partial \theta}\right)\frac{d\theta}{dh}\right]$$

Remarks: G(g) found in COMMON. Uses the following subprograms:
FUNCTION DPH for $\frac{dp}{dh}$; FUNCTION DTHH for $\frac{d\theta}{dh}$;
SUBROUTINE PMNVTH for $\frac{\partial M_n}{\partial \theta}$; SUBROUTINE PARST (0,...)
for $\frac{\partial T}{\partial \theta}\ ,\ \frac{\partial s}{\partial \theta}\ ,\ \frac{\partial T}{\partial M_n}\ ,\ \frac{\partial s}{\partial M_n}\ ,\ \frac{\partial T}{\partial p},\ \frac{\partial s}{\partial p}$.

Usage: Called by SUBROUTINE ABANDC

7. Miscellaneous

Name: FUNCTION ALT(E,V)

Input: E,v : E,V

Output: h(E,v)

Formula(s): $h(E,v) = \dfrac{E - \frac{1}{2} v^2}{g}$

Remarks: g(G) is found in COMMON

Usage: Frequent use throughout program. Referenced by VSTAR, DEDJ, CHKSTAR

Name: FUNCTION PHV(V)

Input: v : V

Output: $\dfrac{\partial h}{\partial v}$

Formula(s): $\dfrac{\partial h}{\partial v} = - \dfrac{v}{g}$

Remarks: g(G) found in COMMON

Usage: Referenced by DDV and DSTV

Name: SUBROUTINE STAND (H,V,P,THETA,RHO,VS,EMN,EMU,PI,S,T,D)

Input: h, v, μ, π : H,V,EMU,PI

Output: $p, \theta, \rho, v_s, M_n$,S,T,D : P,THETA,RHO,VS,EMN,S,T,D

Remarks: This routine calls the fundamental component subroutines PTRVSM, TANDS, and DRAG

Usage: Called by VSTAR, JOVERMU, DEDJ, CHCKSTAR

Name: FUNCTION VNOISE(E)

Input: E

Output: $v_{noise}(E)$

Formula(s): $v_{noise}(E) = \min\{v', \bar{v}\}$, where $\bar{v} = B21(\theta_{max} - B14 - E \cdot B18)$;

$$v' = \begin{cases} \sqrt{2(E - h_o g)}, & \text{if } E - \frac{1}{2}\bar{v}_s^2 \le h_o g \\ \sqrt{2(E - h_s g)}, & \text{if } E - \frac{1}{2}\bar{v}_s^2 > h_s g \\ \bar{v}_s, & \text{otherwise} \end{cases}$$

$$\text{and where } \bar{v}_s^2 = \begin{cases} B19(B20 + E \cdot B18), & \text{if } E < ETEST \\ B17, & \text{if } E \ge ETEST \end{cases}$$

Remarks: The following are found in COMMON: B14, B17, B18, B19, B20, ETEST, HOG ($h_o g$), HSG ($h_s g$), THTMAX (θ_{max}), B21

Usage: Referenced by VSTAR, VSELECT

Name: FUNCTION VSELECT (L,J,K,E,XMU,PI,MXPO,YLAM,VNEW,VOLD,I,JPTS)

Input: All items in the argument string

Output: v, output as VSELECT

Formula(s):

(1) If K = 1, v is found via FUNCTION VSTAR, with λ^* set equal 0.

(2) If K = 2, v is found via FUNCTION VSTAR, with $\lambda^* = \lambda(m_o - \mu)$.

(3) If K = 3, v is the minimum of v_{max}, v_{noise}, and the average of the values of v (at a particular value of μ) from two previous integration stages.

Usage: Called by SUBROUTINE JANDE. This function yields the proper value for v, depending upon whether J = 1 or 2 (i.e., "letdown" or "climbout," respectively) and whether K = 1, 2, or 3. K is set in SUBROUTINE BAKN4TH, and it specifies a method of obtaining v for a particular stage of integration. This function VSELECT is used to

obtain v prior to each call upon SUBROUTINE DEDJ by SUBROUTINE JANDE. The quantity L has the value 0 or 1. L is set to 1 if the calculation of v is at the midpoint of an integration interval, as determined by the Clippinger-Dimsdale technique. Otherwise L = 0.

Name: PVCE (V,E)

Input: v,E : V,E

Output: $\frac{\partial v_c}{\partial E}$

Formula(s): if $v = \bar{v}$, $\frac{\partial v_c}{\partial E} = \frac{bb_8}{\bar{v}}$

if $v = v'$, $\frac{\partial v_c}{\partial E} = \begin{cases} 1/v' \text{ for } v_{test} < HOG \\ bb_7/v' \text{ for } v_{test} > HOG \end{cases}$

$\theta = K_{G_2G_3} + 273$; $\frac{\partial v_c}{\partial E} = \frac{1 - g\frac{\partial h}{\partial E}}{\tilde{v}}$, where $\frac{dh}{dE} = \begin{cases} \frac{(\gamma - 1)/b_{16}^2}{\left(g(\gamma - 1)/b_{16}^2\right) - b_1} & \text{for } h < b_4 = h_{TROP} \\ 1/g & \text{for } h \geq b_4 = h_{TROP} \end{cases}$

$h = h_{TROP}$, $\frac{\partial v_c}{\partial E} = 1/\tilde{v}$

Remarks: Equations for $\bar{v}$ and v' are the same as those in VNOISE. Equations for determining whether $\theta = K_{G_2G_3} + 273$ or $h = h_{TROP}$ are those used in VSTAR, and equations for $\tilde{v}$ are the same as those used in VSTAR.

Usage: Used by ABANDC

Name: SUBROUTINE DJDMU(XMU,EJ,DEJ,H,PI)

Input: μ : XMU--and from COMMON the quantities VMAX and DJNUM = $v_{max} - a$

Output: $\frac{dJ}{d\mu}$, stored in DEJ(1);

h and π (H,PI) are also delivered as output

Formula(s): $\frac{dJ}{d\mu} = \frac{v_{max} - a}{s} = \frac{DJNUM}{S}$

Remarks: h and π are computed by SUBROUTINE HSTAR. SUBROUTINE PTRVSM yields p, θ, ρ, v_s, M_n (given h and v_{max}). SUBROUTINE TANDS yields s (given π, θ, M_n and p)

Usage: Called by SUBROUTINE JOVERMU

Name: SUBROUTINE DEDJ (XMU,PI,V,EJ,DEJ,S,T,D,H,P,VS,THETA, EMN,RHO)

Input: μ,π,v,E : XMU,PI,V,EJ(2)
COMMON m_o, a, cos γ, b : EMO, A, GAMDRAG, BT

Outputs: $\frac{dJ}{d\mu}, \frac{dE}{d\mu}$; DEJ(1), DEJ(2)

Formulas: $\frac{dJ}{d\mu} = \frac{v \cos \gamma - 1}{s} + \frac{1}{b}$

$\frac{dE}{d\mu} = \frac{v(T - D)}{s(m_o - \mu)}$

Remarks: h is found by ALT(E,V)
s, T, D, p, v_s, θ, M_n, and ρ are found by STANDD (H,V,P,THETA,RHO,VS,EMN,XMU,PI,S,T,D)

Usage: Called by SUBROUTINE JANDE. The purpose of this subroutine is to compute the derivatives for the Clippinger-Dimsdale solution of the system of differential equations.

Name: SUBROUTINE ABANDC (N,P,V,VS,THETA,PI,EMN,RHO,XMU,S,T,D, E,AAA,BBB,CCC)

Input: $h,p,v,v_s,\theta,\pi,M_n,\rho,\mu,s,T,D,E$: H,P,V,VS,THETA,PI,MN,RHO, XMU,S,T,D,E
COMMON: m_o, a, cos γ, b : EMO,A,GAMDRAG,BT

Output: A,B,C : AAA,BBB,CCC

Formula(s):

$$A = \frac{-bv}{(m_o - \mu)s}\left[\frac{(T-D)}{m_o - \mu} - \frac{\partial D}{\partial \mu}\right]$$

$$B = \frac{v}{(m_o - \mu)s}\left\{\frac{dT}{dE} - \frac{dD}{dE} - \frac{(T-D)}{s + b(v\cos\gamma - a)}\frac{ds}{dE} + \frac{\partial v_c}{\partial E}\left[\frac{dT}{dv} - \frac{dD}{dv} + (T-D)\left(\frac{1}{v} - \frac{b\cos\gamma + \frac{ds}{dv}}{s + b(v\cos\gamma - a)}\right)\right]\right\}$$

$$C = \frac{1}{s}\left\{\frac{(v\cos\gamma - a)}{a + b(v\cos\gamma - a)}\left[\frac{ds}{dE} + \left(b\cos\gamma + \frac{ds}{dv}\right)\frac{\partial v_C}{\partial E}\right] - \cos\gamma\frac{\partial v_C}{\partial E}\right\}$$

Remarks: Calls DSTE to obtain $\frac{dS}{dE}$ and $\frac{dT}{dE}$, DDE for $\frac{dD}{dE}$, DSTV for $\frac{dS}{dv}$ and $\frac{dT}{dv}$, DDV for $\frac{dD}{dv}$, PARDMU for $\frac{\partial D}{\partial \mu}$, and PVE for $\frac{\partial v_C}{\partial E}$

Usage: Called by JANDE and CHKSTAR; A, B, C stored for use by LAMDDA

Name: CHKSTAR (EMU,OLDMU,E,OLDE,OLDESTR,XJ,OLDJ,OLDBT,PI,OLDPI,AA,B,C)

Input: μ, μ_{OLD}, E, E_{OLD}, E^*_{OLD}, J, J_{OLD}, b_{OLD}, π, π_{OLD} : EMU, OLDEMU, E, OLDE, OLDESTR, XJ, OLDJ, OLDBT, PI, OLDPI

COMMON: v_{max}, E^*, b : VMAX, ESTAR, BT

Output: μ, E, v, J, π, A, B, C : EMU, E, V, J, PI, AA, B, C

COMMON: λ_o, LTDG, b : XLAMO, LTDG, BT

Formula(s): $\lambda_o = 0$

Remarks: At the completion of each step this subroutine is called by JANDE in order to test whether $E \geq E^*$. If $E < E^*$, LTOG is set zero (which causes JANDE to integrate further). If $E \geq E^*$, LTOG is set to 1 (which causes JANDE to stop integrating). For $E \geq E^*$, the value of μ for which $E = E^*$ and the values of E, J, m and b at this value of μ are obtained by linear interpolation. A, B, and C for this value of μ are obtained by calling STANDD followed by ABANDC.

Name: CRUISE (EMU,MXPT,EMU,ZEE,ZPI)

Input: μ, μ_i^*, E_i^*, π_i^* : EMU, ZMU, ZEE, ZPI (i = 1,..., MXPT)

COMMON: v_{max}, a : VMAX, A

Output: COMMON : $E^*(\mu)$, $b(\mu)$: ESTAR, BT

Formula(s): $$b = -\frac{s^*}{v_{max} - a}$$

Remarks: Finds μ^*_{NEEDLE} from the array ZMU such that $\mu^*_{NEEDLE} \leq \mu < \mu^*_{NEEDLE+1}$ and computes $E^*(\mu)$ and $\pi^*(\mu)$ from interpolation on value stored in the array ZEE and ZPI.

EMU, ZEE, and ZPI are computed by JOVERMU. STANDD is used to obtain s^* and b is computed by the above formula.

Usage: Used to store E^* and b in COMMON for use by VSTAR and ABANDC

C. Results

The optimization program was run using the aerodynamics described by Fig. 28; the engine described by Fig. 29 and $a_1 = 1.0$, $a_2 = 1.059$, $a_3 = -0.059$; the atmosphere described by $h_{TROP} = 10{,}000$m, $p_{TROP} = 295$ m bars, $\theta_{TROP} = -60^\circ$C. Other parameters were $m_o = 3.3 \times 10^5$ kg, $\mu_F = 1.5 \times 10^5$ kg, $a = 0$, $\pi_{min} = 0.01$, $h_o = h_s = 1000$ m, $v_o = 150$ m/s, $\gamma = 1.36$, and $\theta_{MAX} = 226.14^\circ$C. It was found that the initial guess in both letdown and climbout was in fact the optimum (i.e., $\lambda_2 = 0$); this same result was obtained in several other runs with different parameters. The resulting optimal trajectories are displayed in Figs. 1 and 2 in the Introduction.

II THE SENSITIVITY PROGRAM

A. Introduction

This program embodies the sensitivity equations given in Part Four, Sec. II. Because it was found by use of the optimization program that $\lambda_2 \approx 0$, a simplification can be made in Eq. (183) for K_M. Make the change of independent variable given by Eq. (165) and let H^* be the Hamiltonian with change of variable and H° without and similarly with f^* and f°. From the result that $\lambda_2 \approx 0$, $f^*_v = H^*_v = 0$; therefore

$$K_M = -\frac{H^*_{xv}}{H^*_{vv}} \tag{221}$$

and, since $H = 0$,

$$H^*_z = H^\circ_z h + H^\circ h_z = H^\circ_z h , \tag{222}$$

where z is any variable and

$$h = \frac{W_f}{W_f - b(v \cos \gamma - a)} . \tag{223}$$

In particular Eq. (222) implies $H^\circ_v = 0$. Furthermore,

$$\begin{aligned} H^*_{zv} &= H^\circ_{zv} h + H^\circ_z h_v + H^\circ_v h_z + H^\circ h_{zv} \\ &= H^\circ_{zv} h + H^\circ_z h_v . \end{aligned} \tag{224}$$

Therefore,

$$K_M = - \frac{H^\circ_{x_m} \frac{h_v}{h} + H^\circ_{x_m v}}{H^\circ_{vv}} \tag{225}$$

where

$$\frac{h_v}{h} = \frac{1}{W_f} \left(\frac{\partial W_f}{\partial v} - \frac{\frac{\partial W_f}{\partial v} - b \cos \gamma}{W_f - b(v \cos \gamma - a)} \right) \tag{226}$$

Most of the subroutines used by the sensitivity program are the same as those used by the optimization program. LAMBDA, BAKN4TH, PVCE, and ABANDC are not used by the sensitivity program. SST calls JANDE twice (for climbout and letdown) rather than BAKN4TH. A new output of JOVERMU and input to JANDE is the array ZPAR, which stores $\partial p/\partial \theta_{TROP}$. CHKCONV, JOVERMV, DJDMU, JANDE, DEDJ, CRUISE, CHKSTAR have been modified to integrate 13 additional differential equations; primary changes in JOVERMU, JANDE and CHKSTAR are modifications of the write statements, and the main change in CHKCONV is to make PE, CE, PH, CH, DP, DC inputs and outputs rather than storing them in COMMON. The changes to DJDMU and DEDJ are more extensive and are described below along with SEN1, SENS2, TOTLS and PRTLS, which are entirely new routines.

B. Greatly Modified Routines

Name: DJDMU (XMU, EJ, DEJ, H, PI, PBTTT, E, S, T, D, P, VS, THETA, EMN, RHO)

Input: μ, J, sensitivities, t: XME, EJ(1), EJ(3)-EJ(14), EJ(15)

Output: $\frac{dJ}{d_\mu}$, $\frac{\text{d sensitivities}}{d_\mu}$, $\frac{dt}{d_\mu}$; h, π, $\frac{\partial b}{\partial \theta_T}$, E, S, T, D, P, v_s, θ, M_n, ρ:

DEJ(1), DEJ(3)-DEJ(14), DEJ(15), H, PI, PBTTT, E, S, T, D,

P, VS, THETA, EMN, RHO

Formula(s):

$\frac{dJ}{d\mu}$ same as before

$$\frac{dJ_{\sigma_i}}{d\mu} = -\left|K_i X_{M_i} S_1\right| \qquad X_M = \begin{bmatrix} \mu \\ p \\ \theta \\ q \\ p_{TROP} \\ h_{TROP} \end{bmatrix}$$

$$\frac{dJ_{\sigma_i^2}}{d\mu} = K_i^2 \times X_{M_i}^2 S_2 + K1_i X_{M_i}^2 S_3$$

$$E = g_o h + \frac{1}{2} v_{max}^2$$

$$\frac{dt}{d\mu} = 1/s$$

$$\frac{db}{d\theta_T} = \frac{1}{b^2} H_\theta$$

Remarks: J_{σ_i} and $J_{\sigma_i^2}$ are the sensitivities to relative errors in the measurement X_{M_i}. H and PI are found by HSTAR. The remainder of the outputs, H_θ, K_i, $K1_i$, S_1, S_2, and S_3 are computed by SENS1

Usage: Called by JOVERMU

Name: DEDJ (XMU; PI, V, EJ, DEJ, S, T, D, H, P, VS, THETA, EMN, RHO)

Input: μ, π, v, E, J, sensitivities, t_i: XMU, PI, V, EJ(1), EJ(2), EJ(3)-EJ(14), EJ(15)

COMMON: m_o, a, cos γ, E^*, b,: EMO, A, GAMDRAG, ESTAR, BT

Output: $\frac{dJ}{d\mu}$, $\frac{dE}{d\mu}$, $\frac{\text{d sensitivities}}{d\mu}$, $\frac{dt}{d\mu}$; S, T, D, H, v_s, θ, M_n, ρ:

DEJ(1), DEJ(2), DEJ(3)-DEJ(14), DEJ(15), S, T, D, H, P, VS,

THETA, EMN, RHO

Formula(s): $\frac{dJ}{d\mu}$ and $\frac{dE}{d\mu}$ as before

$$\frac{dJ_{\sigma_i}}{d\mu} = |K_i \; X_{M_i} \; S_i|$$

$$dJ_{\sigma_i^2} = K_i^2 \; X_{M_i}^2 \; S_2$$

$$\frac{dt}{d\mu} = 1/s$$

Remarks: ALT is called to find h, the remaining outputs K_i, S_1, and S_2 are found by calling SENS2.

Usage: Called by JANDE

C. New Subroutines

Name: SENS1 (EMU, H, V, PI, THETA, P, RHO, VS, EMN, S, T, D, EK, S1, S2, EK1, S3, HTH)

Input: μ, h, v, π: EMU, H, V, PI

COMMON: b_{16} : B_{16}

Output: θ, p, ρ, v_s, M_n, S, T, D; K, S1, S2, K1, S3, H_θ:

THETA, P, RHO, VS, EMN, S, T, D, EK, S1, S2, EK1, S3, HTH

Formula(s): See Sec. 2 of Part Four.

Remarks: STANDD is called to find the atmospheric, aerodynamic, and engine variables. PRTLS followed by TOTLS are called to compute derivatives of the Hamiltonian.

Usage: Called by DJDMU

Name: SENS2 (EMU, H, V, PI, THETA, P, RHO, VS, EMN, S, T, D, EK, S1, S2)

Input: μ, h, v, π: EMU, H, V, PI

Output: θ, P, ρ, v_s, M_n, s, T, D, K, S1, S2:

THETA, P, RHO, VS, EMN, S, T, D, EK, S1, S2

Formula(s): (See Part Four, Sec. II)

Remarks: Same as for SENS1

Usage: Called by DJDE

Name: TOTLS (EMU, H, V, THETA, P, RHO, EMN, S, T, D, ..., HM, HV, HP, JTG)

Input: μ, h, v, θ, p, ρ, M_n, s, T, D, necessary partials, JTG:

EMU, H, V, THETA, P, RHO, EMN, S, T, D, ..., JTG

Output: H_{X_M}, H_v, H_p: HM, HV, HP

Formula(s): (See Part 4, Sec. II)

JTG = 0 implies Cruise

JTG = 1 implies Climbout or letdown

Remarks: Computes derivatives of the Hamiltonian with respect to measurement and controls.

Usage: Called by SENS1 and SENS2

Name: PRTLS (V, H, THETA, P, RHO, VS, ...)

Input: v, h, θ, p, ρ, v_s: V, H, θ, P RHO, VS

Output: Partial derivatives needed by TOTLS: ...

Formula(s): (See Part Four, Sec. II)

Remarks: Computes partial derivatives given in Table VII.

Usage: Called by SENS1 and SENS2

D. Results

The same case that was run with the optimization program was with the sensitivity program. Results are given in Table IV of the Introduction.

REFERENCES

1. John Peschon, Lewis Meier, III, Robert E. Larson, Wade H. Foy, Jr., and Charles H. Dawson, "Information Requirements for Guidance and Control Systems," Final Report, Contract No. NAS2-2457, Stanford Research Institute, Menlo Park, California (May 1966).

2. L. Meier, J. Peschon, B. Ho, R. Larson, and R. Dressler, "Design of Guidance and Control Systems for Optimum Utilization of Information," Final Report, Contract No. NAS2-3476, Stanford Research Institute, Menlo Park, California (May 1968).

3. Sidney M. Serebreny, "A Study of the Sensitivity of a Supersonic Aircraft to the Effect of Various Horizontal Temperature Distributions," Contract No. FAA/BRD-420, SRI Project 3765, Stanford Research Institute, Menlo Park, California (October 1964).

4. Arthur E. Bryson, Jr., Mukund N. Desai, and William C. Hoffman, "The Energy-State Approximation in Performance Optimization of Supersonic Aircraft," AIAA Paper No. 68-877, AIAA Guidance, Control, and Flight Dynamics Conference, Pasadena, California, August 12-14, 1968.

5. A. Kochanski, "Cross Sections of the Mean Zonal Flow and Temperatures Along 80° W," J. Meteorol., Vol. 12, No. 2, p. 95 (April 1955).

6. W. L. Godson and R. Lee, "Hign-Level Fields of Wind and Temperature over the Canadian Arctic," Beitr. Phys., 31 Bund, Heft 1-4, 1959, p. 40 (September 1958).

7. R. Lee and W. L. Godson, "The Arctic Stratospheric Jet Stream During the Winter of 1955-56," J. Meteorol., Vol. 14, No. 2, p. 126 (April 1957).

8. K. L. Behr, Petkovsek, and R. Scherhag, Institut für Meteorologie und Geophysik der Freien Universität Berlin, Meteorologische Abhandlungen, Band XXV/Heft. Preliminary Daily Northern Hemisphere 30-Millibar Synoptic Weather Maps of the Year 1962. First Quarterly Technical Status Report, Contract No. DA-91-591 EUC 2148, U. S. Department of Army, European Research Office (1962).

9. H. S. Meunch and R. Borden, Jr., Atlas of Monthly Mean Stratosphere Charts, 1955-1959; Parts I and II. Air Force Cambridge Research Laboratories, Office of Aerospace Research United States Air Force, Bedford, Massachusetts.

10. "747 Avionics to Include 1970 Concepts," Aviation Week and Space Technology (McGraw-Hill, New York, October 31, 1966).

11. D. M. Petrie, "Automatic Flight Management of Future High Performance Aircraft," J. of Aircraft, Vol. 5, No. 4 (July-August 1968).

12. J. D. Warner, "Multifunction Display Research Program," The Boeing Company, Electrodynamics Technology, Flight Deck Technology Group, January 7, 1969.

13. K. J. Stein, "Norden Expands Attitude Indicator Trails," Aviation Week and Space Technology (McGraw-Hill, New York, January 27, 1969).

14. Bendix DRA-12 Doppler Radar System Description, July 1966.

15. J. D. Warner, The Boeing Company, private communications.

16. S. F. Schmidt, et al., "Case Study of Kalman Filtering in the C-5 Aircraft Navigation System," 1968 JACC Case Studies in System Control, University of Michigan, June 24-25, 1968, pp. 57-110.

17. K. E. Van Every and A. Miele, "Aerodynamic Forces," Chapter 6 of Flight Mechanics, Theory of Flight Paths, pp. 69-94 (Addison-Wesley, Redding, Massachusetts, 1962).

18. Bendix FD-60 Flight Director System, Operators Manual and System Description, January 16, 1967.

Appendix A

SOME ELEMENTARY THERMODYNAMIC RELATIONS

Appendix A

SOME ELEMENTARY THERMODYNAMIC RELATIONS

Definitions

The change in internal energy du of a unit mass of gas equals the heat added minus the external work done by the gas, i.e.,

$$\begin{aligned} du &= dq - dw \\ &= dq - p\,dv \quad , \end{aligned} \tag{A-1}$$

where

q is the heat added
w is the external work done
p is the pressure
v is the specific volume.

The enthalpy h of a unit mass of gas is defined as

$$h = u + pv \quad . \tag{A-2}$$

Therefore, using Eq. (A-1),

$$\begin{aligned} dh &= du + p\,dv + v\,dp \\ &= dq + v\,dp \quad . \end{aligned} \tag{A-3}$$

The specific heats at constant volume and pressure are defined as

$$c_v = \left(\frac{dq}{d\theta}\right)_v$$

$$c_p = \left(\frac{dq}{d\theta}\right)_p \quad , \tag{A-4}$$

where

θ is the absolute temperature.

Since for a perfect gas $u = u(\theta)$ and $pv = R\theta$, where R is the gas constant, it follows that

$$du = \frac{\partial u}{\partial \theta} d\theta$$

and

$$h = h(\theta, p) \quad ,$$

so that

$$dh = \frac{\partial h}{\partial \theta} d\theta + \frac{\partial h}{\partial p} dp \quad . \tag{A-5}$$

Therefore from Eqs. (A-1), (A-3), and (A-5),

$$c_v = \left(\frac{dq}{d\theta}\right)_v = \frac{du}{d\theta}$$

$$c_p = \left(\frac{dp}{d\theta}\right)_p = \frac{dh}{d\theta} \quad . \tag{A-6}$$

Also from Eq. (A-2) by differentiating with respect to θ,

$$\frac{dh}{d\theta} = \frac{du}{d\theta} + \frac{d}{d\theta}(pv) \quad ,$$

i.e.,

$$c_p = c_v + R \quad . \tag{A-7}$$

Isentropic Process with Perfect Gas

For an isentropic process, dq = 0 and the change in internal energy is simply equal to the work done by the gas, i.e.,

$$du = -p \; dv \quad .$$

Using Eq. (A-3),

$$dh = v \; dp \quad . \tag{A-8}$$

Therefore

$$c_v = \frac{du}{d\theta} = - \; p \; \frac{dv}{d\theta}$$

$$c_p = \frac{dh}{d\theta} = v \; \frac{dp}{d\theta} \tag{A-9}$$

and

$$\frac{\theta}{v} \frac{dv}{d\theta} = - \frac{c_v}{R}$$

$$\frac{\theta}{p} \frac{dp}{d\theta} = \frac{c_p}{R}$$

$$\frac{v}{p} \frac{dp}{dv} = - \frac{c_p}{c_v} \quad . \tag{A-10}$$

Assuming that c_p and c_v are constants and defining

$$\gamma = \frac{c_p}{c_v} \quad , \tag{A-11}$$

Equations (A-10) yield

$$pv^{\gamma} = \text{constant}$$

$$v\theta^{\left(\frac{1}{\gamma-1}\right)} = \text{constant}$$

$$p\theta^{\left(\frac{\gamma}{\gamma-1}\right)} = \text{constant} \quad . \tag{A-12}$$

Acoustic Speed and Mach Number

If $k = -v\,(dp/dv)$ is the bulk modulus of a fluid and ρ is its density then $a = \sqrt{K/\rho}$ is the acoustic speed. For a perfect gas, using Eq. (A-10),

$$K = -v\frac{dp}{dv} = p\frac{c_p}{c_v} = p\gamma \quad . \tag{A-13}$$

Therefore

$$a = \sqrt{\frac{p\gamma}{\rho}} = \sqrt{\gamma R\theta} \quad . \tag{A-14}$$

Then for a perfect gas the Mach number is

$$M_n = \frac{V}{a} = \frac{V}{\sqrt{\lambda R\theta}} \quad . \tag{A-15}$$

Steady Isentropic Flow of a Perfect Gas

Conservation of energy implies that the heat supplied plus the work done on the gas minus the external work done by the gas must equal the increase in internal energy plus the increase in kinetic energy, i.e.,

$$dq - (p\,dv + v\,dp) - dw = du + V\,dV$$

or

$$dq - dw = dh + V\,dV = c_p\,dt + V\,dV \quad . \tag{A-16}$$

For an adiabatic flow with no external work, dq = dw = 0 and the only energy changes are from enthalpy to kinetic energy or vice versa. Then

$$dh + V\,dV = 0$$

and

$$h + \frac{V^2}{2} = \text{constant} \quad .$$

By integrating Eq. (A-6) for h,

$$c_p\theta_1 + \frac{V_1^2}{2} = c_p\theta_2 + \frac{V_2^2}{2} = \text{constant} \quad . \tag{A-17}$$

By using $pv = p/\rho = R\theta$, $a^2 = \gamma p/\rho$, and $c_p = R\gamma/(\gamma - 1)$,

$$V_2^2 = a_1^2\left(\frac{2}{\gamma - 1}\right)\left(1 - \frac{\theta_2}{\theta_1}\right) + V_1^2 \quad . \tag{A-18}$$

Total (Stagnation) Conditions

Consider isentropic flow between an initial state with nonzero velocity to a final state with zero velocity. The temperature and pressure at the final state are called the total conditons $\theta^{\star}$, $p^{\star}$ of the gas. From Eqs. (A-18) and (A-12)

$$\theta^{\star} = \theta\left(1 + \frac{\gamma - 1}{2} M_n^2\right)$$

$$p^{\star} = p\left(1 + \frac{\gamma - 1}{2} M_n^2\right)^{\frac{\gamma}{\gamma - 1}} \quad . \qquad \text{A-19)}$$

Appendix B

A DESCRIPTION OF AN ELECTROMECHANICAL FLIGHT DIRECTOR SYSTEM

Appendix B

A DESCRIPTION OF AN ELECTROMECHANICAL FLIGHT DIRECTOR SYSTEM

This appendix describes the basic specifications of the Bendix FD-60 Flight Director System[18] and its related components.

The basic electromechanical flight-director system displays the following information:

(1) Roll attitude
(2) Pitch attitude
(3) Glide-slope deviation
(4) Localizer deviation
(5) Roll command
(6) Pitch command
(7) Speed command
(8) Crab angle
(9) Radar altitude
(10) Rate of turn
(11) Heading mode
(12) Rate-of-turn warning
(13) Glide-slope warning
(14) Gyro warning
(15) Speed warning
(16) Speed-command warning
(17) Flight-director warning
(18) Slip indicator.

1. Cruise Mode of Operation

Pitch attitude is displayed by the displacement of the attitude-horizon sphere against the aircraft fixed reference. The reference point for reading the pitch displacement is a circular dot located at the center of the aircraft fixed reference. Freedom of the servo-driven sphere about the pitch axis is a full 360^{o}.

Roll attitude is displayed by a movable index and fixed reference marks. It is also shown by noting the angular displacement between the aircraft fixed reference and the vertical centerline of the pitch attitude

graduations on the sphere. The sphere is servo-driven and has a full 360° of freedom about the roll axis.

A conventional ball-type slip indicator located at the bottom of the indicator face indicates lateral acceleration. Just below the slip meter is a movable rate-of-turn index and stationary scale that provides turn-rate information.

Integrated pitch and roll steering commands are presented by the pitch and roll command bars, relative to the aircraft fixed reference. To satisfy a command, the pilot flies the aircraft fixed reference to align with the movable command bars. When not required, the command display may be driven out of sight.

2. Approach Mode of Operation

In approach mode, localizer deviation is integrated with vertical flight-path deviation and is presented in three-dimensional form by displacement of the gate display from the aircraft fixed reference.

The gate display consists of two intersecting lines that simulate the intersection of a localizer beam and a glide-slope beam. Alignment of the aircraft fixed reference with the gate display indicates perfect positioning on the approach path. At some specific altitude, depending on the aircraft characteristics, location of the aircraft dot anywhere within the circle indicates that the aircraft is within safe limits for the approach.

The lateral and vertical motions of the gate display are controlled by servo-driven gear trains. When the indicator is used in the cruise mode, the gate symbol is driven laterally out of view behind the roll attitude dial. The vertical movement of the gate symbol is completely independent of the pitch attitude motion of the attitude sphere.

Two transilluminated rings are mounted flush inside of the gate display. When the outer ring is illuminated, minimum decision altitude is indicated. When the inner ring is illuminated, flare is indicated.

Radar altitude is displayed by a crosshatched ground symbol that moves vertically over a range of zero to 200 feet altitude. At altitudes over 200 feet, the symbol is driven out of sight and stored in the lower portion of the instrument. At zero altitude indication, the ground symbol is aligned with the bottom of the aircraft fixed reference.

Crab-angle/roll-out information is displayed by a bar index moving laterally against a fixed scale to indicate direction and amount of lateral displacement. The direction and magnitude are derived from the angular error existing between the aircraft heading and the selected runway heading. This display has potential application in providing steering roll-out information after the aircraft has touched down on the runway and is completing its roll out. The crab-angle display is capable of being driven out of view when not required.

3. Components

The flight director is composed of the following five components:

(1) Horizon and Director Indicator

(2) Course Deviation Indicator

(3) Flight Instrument Amplifier

(4) Flight Steering Computer

(5) Control Panel.

The following is a brief description of the function of each of these elements.

The Horizon and Director Indicator (HDI) displays aircraft attitude in roll and pitch through a conventional type of artificial horizon.

Glide slope, expanded localizer, and speed command are each displayed by a moving bar that is read against a fixed scale. When not in use, these bars are biased out of view. Integrated pitch and roll steering commands are presented on a split command bar.

The command bar is positioned by signals from the flight steering computer, relative to a fixed aircraft reference. To satisfy a command, the pilot flies the fixed aircraft reference to align with the movable command bar. When the command bar is not in use, it is automatically recessed out of sight. The instrument then functions solely as a remote attitude reference indicator.

Illuminated annunciators indicate the active mode of operation. Each of these, when not energized, appears as black markings on a black background.

There are five warning flags, one each for gyro, computer, glide-slope indicator, localizer, and speed command or radar altimeter. These signals indicate a malfunction in the system.

The Course Deviation Indicator (CDI) provides a pictorial presentation of aircraft displacement relative to VOR radials, localizer, and glide-slope beam. It also gives heading reference with respect to magnetic north.

The pilot selects the desired VOR radial by rotating the bearing selector on the instrument; the VOR radial is then displayed in digital form by a counter on the face of the unit. A course cursor is simultaneously positioned to indicate the selected course on the compass dial in relation to aircraft heading. A to-from indication displays the relationship of the aircraft to the selected radial.

Heading is displayed on the outer azimuth ring of the compass card. Riding with this compass card is a triangular-shaped cursor positioned

by manual rotation of the heading knob located on the instrument. This establishes a magnetic reference for the flight steering computer, similar to the course output, and is used in preselect-heading and variable-angle capture of the ILS.

Other displays are the course-deviation needle and the glide-slope needle. The course deviation needle indicates lateral and angular displacement of the aircraft from the preselected course. Positioned by signals from the localizer/VOR radio receiver, the needle rotates with the compass dial and the course cursor, and is parallel to the course cursor and its reciprocal. The glide-slope needle indicates displacement of aircraft from the glide-slope beam. Positioned by signals from the glide-slope radio receiver, the needle moves in a horizontal plane and does not rotate with changes in compass heading.

In the event of an unreliable compass indication, the course crank is pulled out (emergency mode). This disconnects the compass servo system and permits manual rotation of the compass card and the course cursor relative to the vertical axis of the instrument without disturbing the preselected course setting. This allows continued use of the data from the radio aids, displayed in a clearly interpretable manner.

The Flight Instrument Amplifier contains the electronics equipment required to amplify the attitude, heading, and command signals to operate the servomechanisms in the HDI and the CDI. In addition, it contains in-line servo monitors that sense the tracking accuracy of the servoed instrument displays with respect to their input sensors.

Servo amplifiers, on modularized, plug-in cards, provide the outputs for positioning the compass card on the CDI and the roll and pitch attitude and command on the HDI. Failure of any one amplifier component will not cause servo-system failure. Also, individual power supplies are

provided for heading, attitude, and command displays, to prevent malfunction in one circuit from affecting the other circuits.

The overall system logic for the warning flags makes use of the servo in-line monitoring in conjunction with the monitoring of such input reference systems as the compass, the vertical gyro, and the navigation receivers.

The Flight Steering Computer is the heart of the flight-director system. It combines compass heading, attitude, altitude, and navigation receiver data into computed roll and pitch command signals. The computer contains the logic, shaping, and gain scheduling circuitry to produce the output signals that position the command bar on the Horizon and Director Indicator. The modes provided by the computer are:

- Heading selection
- Variable-angle capture of localizer/VOR
- Automatic glide-slope engage
- Go-around (programmed for fixed pitch-up and wings-level command, or for speed command information computed by auxiliary equipment)
- Altitude hold
- Pitch attitude command.

The logic associated with activation of the computer warning flag and the solenoid-held mode selector switches is incorporated within the computer. Interlocks are provided for use with the mode selector switch to cross check that the computer is programmed to the selected mode.

The localizer and glide-slope flag circuit outputs are also monitored. A failure in either navigation receiver results in the appearance of the computer warning flag, when operating in the localizer or glide-slope mode. System logic is arranged to integrate the vertical gyro and compass

system in-line monitoring with the computer and flight instrument amplifier warning sensors, thus providing an extensive check as to the operation of the instrument displays.

Limiters, smoothing of the VOR displacement signal, gain scheduling of the localizer and glide slope, automatic drift (crosswind) correction, and automatic mode switching associated with localizer/VOR and glide slope are integrated with the logic contained in the computer.

The Control Panel contains the controls by which the pilot can select the modes of operation of the system. The unit consists of the following items: mode selector switch, altitude-hold switch, and mode light controls.

The mode selector switch is readily accessible to the pilot and provides for the following modes: OFF, GO AROUND, HDG (select heading), VOR/LOC, GS AUTO (glide slope with automatic capture), and GS MAN (manual override of automatic glide slope).

Go-around mode is selected either by rotating the mode selector to GO AROUND or by momentarily depressing a disconnect button usually located on the control wheel. The latter method automatically moves the mode selector switch to the GO AROUND position.

The altitude-hold switch enables the pilot to maintain the altitude of the aircraft at the time the switch is engaged. Computed commands to the Horizon and Director Indicator will pictorially command a climb or dive maneuver necessary to maintain this altitude.

A block diagram of the entire system is shown in Fig. B-1.

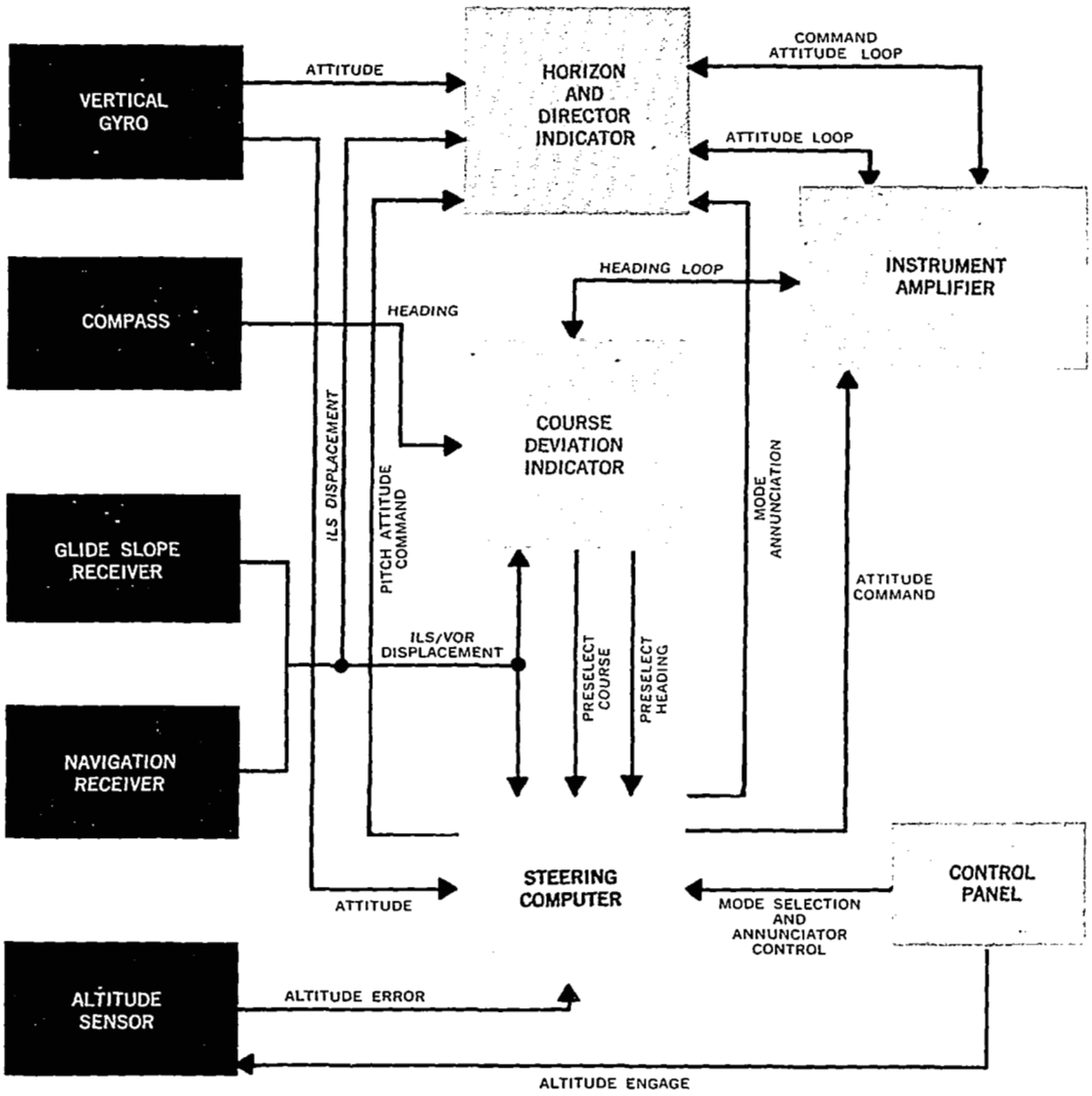

FIGURE B-1 FLIGHT DIRECTOR SYSTEM BLOCK DIAGRAM, COURTESY OF BENDIX AVIONICS

Appendix C

STANDARD JET-TRANSPORT ENGINE INSTRUMENTATION

Appendix C

STANDARD JET-TRANSPORT ENGINE INSTRUMENTATION

Aircraft engine instruments are required on all aircraft. Although the FAA has established minimum requirements for engine instrumentation, nearly all aircraft greatly exceed these minimums. The following paragraphs briefly describe commercially available engine instruments and their basic functions.

The following ranges and accuracies represent the average instrumentation performance for jet transport aircraft. Accuracy and cost of sensors must be evaluated in detailed trade-off studies.

1. Fuel Flow Meter

The fuel flow meter was discussed in the body of the report.

2. Exhaust Gas Temperature Indicator

The exhaust gas temperature instrument is composed of a chromel-alumel thermocouple attached to the exit nozzle of the aircraft engine. A cold reference junction and an amplifier are required to drive pilot displays. The response speed of thermocouples varies with their design characteristics and with their placement in the gas stream. The response times may vary from 5 seconds to 30 seconds for full-scale deflection, according to the overall system design characteristics and cost. Range and accuracy are

Range	Accuracy
0 to 1000°C	±5°C
200 to 700°C	±5°C .

3. Percent RPM Meter

The percent RPM instrument is simply a tachometer. Because of very high turbine speeds, the instrument is calibrated in terms of percent maximum design speed. The sensor pick-up is generally located on the portion of the engine that rotates more slowly than the turbine. For example, the rotor on the engine generator is an excellent candidate. The response of this instrument is very rapid; for most sensors its response time is about 5 seconds. It should be noted that the response of the engine to a step change in throttle position is of the same magnitude. Range and accuracy are

Range	Accuracy
0-110 percent	±0.4 percent
50-110 percent	±0.4 percent
90-110 percent	±0.25 percent .

4. Oil Temperature Gauge

The oil-temperature sensors may be of either the resistance bulb type or the thermocouple type. The response of the bulb thermometers is almost instantaneous, whereas response for the thermocouple is nearly 5 seconds. The reliability of the bulb is much higher since amplifiers and reference junctions are not required. The resistance bulb thermometers, however, have limited range. Range and accuracy are

Range	Accuracy
-50 to +150°C	±2°C
0 to 160°C	±3°C .

5. Oil Pressure Gauge

The oil pressure gauge is usually a simple diaphragm pressure-sensitive device. Where the pressure source is very remote from the

instrument display, it is necessary to use a pressure-transmitting device. This device converts the pressure signal to an electrical signal that is amplified and transmitted to the cockpit display. Range and accuracy are

Range	Accuracy
0-100 psig	±1 psig
20-100 psig	±2 psig .

6. Generator Voltage Meter

The output of the voltage generator is measured with a voltmeter. In certain instances these signals must also be telemetered to the cockpit because of the distance from the source. Range and accuracy are

Range	Accuracy
10-35 V	±0.25 V .

7. Generator Current Meter

An ammeter, which may also require telemetry, is used to measure generator current. The range and accuracy are

Range	Accuracy
0-450 A	±4.5 A .

8. Hydraulic Pressure Gauge

A pressure-sensitive diaphragm device is used, along with a pressure-transmitting device, to carry the information from the source to the display. Range and accuracy are

Range	Accuracy
0-5000 psig	±50 psig .

9. Turbine-Inlet Temperature Gauge

The turbine-inlet temperature thermocouple placement requires very special attention. The hot ionized gas from the combustor causes severe noise and bias problems, which are due to the excess of electrons in the vicinity of the thermocouple probe. Special calibration and shielding are required for reliable measurements. Range and accuracy are

Range	Accuracy
0-1000°C	±5° .

10. Exhaust Pressure Ratio Gauge

The oil pressure gauge is usually a simple diaphragm pressure-sensitive device. Where the pressure source is very remote from the instrument display, it is necessary to use a pressure-transmitting device. This device converts the pressure signal to an electrical signal that is amplified and transmitted to the cockpit display. Range and accuracy are

Range	Accuracy
1-2 dimensionless	±.5 percent .

11. Fuel Pressure Gauge

The oil pressure gauge is usually a simple diaphragm pressure-sensitive device. Where the pressure source is very remote from the instrument display, it is necessary to use a pressure-transmitting device. This device converts the pressure signal to an electrical signal that is amplified and transmitted to the cockpit display. Range and accuracy are

Range	Accuracy
Dependent on type of fuel feed	±.5 percent .

12. Outside Air Temperature Indicator

The outside air temperature gauge (free air thermometer) is usually of the bimetallic-strip, direct-reading type. The fact that two dissimilar metals have different expansion rates with respect to temperature variations is used to register temperature. Two strips of metal are welded to form a coil spring. One end is anchored, and the other is attached to the indicating hand. The pick-up (probe) is located in the free airstream and the dial faces the pilot. Range and accuracy are

Range	Accuracy
-50 to +50°C	±2°C .

13. Throttle Setting Indicator

A linear potentiometer is used to measure throttle setting. The range and accuracy are

Range	Accuracy
0-75°	±0.5 percent .

14. Total Temperature

The total temperature is defined as the temperature of the air entering the compressor of the engine if it were isentropically expanded to zero velocity. The equation describing this temperature is:

$$T_S = T_R \left(1 - \frac{\gamma}{M}\right)^{\gamma-1/\gamma} .$$

No device yet exists for measuring this.

15. Engine Temperatures

Engine temperatures are measured with various types of thermocouple junctions. A cold reference junction and amplifier may be required to drive pilot displays. Sensor locations and mounting techniques are specified by the engine manufacturers. The range and accuracy are

Range	Accuracy
0 to 1000°C	±5°C .

16. Ram Air Temperature

The ram air temperature is the temperature of the air entering the engine compressor. A thermocouple or resistance bulb may be used as a sensing device. Since this measurement is not now made, range and accuracy of the contemplated instrument are unknown.

17. Vibration Monitor

The exact design of this device has not yet been fixed.

18. Oil Filter Pressure

The pressure at the oil filter exit is measured with a diaphragm pressure-sensing device. Range and accuracy are

Range	Accuracy
0-60 psig	±1 psig .

19. Oil Breather Pressure

The vent pressure to the atmosphere is measured with a diaphragm pressure gauge. Range and accuracy are

Range	Accuracy
0-16 in Hg	±0.5 percent .

20. Scavenge and Chip Detector

A description of this instrument could not be obtained within the time frame of this study.

21. Recording Equipment

Extensive maintenance and flight data are recorded continuously during aircraft operation. The recorded variables are generally more accurate than displayed information since data can be recorded directly from sensor amplifiers. At present data are recorded on magnetic tape for further processing on landing. On-board jet-transport data processing is limited to simple filtering.

Appendix D

EXACT FORMS OF $\mathfrak{I}_1$ AND $\mathfrak{I}_2$

Appendix D

EXACT FORMS OF $\mathfrak{J}_1$ AND $\mathfrak{J}_2$

From Eqs. (20) to (27),

$$\mathfrak{J}_1 \triangleq \Delta\dot{\bar{x}} = f(x,u,t) - f(x^\circ,u^\circ,t) + w(t) \tag{D-1}$$

$$\mathfrak{J}_2 \triangleq (\Delta x \Delta\dot{x}^T) = \Delta x(t)\,\mathfrak{J}_1^T + \mathfrak{J}_1 \Delta x^T(t) + \hat{Q}(t) \; . \tag{D-2}$$

The presence of the term $\hat{Q}$ is required because $w(t)$ is white noise. Its presence may be shown rigorously by use of the Ito calculus.

From Eqs. (30), (D-1), and (D-2),

$$\begin{aligned}
\mathcal{H} &= E\{\ell(x,u,t) + \lambda^T \mathfrak{J}_1 + \mathrm{tr}[P\mathfrak{J}_2]\} \\
&\approx \ell(x^\circ,u^\circ,t) + H_x^\circ \Delta\bar{x} + H_u^\circ[(K + \Delta K)\Delta\bar{x} + \Delta u] \\
&\quad + \frac{1}{2}\mathrm{tr}\{H_{xx}^\circ \bar{P} + 2H_{xu}^\circ [K(\bar{P} + \tilde{P}) + \Delta K(\bar{P} + \tilde{P}) + \Delta u \Delta\bar{x}^T] \\
&\quad + H_{uu}^\circ [K(\bar{P} + 2\tilde{P} + \hat{P})K^T + 2K\Delta\bar{x}\Delta u^T + 2K(\bar{P} + \tilde{P} + \tilde{P}^T + \hat{P})\Delta K^T \\
&\quad + 2\Delta K\Delta\bar{x}\Delta u^T + \Delta K(\bar{P} + 2\tilde{P} + \hat{P})\Delta K^T + \Delta u \Delta u^T]\} \\
&\quad + 2\mathrm{tr}\{P[\bar{P} f_x^T(x^\circ,u^\circ,t) + (\bar{P} + \tilde{P}^T)K^T f_u^T(x^\circ,u^\circ,t) \\
&\quad + (\bar{P} + \tilde{P}^T)\Delta K^T f_u^T(x^\circ,u^\circ,t) + \Delta\bar{x}\Delta u^T f_u^T(x^\circ,u^\circ,t) + \tfrac{1}{2}\hat{Q}]\}.
\end{aligned} \tag{D-3}$$

Rearranging terms in Eq. (D-3) yields the results reproduced in Eqs. (31) to (35).

Appendix E

NOISY MEASUREMENTS AND DISCONTINUITIES IN THE DERIVATIVES OF THE HAMILTONIAN

Appendix E

NOISY MEASUREMENTS AND DISCONTINUITIES IN THE DERIVATIVES OF THE HAMILTONIAN

For $g(x^\circ, u^\circ, t) = 0$, the term $\Delta\mathcal{H}_1$ must be added to $\mathcal{H}_1$, as defined in Eq. (32) where

$$\Delta\mathcal{H}_1 \triangleq [\tilde{H}^\circ_x + \tilde{H}^\circ_u |K + \Delta K|] \Delta\tilde{x} + \tilde{H}^\circ_u \Delta\tilde{u} + \frac{1}{2}\tilde{H}^\circ_{xx}\Delta\tilde{x}^2 + (2P\tilde{f}^\circ_u + \tilde{H}^\circ_{xu})\Delta\tilde{x}\Delta u + \tilde{H}^\circ_{uu}\Delta\tilde{u}^2$$

$$\tilde{f}^\circ_u \triangleq \frac{1}{2}\lim_{\epsilon\to 0}[f_u(\lambda, x^\circ + \epsilon, u^\circ, t) - f_u(\lambda, x^\circ - \epsilon, u^\circ, t)]$$

$$\tilde{H}^\circ_x \triangleq \frac{1}{2}\lim_{\epsilon\to 0}[H_x(\lambda, x^\circ + \epsilon, u^\circ, t) - H_x(\lambda, x^\circ - \epsilon, u^\circ, t)]$$

$$\tilde{H}^\circ_u \triangleq \frac{1}{2}\lim_{\epsilon\to 0}[H_u(\lambda, x^\circ, u^\circ + \epsilon, t) - H_x(\lambda, x^\circ, u^\circ - \epsilon, t)]$$

$$\tilde{H}^\circ_{xx} \triangleq \frac{1}{2}\lim_{\epsilon\to 0}[H_{xx}(\lambda, x^\circ + \epsilon, u^\circ, t) - H_{xx}(\lambda, x^\circ - \epsilon, u^\circ, y)]$$

$$\tilde{H}^\circ_{xu} \triangleq \frac{1}{2}\lim_{\epsilon\to 0}[H_{xu}(\lambda, x^\circ + \epsilon, u^\circ + \epsilon, t) - H_{xu}(\lambda, x^\circ - \epsilon, u^\circ - \epsilon, t)]$$

$$\tilde{H}^\circ_{uu} \triangleq \frac{1}{2}\lim_{\epsilon\to 0}[H_{uu}(\lambda, x^\circ, u^\circ + \epsilon, t) - H_{uu}(\lambda, x^\circ, u^\circ - \epsilon, t)]$$

$$\Delta\tilde{x} \triangleq \int_{-\infty}^{\infty} |\xi|\, N(\xi;\, \Delta\bar{x}, \bar{P} - \Delta\bar{x}^T\Delta\bar{x})\, d\xi$$

$$\Delta\tilde{x}^2 = \int_{-\infty}^{\infty} |\xi| \xi N(\xi; \Delta\bar{x}, \bar{P} - \Delta\bar{x}^T \Delta\bar{x}) d\xi$$

$$\Delta\tilde{u} \overset{\Delta}{=} \int_{-\infty}^{\infty} |\xi| N(\xi; \Delta\bar{u}, \sigma_u^2) d\xi$$

$$\Delta\tilde{u}^2 = \int_{-\infty}^{\infty} |\xi| \xi N(\xi; \Delta\bar{u}, \sigma_u^2) d\xi$$

$$\Delta\bar{u} = \Delta u + \left(K + \frac{g_x^\circ(x^\circ, u^\circ, t)}{g_u(x^\circ, u^\circ, t} \right) \Delta\bar{x}$$

$$\sigma_u^2 = K\hat{P}K^T + 2K\tilde{P}\left(K + \frac{g_x^\circ}{g_u^\circ}\right) + \left(K + \frac{g_x^\circ}{g_u^\circ}\right) \bar{P} \left(K + \frac{g_x^\circ}{g_u^\circ}\right)^T$$

If

$$K = -\frac{g_x^\circ}{g_u^\circ}$$

then $\tilde{H}_x^\circ + \tilde{H}_u^\circ |K| = 0$, and $\Delta\bar{u} = \Delta u$, and $\sigma_u^2 = K\hat{P}K^T$. Let $\Delta K = \gamma K$; then γ may be chosen so that $\mathcal{H}_1$ take the form given in the body of the report.

Appendix F

SONIC BOOM AND STRUCTURAL CONSTRAINTS

Appendix F

SONIC BOOM AND STRUCTURAL CONSTRAINTS

First consider the constraint on the total temperature:

$$\theta^* \leq \theta_{MAX} \ . \tag{F-1}$$

For $h \geq h_{TROP}$, from Eqs. (18) and (125),

$$\begin{aligned} \theta^* &= \theta_{TROP}\left(1 + \frac{\gamma - 1}{2} M_n^2\right) \\ &= \theta_{TROP}\left(1 + \frac{\gamma - 1}{2} \frac{v^2}{\gamma R\ \theta_{TROP}}\right) \\ &= \theta_{TROP} + \frac{1}{2} \cdot \frac{\gamma - 1}{\gamma} \cdot \frac{v^2}{R} \ . \end{aligned} \tag{F-2}$$

Combining Eqs. (F-1) and (F-2) yields

$$v \leq \sqrt{(\theta_{MAX} - \theta_{TROP}) \frac{2\gamma R}{\gamma - 1}} \triangleq v_{max} \ . \tag{F-3}$$

For $h \leq h_{TROP}$,

$$\begin{aligned} \theta^* &= [\theta_{TROP} + k_{LPS}\ (h_{TROP} - h)\ ] + \frac{1}{2} \frac{\gamma - 1}{\gamma} \frac{v^2}{R} \\ &= \left[\theta_{TROP} + k_{LPS} \left(h_{TROP} - \frac{E - \frac{1}{2}v^2}{g_0}\right)\right] + \frac{1}{2} \frac{\gamma - 1}{\gamma} \frac{v^2}{R} \end{aligned} \tag{F-4}$$

and combining Eqs. (F-1) and (F-4) yields

$$v \leq \sqrt{\left[\theta_{MAX} - \theta_{TROP} - k_{LPS}\left(h_{TROP} - \frac{E}{g_0}\right)\right] \frac{2\gamma R}{\gamma - 1 + \gamma R \frac{k_{LPS}}{g_0}}} \triangleq \bar{v}(E). \quad \text{(F-5)}$$

Now consider the constraint that the SST be above given altitudes subsonically and supersonically. First note that at the tropopause an SST traveling at Mach 1 has energy E_{TROP} given by

$$E_{TROP} = \frac{1}{2} \gamma R \theta_{TROP} + h_{TROP} g_0 . \quad \text{(F-6)}$$

If $E \geq E_{TROP}$ then an SST traveling at Mach 1 will have velocity $\bar{v}_s(E)$ that obeys

$$\bar{v}_s(E)^2 = \sqrt{\gamma R \theta_{TROP}} . \quad \text{(F-7)}$$

If $E < E_{TROP}$ then an SST traveling at Mach 1 will have a velocity $\bar{v}_s(E)$ that obeys

$$\begin{aligned} \bar{v}_s^2(E) &= \gamma R \theta \\ &= \gamma R \left[\theta_{TROP} + k_{LPS}(h_{TROP} - h)\right] \\ &= \gamma R \left[\theta_{TROP} + k_{LPS}\left(h_{TROP} - \frac{E - \frac{1}{2}\bar{v}_s^2}{g_0}\right)\right] . \end{aligned} \quad \text{(F-8)}$$

Hence for $E < E_{TROP}$

$$\bar{v}_s^{-2} = \frac{\gamma R}{1 - \frac{1}{2}\gamma R \frac{k_{LPS}}{g_0}} \left[\theta_{TROP} + k_{LPS} \left(h_{TROP} - \frac{E}{g_0} \right) \right] . \qquad \text{(F-9)}$$

Let

$$v'(E) \triangleq \begin{cases} 2(E - h_0 g_0) & \text{if } E - \frac{1}{2} \bar{v}_s^{-2} \leq h_0 g_0 \\ 2(E - h_s g_0) & \text{if } E - \frac{1}{2} \bar{v}_s^{-2} > h_s g_0 \\ \bar{v}_s & \text{otherwise} \end{cases} . \qquad \text{(F-10)}$$

Then $v < v'$ implies that $h > h_0$ for $M_n \leq 1$ and $h > h_0$ for $M_n > 1$.

The above constraints can be summarized by

$$v_c(E) = \text{minimum } \{v_{max}, \bar{v}(E), v'(E)\} . \qquad \text{(F-11)}$$

NASA-Langley, 1970 —— 2